FACULTAD DE CIENCIAS

DEPARTAMENTO DE BIOLOGÍA MOLECULAR

"Study of autophagy regulation and innate immunity in African Swine Fever Virus infection"

DOCTORAL THESIS

Raquel Muñoz Moreno

Madrid, 2014

FACULTAD DE CIENCIAS
DEPARTAMENTO DE BIOLOGÍA MOLECULAR
UNIVERSIDAD AUTÓNOMA DE MADRID

"Study of autophagy regulation and innate immunity in African Swine Fever Virus infection"

Memoria presentada para optar al grado en Doctor en Ciencias por:

Raquel Muñoz Moreno

DIRECTORAS DE TESIS

Covadonga Alonso Martí
Inmaculada Galindo Barreales

Tutor académico

José Mª Almendral del Río

El presente trabajo de tesis ha sido realizado en el Departamento de Biotecnología del Instituto Nacional de Investigaciones agrarias y alimentarias (INIA) financiada por una Beca de Formación de Personal Investigador (FPI) otorgada por el Ministerio de Ciencia e Innovación (MICINN)

INFORME DEL DIRECTOR DE TESIS PARA LA AUTORIZACIÓN DE DEFENSA DE TESIS DOCTORAL

(Doctoral Thesis Supervisor's report to dissertation authorization)

(En el caso de existir más de un director de la tesis doctoral, deberá presentarse un informe de cada uno de los co-directores)
(In case of more than one Thesis Supervisor, a report of each one must be submitted)

D/Dª **COVADONGA ALONSO MARTÍ**
(Thesis Supervisor´s name and surname)

Director/a de la tesis doctoral de D/Dª **Raquel Muñoz Moreno** ***(PhD Candidate´s name and surname),*** **informa favorablemente** la solicitud de autorización de defensa de la tesis doctoral con el Título ***(Title of the PhD Dissertation):***

"Study of autophagy regulation and innate immunity in African Swine Fever Virus infection " presentada por dicho/a doctorando/a.

(favorably reports on the application for dissertation authorization submitted for the PhD Candidate)

Programa de Doctorado ***(Doctoral program)*****:** RD1393/ 2007
La tesis está sometida a procesos de confidencialidad: SÍ ☐ NO ☒X
(Thesis is under confidentiality procedures: Yes / No)
La tesis se presenta como compendio de publicaciones: SÍ ☐ NO ☒X
(Thesis is submitted as a compendium of publications: Yes / No)

Resultados y valoración ***(Results and assessment):***

ANTECEDENTES DE LA CUESTIÓN Y OBJETIVOS PROPUESTOS ***(Background of the field and main goals)*** Los antecedentes de la cuestión están bien presentados y estructurados y son muy informativos sobre el estado de la cuestión de los temas tratados.
DESARROLLO DEL TRABAJO Y METODOLOGÍA ***(Procedure and Development of the general matter and methodology)*** El doctorando ha realizado un trabajo brillante, ordenado y minucioso demostrando gran capacidad de trabajo e iniciativa. La metodología es apropiada y rigurosa incluyendo numerosos abordajes técnicos incluyendo rastreo por doble híbrido en levaduras, utilización de RNA interferentes, establecimiento de líneas estables, etc. La memoria está bien redactada y ordenada de forma sistemática y comprensiva. Los resultados son relevantes y novedosos abordando cuestiones aun no bien clarificadas sobre la regulación de la autofagia en las infecciones víricas y su posible papel en el ciclo replicativo del virus. Asimismo, aborda aspectos novedosos sobre la posible relación entre la autofagia y la vía endocítica y las proteínas de respuesta al interferón IFITM.
APORTACIONES DE CARÁCTER GENÉRICO O EXPERIMENTAL ***(Contribution to the experimental and general field)*** Se caracteriza el gen vírico responsable de la regulación de la autofagia, que es un gen esencial para la replicación del virus de la Peste porcina africana. Demuestra la relevancia que este proceso tiene para la infección y las condiciones del mismo. Se describen las bases para la búsqueda de nuevas dianas para las proteínas de la inmunidad innata en las moléculas que regulan la endocitosis y la autofagia.

PUBLICACIONES A QUE HAYA DADO LUGAR
(Publications appeared already)

1. Alonso, C., Galindo, I., Cuesta-Geijo, M.A., Cabezas, M., Hernaez, B., Munoz-Moreno, R., 2013. African swine fever virus-cell interactions: from virus entry to cell survival. Virus Res 173, 42-57.

2. Galindo, I., Hernaez, B., Munoz-Moreno, R., Cuesta-Geijo, M.A., Dalmau-Mena, I., Alonso, C., 2012. The ATF6 branch of unfolded protein response and apoptosis are activated to promote African swine fever virus infection. Cell death & disease 3, e341.

3. Hernaez, B., Cabezas, M., Munoz-Moreno, R., Galindo, I., Cuesta-Geijo, M.A., Alonso, C., 2013. A179L, a new viral Bcl2 homolog targeting Beclin 1 autophagy related protein. Curr Mol Med 13, 305-316.

4. Quetglas, J.I., Hernaez, B., Galindo, I., Munoz-Moreno, R., Cuesta-Geijo, M.A., Alonso, C., 2012. Small rho GTPases and cholesterol biosynthetic pathway intermediates in african Swine Fever virus infection. J Virol 86, 1758-1767.

5. Cuesta-Geijo, Miguel Angel, Michele Chiappi, Raquel Muñoz-Moreno, Inmaculada Galindo, Pedro M. Juiz-González, Lucía Barrado, José L. Carrascosa and Covadonga Alonso., 2014. Endosomes and lipids are platforms for African swine fever virus replication. eLife 2014. (Manuscript under revision)

VALORACIÓN GLOBAL ***(Final evaluation)***

Es un trabajo novedoso con un abordaje bien enfocado y altamente informativo que lleva a cabo los objetivos propuestos de una forma clara y concisa llegando a conclusiones relevantes desde el punto de vista científico.

(Rellenar solo en el caso de que la tesis se presente como compendio de publicaciones):
(To fill in only in case that thesis is submitted as a compendium of publications):

Se autoriza la presentación de la tesis como compendio de publicaciones: SÍ ☐ NO ☐
(Authorizing the submission of the thesis as a compendium of publications: Yes /No)

Fecha
(Date): 25 de julio de 2014

Firma
(Signature): Covadonga Alonso

(En el caso de que se trate de directores no vinculados al programa de doctorado cursado por el doctorando, se incluirá a continuación la ratificación razonada del tutor)
(In case of Thesis Supervisors not related to the doctoral program followed by the PhD Candidate, a Thesis Advisor's ratification must be submitted)

INFORME DEL DIRECTOR DE TESIS PARA LA AUTORIZACIÓN DE DEFENSA DE TESIS DOCTORAL
(Doctoral Thesis Supervisor's report to dissertation authorization)

(En el caso de existir más de un director de la tesis doctoral, deberá presentarse un informe de cada uno de los co-directores)
(In case of more than one Thesis Supervisor, a report of each one must be submitted)

D/Dª **INMACULADA GALINDO BARREALES**
(Thesis Supervisor´s name and surname)

Director/a de la tesis doctoral de D/Dª **Raquel Muñoz Moreno** ***(PhD Candidate´s name and surname)*** **informa favorablemente** la solicitud de autorización de defensa de la tesis doctoral con el Título ***(Title of the PhD Dissertation):***

"Study of autophagy regulation and innate immunity in African Swine Fever Virus infection" presentada por dicho/a doctorando/a.

(favorably reports on the application for dissertation authorization submitted for the PhD Candidate)

Programa de Doctorado ***(Doctoral program)*****:** RD1393/ 2007
La tesis está sometida a procesos de confidencialidad: SÍ ☐ NO X
(Thesis is under confidentiality procedures: Yes / No)
La tesis se presenta como compendio de publicaciones: SÍ ☐ NO X
(Thesis is submitted as a compendium of publications: Yes / No)

Resultados y valoración ***(Results and assessment):***

ANTECEDENTES DE LA CUESTIÓN Y OBJETIVOS PROPUESTOS
(Background of the field and main goals)

La autofagia es un mecanismo de defensa celular que elimina directamente patógenos intracelulares y juega un papel crucial en la respuesta inmune innata y adaptativa de la célula frente a patógenos intracelulares. Algunos virus han desarrollado herramientas para contrarrestar, o incluso aprovechar, esta respuesta celular. El objetivo de esta Tesis se ha dirigido a estudiar la regulación de la autofagia en la infección por el virus de la Peste Porcina Africana.

DESARROLLO DEL TRABAJO Y METODOLOGÍA
(Procedure and Development of the general matter and methodology)

La doctoranda ha adquirido una gran experiencia en técnicas de Virología, Biología Celular y Molecular. La metodología que ha empleado en este trabajo es la apropiada y coherente con los objetivos e incluye la generación de líneas celulares estables, rastreo de interacción proteína-proteína mediante el sistema del doble hibrido en levaduras y mediante co-inmunoprecipitación, microscopía confocal, etc. La memoria está bien escrita y los resultados son novedosos.

APORTACIONES DE CARÁCTER GENÉRICO O EXPERIMENTAL
(Contribution to the experimental and general field)

Los resultados obtenidos en la Tesis demuestran que el virus de la Peste Porcina Africana interrumpe activamente la maquinaria autofagia celular normal necesaria para la formación de autofagosomas.
Los resultados han permitido poner las bases para el desarrollo de nuevos tratamientos antivirales utilizando como dianas proteínas que regulan la autofagia y proteínas de la inmunidad innata como los IFITMs.

PUBLICACIONES A QUE HAYA DADO LUGAR ***(Publications appeared already)***

1. Alonso, C., Galindo, I., Cuesta-Geijo, M.A., Cabezas, M., Hernaez, B., Munoz-Moreno, R., 2013. African swine fever virus-cell interactions: from virus entry to cell survival. Virus Res 173, 42-57.

2. Galindo, I., Hernaez, B., Munoz-Moreno, R., Cuesta-Geijo, M.A., Dalmau-Mena, I., Alonso, C., 2012. The ATF6 branch of unfolded protein response and apoptosis are activated to promote African swine fever virus infection. Cell death & disease 3, e341.

3. Hernaez, B., Cabezas, M., Munoz-Moreno, R., Galindo, I., Cuesta-Geijo, M.A., Alonso, C., 2013. A179L, a new viral Bcl2 homolog targeting Beclin 1 autophagy related protein. Curr Mol Med 13, 305-316.

4. Quetglas, J.I., Hernaez, B., Galindo, I., Munoz-Moreno, R., Cuesta-Geijo, M.A., Alonso, C., 2012. Small rho GTPases and cholesterol biosynthetic pathway intermediates in african Swine Fever virus infection. J Virol 86, 1758-1767.

5. Cuesta-Geijo, Miguel Angel, Michele Chiappi, Raquel Muñoz-Moreno, Inmaculada Galindo, Pedro M. Juiz-González, Lucía Barrado, José L. Carrascosa and Covadonga Alonso., 2014. Endosomes and lipids are platforms for African swine fever virus replication. eLife 2014. (Manuscript under revision)

VALORACIÓN GLOBAL ***(Final evaluation)***

A lo largo del proyecto la doctoranda ha demostrado tener grandes cualidades científicas y humanas para llevar a cabo los objetivos propuestos, demostrando gran capacidad de trabajo e iniciativa.

(Rellenar solo en el caso de que la tesis se presente como compendio de publicaciones):
(To fill in only in case that thesis is submitted as a compendium of publications):
Se autoriza la presentación de la tesis como compendio de publicaciones: SÍ ☐ NO ☐
(Authorizing the submission of the thesis as a compendium of publications: Yes /No)

Fecha
(Date): 29 Agosto 2014

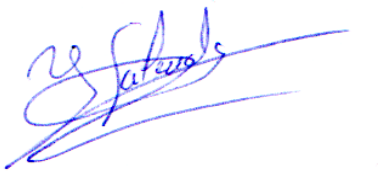

Firma
(Signature): Inmaculada Galindo

(En el caso de que se trate de directores no vinculados al programa de doctorado cursado por el doctorando, se incluirá a continuación la ratificación razonada del tutor) ***(In case of Thesis Supervisors not related to the doctoral program followed by the PhD Candidate, a Thesis Advisor's ratification must be submitted)***

RATIFICACIÓN RAZONADA DE LA AUTORIZACIÓN DE DEFENSA DE LA TESIS DOCTORAL POR EL TUTOR

D/Dª : José Mª Almendral del Río

Tutor/a de D/Dª Raquel Muñoz Moreno

en el programa de doctorado RD1393/2007

A la vista de las razones expuestas en el informe del Director/es de las tesis, se ratifica el referido informe para la autorización de la defensa doctoral presentada por dicho/a doctorando/a.

Fecha: 05/0

Firma:

Ratificación del informe por la Comisión Académica del programa de doctorado (*)

El Responsable de la Comisión Académica ratifica el informe favorable del director de tesis para la autorización de defensa de la tesis

doctoral presentada por dicho/a doctorando/a.

Madrid, a de de 20

Marque lo que proceda:

Programa de doctorado del RD 185/1985 Programa de doctorado del RD 778/1998	Director del Departamento Correo electrónico: ...	
	Director en funciones Correo electrónico: ...	
	Subdirector Correo electrónico: ...	Fdo.: ....
Programa de doctorado del RD 56/2005 Programa de doctorado del RD1393/2007	Coordinador del programa Correo electrónico: ...	Fdo.: ....
Programa de doctorado del RD 99/2011	Responsable de la Comisión Académica Correo electrónico: ...	Fdo.: ....

ACKNOWLEDGEMENTS

Parece que fue ayer, pero ya han pasado más de 4 años desde que entré a formar parte de este laboratorio. Siempre vi lejano este momento y sin embargo aquí estoy, escribiendo las últimas líneas que marcan el final de una etapa muy importante de mi vida.

Mis primeras palabras de agradecimiento son para la Dra. Covadonga Alonso. Gracias por haberme dado la oportunidad de realizar la tesis doctoral en tu laboratorio, por haber confiado siempre en mi a lo largo de estos años, por transmitirme tu pasión por la ciencia y por haber estado ahí tanto fuera como dentro del laboratorio y tanto en lo profesional como en lo personal. Eres una persona en quien se puede confiar y todo un ejemplo de trabajo y superación. No te quepa la menor duda de que me voy con la certeza de no haber podido estar en un lugar mejor y de que si se me presentase de nuevo la oportunidad, sin dudarlo repetiría la experiencia.

Gracias a también a Inma (IG). Has estado siempre ahí durante estos cuatro años y sólo puedo decir que trabajar a tu lado ha sido un placer. Gracias por escucharme, por ayudarme siempre que me ha surgido cualquier duda y por haberme dado ánimos en los momentos duros. Si hoy he conseguido llegar hasta aquí, gran parte de ese mérito es tuyo. ¡No cambies nunca!

También agradecerle a Miguel Ángel su gran ayuda, en especial durante estos últimos meses. Me ha encantado ser tu compi de enfrente este ultimo año y quería felicitarte por la paciencia que has demostrado tener a la hora de soportar las continuas "perrerías" por parte de tus compis de laboratorio, entre las cuales por supuesto me incluyo –y que tanto te gustan y te/nos han hecho reír-. Era el precio a pagar por haber sido durante tanto tiempo el único chico del laboratorio. ¡Eres un tío estupendo y ten por seguro que voy a echar mucho de menos tantos buenos ratos!

También a Inma Dalmau y a Marta, que hace ya tiempo que se fueron pero que sin duda han dejado una huella imborrable en mí. Dalmau, espero que la presentación de mi tesis sea la excusa perfecta para que te vuelvas a pasar por aquí, ¡me haría muchísima ilusión! Marxu, sabes tu ayuda en todo este tiempo ha sido de vital importancia. Hemos trabajado en numerosas ocasiones juntas y aunque más de una vez surgieron contratiempos (sobre todo a la hora del screening de la librería, ¿te acuerdas?), siempre supimos salir airosas de la situación. En resumen:¡formábamos un buen equipo! Sabes que se te echa mucho de menos desde que te fuiste (yo ya sabes que ¡desde antes de que te fueses!), pero me alegro de que todo te este yendo bien y de que nos podamos seguir viendo por los pasillos del INIA o pasando un buen rato desayunando en la cafetería.

Como no, también tengo guardadas unas palabras de agradecimiento para Bruno. Tú me guiaste durante mi primera etapa en el laboratorio y aunque sólo coincidimos durante algo más de un año, fuiste para mi un gran maestro y de ti aprendí un montón de técnicas de laboratorio. Gracias "crack" por volcarte conmigo, por tu paciencia, tu saber hacer y por el tan buen rollo que desprendiste y me contagiaste desde el primer día.

Gracias también al resto de personas que han pasado por el laboratorio durante estos años como Berta o Nerea y en especial a los dos últimos fichajes del laboratorio: "Rasca y Pica", también conocidos como Pedro y Lucía. Habéis conseguido que me ría como no lo hacía en mucho tiempo. Pedro, tus anécdotas varias como médico no han tenido desperdicio alguno y si a eso le sumas las reflexiones y comentarios de Lucía eso ya se convertía en lo que llaman los americanos el "cherry on top". Eso sí Cova, quiero que sepas que a pesar de todo el cachondeo y las reincidentes carcajadas - que sin duda habrás oído mas de una vez desde tu despacho-, ¡¡hemos currado y trabajado como los que más!! (aunque estoy segura de que eso ya lo sabías). Pedro, te deseo mucho éxito en tu futuro profesional, eres un tío súper divertido; sencillamente genial. Lucía, espero haberte servido de apoyo desde que entraste en el laboratorio y que te haya podido enseñar alguna que otra cosilla. Sabes que para cualquier cosa que necesites, estaré ahí para intentar ayudarte en todo lo posible.

Mi más sincero agradecimiento también al Dr. Escribano. Sabes que siempre me he sentido atraída por el mundo empresarial. Gracias a ti he podido seguir muy de cerca lo que es hacer ciencia de calidad y me has transmitido que si se tiene una buena idea, carácter emprendedor y ganas, puedes llegar a crear con éxito tu propia empresa. Me pareces todo un ejemplo de lucha y perseverancia y me has mostrado con tu propio ejemplo que si uno se marca una meta, por alta que esté, con trabajo y esfuerzo se puede conseguir.

También quería dar las gracias al resto de personas que componen el labo de enfrente. A Javi y Eva: gracias por hacerme más amenos muuuuuchos fines de semana. Siempre que me tocaba venir, el hecho de encontraros por aquí y tener gente con quien charlar me hacia la situación mucho más llevadera. También a Susana, y por supuesto a dos de mis más fieles compañeras de ´realities´: Carmen y Silvia. Que sepáis que sois unas Masterchefs estupendas, que me ha encantado conoceros y poder compartir tantos buenos momentos. Os echare mucho de menos pero prometo conectarme desde el otro lado del charco y seguir comentando con vosotras y el resto componentes del grupo los diferentes shows televisivos que vayan surgiendo.

Asimismo agradecerle a gente de otros laboratorios, en especial a María, Yanín, Estela, Ana y Maite. Me habéis salvado de numerosos apuros, los típicos en los que das cuenta de que no has hecho un pedido (o no te ha llegado) y te falta el anticuerpo, o la placa o el medio de turno. Gracias por haber sido tan serviciales a lo largo todo este tiempo y gracias también por hacer tan amenos y divertidos los momentos del desayuno y/o comida.

En general gracias también al resto de personas que componen el Dpto. de Biotecnología del INIA. Entre todos, y cada uno a vuestra manera, habéis contribuido a que ir a trabajar cada día haya sido todo un placer.

Fuera de los muros que componen el INIA, me gustaría agradecerle profundamente al Dr. Adolfo García Sastre la oportunidad que me brindó el año pasado de realizar una estancia en su laboratorio, en el Hospital Mount Sinai de Nueva York. Supuso para mí un reto profesional y un sueño hecho realidad.

Una persona que se merece una mención especial en este apartado de mi tesis doctoral es Carles. Fuiste un pilar muy importante durante toda mi estancia en Nueva York, eres un gran científico y sobre todo una de las mejores personas que he conocido. Resumiéndolo de alguna manera, te puedo decir que eres sin duda el mayor descubrimiento de todos estos años de investigación. Haces que mi vida merezca la pena, que me haya sentido motivada todos y cada uno de los días desde que empecé a redactar esta tesis y para que negarlo, una razón más para querer volver a Nueva York. En definitiva, gracias por hacer de mi una mejor persona y por haberme devuelto la felicidad que sin darme cuenta había perdido. Te quiero.

El último apartado de los agradecimientos me lo he reservado para las personas que han sido más importantes para mi desde el principio de mi existencia: mi familia. Tengo que daros las gracias por tantas cosas que no sé por donde empezar. Gracias a mis padres: gracias a vosotros soy quien soy a día de hoy. Siempre os habéis sacrificado y esforzado por darnos una buena educación, y nos habéis inculcado tanto a Paula como a mi valores que nos han hecho crecer como personas. Si hoy he llegado hasta aquí, ha sido sin duda gracias a vosotros. Gracias por vuestro apoyo, por haberme escuchado y aconsejado SIEMPRE en los buenos momentos (y también en los menos buenos) y por haber hecho de mi una persona fuerte que no se rinde ante nada y que jamás tira la toalla. Me siento muy afortunada de que seáis mis padres porque iguales quizás los habrá, pero desde luego no mejores. Gracias también a Paula, eres mi hermana pero ante todo eres mi amiga. Quiero que sepas que me siento muy orgullosa de ti y que

estoy muy contenta de que hayamos podido convivir juntas durante estos últimos meses en Madrid, la verdad es que te voy a echar mucho de menos. Gracias por ser tan servicial, por escuchar, por tus continuos detalles y por preocuparte siempre de que los que estamos a tu alrededor seamos felices. Gracias a la yaya Cónsola, eres una segunda madre para mi y quiero que sepas que te quiero un montón. Eres de las mejores personas que existen sobre la Tierra: cariñosa, generosa y con un corazón que no te cabe en el pecho. Gracias por preocuparte siempre por nosotros y por rezarme la oración cada vez que he tenido un examen o algún acontecimiento importante, la verdad es que en la mayoría de casos siempre ha funcionado o como poco, ha logrado que me sintiese mejor y más segura de mi misma. Gracias también a mi yayo Víctor; te fuiste cuando tan sólo era una niña, pero quiero que sepas que el sentimiento de indignación e impotencia que sentí en aquel momento al oír la palabra "cáncer", despertaron aún más en mí el interés por la ciencia y el descubrimiento; por tanto, quiero que sepas que una parte de este trabajo va dedicada especialmente a ti. Gracias también a mis abuelos, María y Macario, sois el vivo ejemplo del respeto y de que el amor lejos de desaparecer, va aumentando con el paso de los años. Gracias también al resto de mi familia: a mis tíos (Víctor, Anabel, María y Juan) y a mi primo Joan.

En definitiva, quiero que sepáis que sois la mejor familia que se puede tener y sólo espero y deseo que os sintáis tan orgullosos de mi como yo lo estoy de vosotros.

"Research is to see what everybody else has seen,

and to think what nobody else has thought"

Albert Szent-Gyorgyi (1893-1986)

ABSTRACT

In this current work, we have investigated the role of the African swine fever virus (AFSV) in the context of autophagy and in the innate immune response of the host cell. These two processes have been recently linked together in the early cell defense mechanism against external pathogens, including viruses. We have characterized a complex regulation of the autophagic process mediated by the ASFV, using the autophagosome-related LC3 protein. Upon viral entry, ASFV inhibits autophagy persistently throughout the infectious cycle to facilitate replication and to avoid virus clearance. Further analysis revealed that ASFV-mediated autophagy inhibition depends on the specific interaction of ASFV Bcl2 homolog and apoptotic inhibitor A179L with autophagy-related cell protein Beclin1.

The ASFV-mediated autophagy inhibition is a tightly regulated process, since altering key autophagy factors impairs infectivity, the formation of the ASFV viral factories and the replication of the virus overall. Analysis of viral factory formation and distribution revealed that even though viral factories of ASFV resemble sequestering of cytoplasmic material in structures called aggresomes, they are not consistent with aggresome formation mechanisms. In fact, inhibition of canonical BAG3 and HDAC6-mediated aggresome formation pathways, did not alter the formation of ASFV viral factories.

Finally, our studies established a link between autophagy, ASFV infection and innate immunity by the expression of the interferon-induced transmembrane (IFITM) protein family, which possesses antiviral properties against several viruses. ASFV infection was impaired by IFITM2 and IFITM3 but not IFITM1, due to alterations in endosomal compartments, changes in the cholesterol homeostasis, as well as induction of autophagy.

Taking together these results, we propose that the mechanism underlying the antiviral effect of IFITM against ASFV could be inhibiting ASFV infection through the endosomal pathway. Interestingly, expression of IFITM2 induces accumulation of autophagosomal marker LC3, colocalizing with late endosomal compartments. Future studies will reveal more details about the crosstalk between autophagy and IFITM-related innate immunity in ASFV infection, allowing better and more efficient antiviral intervention strategies against the disease.

RESUMEN

En el presente trabajo hemos investigado el papel que juega el Virus de la Peste Porcina Africana (VPPA) en el proceso de autofagia y respuesta inmune celular. Se ha descrito recientemente la estrecha relación que existe entre ambos procesos por formar parte del mecanismo de defensa de la célula ante la llegada externa de patógenos como son los virus. Haciendo uso de la proteína LC3, que se encuentra asociada a los autofagosomas, hemos logrado caracterizar la compleja regulación de la autofagia llevada a cabo por el VPPA. Tras la entrada del virus en la célula, el VPPA inhibe la autofagia y dicha inhibición persiste a lo largo de todo el ciclo infectivo para facilitar su posterior replicación y evitar así ser eliminado. Análisis posteriores han revelado que esta inhibición del proceso autofágico está mediado por la interacción específica entre el homólogo celular a Bcl2 e inhibidor de apoptosis codificado por VPPA (A179L) y la proteína Beclin1.

Esta inhibición de la autofagia mediada por el virus es un proceso minuciosamente regulado ya que si se alteran alguno de sus componentes, se bloquea la formación de las factorías virales y la consecuente replicación del virus. Haciendo un análisis de las factorías virales y de su distribución hemos podido concluir que a pesar de que son orgánulos muy similares a los agresomas, realmente no se trata de la misma estructura. De hecho, la inhibición de las dos principales vías implicadas en la formación del agresoma mediadas por las proteínas BAG3 y HDAC6 no afectó a la formación de las factorías virales.

Finalmente nuestros estudios nos han permitido establecer un vínculo entre la autofagia, la infección por VPPA y la inmunidad innata mediante el estudio de una familia de proteínas transmembrana que se inducen en respuesta a interferón (IFITMs), y que se ha descrito que poseen propiedades antivirales frente a algunos virus. La infección por VPPA se vio afectada en presencia de IFITM2 y 3 pero no de IFITM1, debido a alteraciones en compartimentos endosomales , cambios en la homeostasis del colesterol e inducción de autofagia.

Haciendo una valoración global de los resultados obtenidos, hemos propuesto que el papel antiviral propiciado por los IFITMs es debido a alteraciones que producen en la ruta endosomal. Además, la expresión de IFITM2 induce la acumulación de LC3 que se distribuye colocalizando con compartimentos endosomales tardíos. Futuras investigaciones revelarán mas detalles a cerca de la interrelación existente entre autofagia y la regulación de la inmunidad innata en la infección por VPPA, permitiendo así desarrollar mejores y mas eficientes terapias antivirales frente a esta enfermedad.

INDEX

ACRONYMS

A

AD: Activation domain
Akt: Protein kinase B
ASF: African swine fever
ASFV: African Swine Fever Virus
ATCC: American Type Culture Collection
ATG: Autophagy-related gene
ATP: Adenosine triphosphate

B

BAG3: Bcl-2-associated athanogene 3
Bcl2: B-Cell lymphoma 2

C

cBcl2: Cellular Bcl2
CIL: Conserved intracellular loop
CMA: Chaperone-mediated autophagy

D

DENV: Dengue virus
DMEM: Dulbecco´s modified eagle´s medium
DNA: Deoxyribonucleic Acid
dsDNA: double stranded DNA

E

EEA1: Early endosome antigen 1
EBOV: Ebola virus
EGFR: Epidermal growth factor receptor
eIF: Eukaryotic initiation factor
EM: Electron microscopy
EMEM: Eagle's modified essential medium
ER: Endoplasmic reticulum
Eps15: Epsin15

F

FBS: Fetal bovine serum

G

GABARAP: γ-aminobutyric acid type A [GABA] receptor-associated protein
GABARAPL1: GABARAP-like 1
GABARAPL2: GABARAP-like 2
GABARAPL3: GABARAP-like 3
ϒ-HV68: Gamma-herpesvirus 68
GERL: Golgi–ER–lysosome
GF: Growth factor

GFP: Green fluorescent protein
GFR: Growth factor receptor
GTP: Guanidine-5'-triphosphate

H

HBSS: Hanks balanced salt solution
HCV: Hepatitis C virus
HDAC6: Histone deacetylase 6
hEGF: Human epidermal growth factor
hpi: Hours post-infection
HSV-1: Herpes simplex virus-1

I

IAV: Influenza A virus
IFITM: IFN-inducible transmembrane protein
IF: Immunofluorescence
IFN: Interferon

K

Kbp: Kilobase pairs
KSHV: Kaposis sarcoma herpesvirus
LAS AF: Leica Application Suite advanced fluorescence software
LB: Lysogeny broth
LE: Late endosome
LiAc: Lithium acetate

M

MAP1LC3A: Microtubule-associated protein 1 light chain 3A
MAP1LC3B: Microtubule-associated protein 1 light chain 3B
MAP1LC3C: Microtubule-associated protein 1 light chain 3C
MARV: Marburg virus
MEF: Mouse embryonic fibroblast
MGF: Multigene Family
MHV68: Murine γ-herpesvirus 68
moi: Multiplicity of Infection
mpi: Minutes post-infection
mQ: MilliQ
mRNA: Messenger RNA
MTOC: Microtubule-organizing center
mTOR: Mammalian target of rapamycin
µg/ml: Micrograms per milliliter
µl: Microliter
MVB: Multivesicular Body

N

NCLDV: Nucleo-cytoplasmic DNA virus
ng: Nanogram
nM: Nanomolar

O

OIE: World Organisation for Animal Health
ORF: Open Reading Frame

P

PBS: Phosphate buffered saline
PCR: Polymerase chain reaction
PE: Phosphatidyl ethanolamine
PFA: Paraformaldehyde
PFU: Plaque-forming units
PIP2: Phosphatidylinositol 4,5-bisphosphate
PIP3: Phosphatidylinositol 3,4,5-trisphosphate
PI3K: Phosphoinositide 3-kinase
pmol: Picomol
PTEN: Phosphatidylinositol-3,4,5-trisphosphate 3-phosphatase

Q

qRTPCR: Quantitative real-time PCR

R

RIPA buffer: Radioimmunoprecipitation assay buffer
RNA: Ribonucleic acid

S

SARS CoV: Severe acute respiratory syndrome coronavirus
Scr: Scramble
SDS: Sodium dodecyl sulfate
shRNA: Short hairpin RNA
siRNA: Small interfering RNA
S6K1: 40S ribosomal protein S6 kinase 1

T

TBE: Tris/borate/EDTA
TEMED: N,N,N´,N´-tetramethilethilendiamine
TM: Transmembrane domain
Trp: Tryptophan

U

UBC: ubiquitin-conjugating enzyme

V

vBcl2: Viral Bcl2
VF: Viral Factory

W

WB: Western Blot
WT: Wild type

#

3AT: 3-Amino-1,2,4-triazole
3MA: 3-Methyladenine
4E-BP1: 4E-binding protein 1

INTRODUCTION

1. African Swine Fever

1.1 Brief description and current situation

African Swine Fever **(ASF)** is a highly contagious disease affecting wild and domestic pigs alike, causing severe economic losses for the pig industry worldwide. ASF is classified as a notifiable disease by the World Organization for Animal Health (OIE). The disease is endemic in most sub-Saharan countries in Africa, where it also has serious implications for food safety by limiting the availability of an important source of human dietary protein (Costard et al., 2009b). ASF is caused by the African Swine Fever Virus (ASFV), which is a member of the *Asfarviridae* family. ASFV is the only DNA virus that is transmitted by arthropods (ticks from the genus *Ornithodoros)*, acting as its major reservoirs (Kleiboeker, 2002; Kleiboeker and Scoles, 2001; Plowright et al., 1969).

ASFV causes unapparent persistent infections in its natural hosts, namely warthogs (*Phacochoerus africanus*), bushpigs (*Potamochoerus porcus*, *P. Larvatus*) and soft ticks (*Ornithodoros moubata*) (Anderson et al., 1998; Kleiboeker et al., 1999). In contrast, ASFV in domestic pigs causes an acute hemorrhagic fever, leading the death of all infected animals. In fact, animals with acute ASF display fever and a tendency to crowding, loss of appetite, inactivity and apathy as well as early leukopenia induced by lymphopenia and changes in monocyte numbers (Colgrove et al., 1969; Pan and Hess, 1984). However, less virulent isolates that emerged during the circulation of the virus in domestic pigs have led to an increase of subacute and unapparent infections, thereby increasing the prevalence (Bech-Nielsen et al., 1995; Mebus and Dardiri, 1980; Penrith et al., 2004).

ASF was first observed in Kenyan pigs in 1909 and it was later reported in 1921 as a distinct entity from classical swine fever (Montgomery, 1921). In the present, ASF is still endemic in Africa and in Sardinia, affecting domestic pigs, wild boar and feral pigs. In 2007, it spread from Africa to the Caucasus region and subsequently to the Russian Federation. This epidemic outbreak caused acute disease in domestic pigs and wild boars (Beltrán-Alcrudo et al., 2009; Beltrán-Alcrudo et al., 2008). Due to the general lack of biosecurity measures and poor implementation of disease control protocols, the illegal movement of infected pigs and related products, as well as the existence of areas of interaction between free-ranging pigs and wild boar, there is a substantial risk that ASF may persist in these regions and/or spread

to other areas of Europe (Costard et al., 2009a; Wieland et al., 2011), as illustrated by the recent detection of ASFV in meat products in northern Russia (PROMed-Mail, 2012) and the introduction of ASF into Ukraine and other neighboring countries (Roberts et al., 2014).

A previous epidemic outbreak affected Spain and jumped to the American continent. The first reported case of ASF in Spain dates from 1960 in Badajoz, linked to pig imports from Portugal originated in Mozambique (Polo-Jover and Sánchez-Botija, 1961). Thanks to rigorous control programs that were adopted by the Spanish Government, ASF was eradicated from the Iberian Peninsula in the late 1990s, after 30 years of endemicity (Arias et al., 2002; Perez et al., 1998). This is a very relevant disease from the economic point of view. Unluckily, there is not an effective vaccine available for ASF. Therefore, a deeper knowledge of virus–host interactions is required in order to overcome the existing gaps that could set the context in which a protective vaccine would be possible.

ASF is one of the most important infectious diseases threatening porcine production. With its recent introduction in the Caucasus and Russian Federation, it has become a world threat, as the risk of ASFV dissemination to the rest of Europe, China and other major pig producing countries from South-East Asia has substantially increased.

ASFV is a major constraint for pig production and results in killing large numbers of animals, not only due to the high lethality rate of the virus but also due to the fact that massive culling is the only method to control the disease. ASFV outbreaks further imply major economic losses in affected countries because of market and trade bans and closing of borders to animals and pork products. Pork meat provides an affordable source of high protein quality in endemic areas in Africa and the eradication of this disease would directly alleviate poverty.

2. African Swine Fever Virus

African Swine Fever Virus (ASFV) is a large, enveloped virus with icosahedral morphology and an average diameter of 200nm. It consists on a double-stranded DNA genome of 170-190 kylobases (kb), containing terminal inverted repeats at its ends and closed by hairpin loops (Salas, 1999).

ASFV replication cycle is mainly cytoplasmic but an early stage of replication in the nucleus has also been reported (Garcia-Beato et al., 1992; Rojo et al., 1999). Transcription of viral

genes is strongly regulated and the synthesis of different recognizable classes of mRNA -including immediate-early, early, intermediate and late transcripts- has also been described (Almazan et al., 1992; Rodriguez et al., 1996). Viral morphogenesis takes place exclusively in cytoplasmic viral factories (VFs), in which the late phase of viral replication also occurs. Because of all these replication characteristics and also as a result of comparative genome analysis, ASFV has been included in the monophyletic group of large nucleo-cytoplasmic DNA viruses (NCLDV) and nowadays it is the sole member of the *Asfarviridae* family (Iyer et al., 2001).

2.1 Structure and composition of the viral particle

The ASFV particle is composed by several concentric domains: an internal core formed by the central genome that contains the nucleoid coated by a thick protein layer named core shell, an inner lipid envelope surrounding the core and finally the capsid, which is the outermost layer of the intracellular virions **(Figure I1)**. The extracellular virions possess an additional external envelope that is acquired from the plasma membrane after budding. The ASFV viral particle combines the following layers:

a) The outer envelope: Morphology of the external envelope of extracellular virus is similar to the plasma membrane. This results from the budding process at the virus exit from the cell (Breese and DeBoer, 1966). The virus attachment protein p12 has been reported to localize into the outer envelope by immunoelectron microscopy studies of purified extracellular virus.

b) The capsid: The structure of the capsid has been extensively studied by electron microscopy and it is formed by about 2000 capsomers assembled as hexagonal prisms. They are 13 nm-long, 5-6 nm in width and they display a central hole (Carrascosa et al., 1984). Protein p72, which is encoded by the *B646L* gene, is the major capsid protein (Garcia-Escudero et al., 1998) and it represents about one third of the protein mass in the viral particle. Another protein present in the capsid is pE120R, which is involved in the transport of the mature ASFV particles from the viral factory to the plasma membrane to exit the cell (Andres et al., 2001).

c) The inner envelope: When visualized by electron microscopy (EM), the inner envelope of mature particles look like a single lipid membrane (Andres et al., 1998; Carrascosa et al.,

1984) that is derived from the endoplasmic reticulum (Cobbold et al., 1996; Rouiller et al., 1998) through a mechanism that is still poorly understood. Furthermore, membrane proteins p54 (Rodriguez et al., 2004), p17 (Suarez et al., 2010) and pE248R (Rodriguez et al., 2009) are also constituents of this envelope.

d) The core shell: The core shell is a thin protein layer of about 30nm that has been defined as an independent domain of the virus core, encompassing the central nucleoid (Andres et al., 1997).

e) The nucleoid: It is an electrodense structure of 80 nm that contains the viral genome (Andres et al., 1997) and nucleoproteins such as the DNA-binding protein p10 (Andres et al., 2002; Munoz et al., 1993) or protein pA104R (Andres et al., 2002; Borca et al., 1996) which is closely to the histone-like proteins of bacteria.

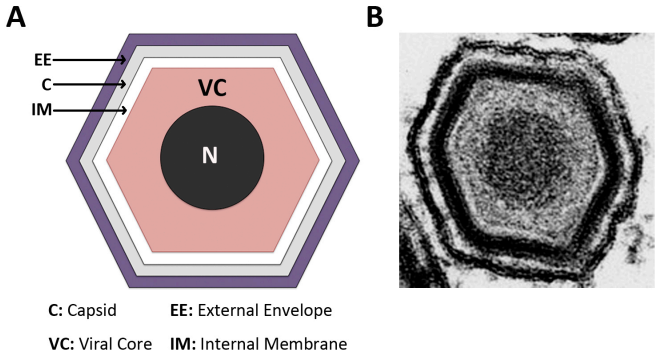

Figure I1. Structure of ASFV virion. (A) Representative scheme of ASFV virion structure showing the corresponding layers forming the viral particle: The external envelope (EE), the capsid (C), the internal membrane (IM), the viral core (VC) and the nucleoid (N) **(B)** Electron microscopy image of ASFV.

2.2 Functionality of the ASFV genome

ASFV genome structure is very similar to the one from poxvirus, as it is comprised of a double stranded DNA (dsDNA) with terminal inverted repeats and hairpin loops (Gonzalez et al., 1986). Genome length fluctuates among the different ASFV isolates, oscillating from 170 to 193 kilobase pairs (kbp) (Chapman et al., 2008; de Villiers et al., 2010; Yanez et al., 1995).

Due to its large genome, ASFV encodes around 151 and 167 open reading frames (ORFs), separated by 200-bp long non-coding sequences. Moreover, transcription occurs from both DNA strands. Differences found in genome length and in number of genes are due to the gain or loss of ORFs of the different multigene families (MGF) encoded by ASFV.

An ASFV isolate (BA71V) was cell-culture adapted to replicate in Vero cells (Enjuanes et al., 1976b; Gonzalez et al., 1986; Yanez et al., 1995). Furthermore, complete sequencing of the 12 wild type (WT) isolates from different geographical areas has recently been achieved.

There is a short sequence located in the 5' end of each gene that contains the promoter region. The viral RNA polymerase complex is responsible of recognizing the aforementioned promoter regions. They are rich in A+T, as well as being recognized by transcription factors encoded by ASFV that are specific for the different viral stages: early gene expression (immediate early and early), intermediate gene expression and late gene expression.

2.3 ASFV gene expression

Gene expression of ASFV appears to follow a cascade mechanism similar to that described for poxviruses (Moss, 2001). Immediate early and early genes are expressed before DNA replication begins. This is possible due to the action of several enzymes that are packed in the viral core and are involved in the viral transcription. ASFV early genes also encode for other enzymatic proteins that take part in the nucleotide metabolism, DNA replication and expression of transcription factors that are crucial for late gene expression (Almazan et al., 1992; Almazan et al., 1993; Kuznar et al., 1980; Salas et al., 1981).

DNA replication takes place by a self-initiation mechanism (Baroudy et al., 1982) and makes use of the viral DNA polymerase (Martins et al., 1994; Moreno et al., 1978). DNA replication involves two phases: a first and brief replication phase that occurs in the host cell nucleus (Garcia-Beato et al., 1992; Rojo et al., 1999; Tabares and Sanchez Botija, 1979) and a second replication phase with a maximum peak at 8 hours post-infection (hpi). This second replication phase takes place in VFs. Enzymes required for viral replication are expressed immediately after viral core penetration, when it is partially decapsidated in the cytoplasm (Salas et al., 1983). The current hypothesis is that short sections of viral DNA are synthesized at early times post infection in the nucleus and then transported to VFs, where they are later used in the prime synthesis of full length genomic DNA within the replicative cycle.

After replication of the viral DNA has been initiated (approximately at 6 hpi), transcription of intermediate and late genes begin (Rodriguez et al., 1996; Salas et al., 1986). These genes codify for structural proteins of the virion, as well as polymerases and early transcription factors that will be packed into the new virions (Kuznar et al., 1980; Pena et al., 1993; Salas

et al., 1988). However, little is known about specific regulatory mechanisms that control ASFV gene expression during this timed sequence of events.

2.3.1 ASFV gene products

ASFV genome contains several genes that codify host, virulence and regulatory proteins for several cellular functions. For example, gene *DP71L* present in BA71V isolate (Yanez et al., 1995) and *23-NL* in Malawi isolate (Zsak et al., 1996) inhibits protein synthesis induced by phosphorylation of eIF-2α through PKR or other kinases as PERK (Rivera et al., 2007a; Zhang et al., 2010). Furthermore *MGF360* and *530* (Zsak et al., 2001b) determine the tropism, virulence and suppression of IFN response (Afonso et al., 2004; Zsak et al., 2001a). ASFV also contains genes involved in the immune system evasion as *EP402R* or *CD2v*, a gen homologue to cellular *CD2* (Borca et al., 1998; Borca et al., 1994), and also *A238L* that is homologue to IκB cellular proteins and acts blocking the transcription activation of immunoregulatory genes (Granja et al., 2008; Miskin et al., 1998). The virus also regulates the apoptotic response of infected cells through gene *A179L* that acts as a viral homologue to antiapoptotic cellular protein Bcl-2. The protein encoded by *A179L* impedes the programmed cell death of infected cells before the complete viral genome replication has been completed (Brun et al., 1996; Hernaez et al., 2004a). The ASFV gene *I215L* is the only known viral encoded ubiquitin-conjugating enzyme E2, UBCv1 (Hingamp et al., 1992; Rodriguez et al., 1992). UBCv1 catalyzes the attachment of ubiquitin to substrate proteins, which tags them for proteolytic degradation via the proteasome. In addition to UBC enzymes, ubiquitin-activating E1 and E3 or ubiquitin protein ligase enzymes are involved in attaching ubiquitin to substrate proteins (Scheffner et al., 1995). Selective protein degradation mediated by protein ubiquitination regulates many processes including transcription and cell cycle control (Ciechanover, 1994; Pahl and Baeuerle, 1996; Smith et al., 1996). However, recent evidence also suggests the involvement of ubiquitin as a specificity factor for selective autophagy (Kraft et al., 2010). Recombinant UBCv1 can be self-ubiquitinated *in vitro*. It also can ubiquitinate histones and the ASFV virion protein pp62 (polyprotein pp62), which is posttranslationally processed resulting in two major structural proteins of 35 kDa (p35) and 15 kDa (p15) (Hingamp et al., 1992; Hingamp et al., 1995; Simon-Mateo et al., 1997). Furthermore, SMCp protein has also been described as an *in vivo* substrate for UBCv1 (Bulimo et al., 2000).

2.4 ASFV infectious cycle

2.4.1 Entry of ASFV into the host cell

ASFV infectious cycle starts with the viral adsorption and subsequently entry into the host cell, lasting between 18 and 24 hpi (Costa, 1990). Targets of ASFV infection are mainly macrophages and monocytes from lymphatic tissues; also megakaryocytes and polymorphonuclear leukocytes, present in blood and bone marrow (Plowright et al., 1968; Ramiro-Ibanez et al., 1996; Ramiro-Ibanez et al., 1997). The virus was adapted to grow in Vero cells and lead to the creation of the non-virulent isolate BA71V (Enjuanes et al., 1976b). This isolate is currently the most characterized of all and it has enabled great progress in the study of the ASFV infectious cycle.

ASFV enters the host cell by receptor-mediated endocytosis and its entry is temperature and acid pH-dependent (Alcami et al., 1989; Valdeira and Geraldes, 1985). Cell receptors involved in this process are still unknown. However, viral proteins such as p12 and p54, that are involved in host cell recognition, as well as p30, which plays a role in viral internalization, have been identified so far (Angulo et al., 1992, 1993; Gomez-Puertas et al., 1998).

ASFV entry into host cells takes place by clathrin-mediated endocytosis, which requires dynamin GTPase activity. Moreover, the clathrin-coated pit component Epsin15 (Eps15) was identified as a relevant cellular factor during infection. (Hernaez and Alonso, 2010). In addition to this, alternative pathways for ASFV entry, such as macropinocytosis (Sanchez et al., 2012) or phagocytosis (Basta et al., 2010), have been recently proposed. However, whether these alternative pathways are effective in achieving a productive ASFV infection remains unknown. It will be interesting to unveil if ASFV could use all entry pathways in a cooperative fashion (Alonso et al., 2013). Successful infection of ASFV is also dependent on cholesterol, as treatment of cells with β-methyl cyclodextrin, which removes cholesterol from cellular membranes, severely affects ASFV infection (Bernardes et al., 1998; Hernaez and Alonso, 2010). Furthermore, the activity of PI3K enzyme, GTPase Rac1 activation and the integrity of the cholesterol biosynthetic pathway are all necessary in the early steps of infection (Quetglas et al., 2012).

2.4.2 Morphogenesis and final steps of the infection

The final steps of the infectious cycle include the assembly and release of mature virions (Smith and Enquist, 2002). *De novo* synthetized virions assembly leads to an accumulation of viral membranes inside the VF that emerge as opened and curved structures and constitute the precursors of the internal viral membrane. It has been demonstrated that they have their origin in endoplasmic reticulum (ER) cisternae that are located in the VF periphery (Andres et al., 1998).

The assembly of new virions also includes the acquisition of the viral DNA together with the enzymes that the virus will include inside *de novo* synthetized capsids (Nunes et al., 1975). The DNA incorporation process is not always successful. In fact, empty viral particles close to the plasma membrane are frequently found. Finally, new virions can exit infected cells by gemmation process (Breese and Hess, 1966). These extracellular virions are surrounded by a fragile lipid envelope. However, this process is not very efficient, as the extracellular virus fraction represents a small percentage when compared to intracellular virus fraction.

The cytopathic effect produced ASFV infected cells is thought to be a second mechanism to massively liberate new synthetized virions. The late apoptosis described in infected cells (Hernaez et al., 2004b, 2006; Ramiro-Ibanez et al., 1996; Ramiro-Ibanez et al., 1997) ends with the generation of apoptotic bodies that are full of mature virions. In the final phase of the apoptotic process, a plasma membrane blebbing is produced. This blebbing inhibition has been shown to severely decrease the release of virions to the extracellular media (Galindo et al., 2012). Additionally, phagocytic cells can absorb apoptotic bodies. This fact implies the diffusion of virions to other cells without alerting the immune system (Teodoro and Branton, 1997).

2.5 ASFV delivery to perinuclear sites requires microtubules

Microtubules are essential components of the cytoskeleton, as they provide structural support to the cell and they also constitute the major long-rage intracellular transport mechanism within the cytoplasm. Movement along microtubules can be either through the use of motor proteins or by growth of the tubules themselves. Microtubules are organized at the centrosome, which is also called the microtubule-organizing center (MTOC), and dynein motors are responsible for driving the cargo towards the MTOC by a retrograde

transport, while kinesin motors transport them to the periphery by an anterograde transport.

Incoming ASFV virions are associated with microtubules (Quetglas et al., 2012), as they eventually localize to regions of the cell that are close to the nucleus (VFs). This movement in infected cells can be easily followed by using recombinant ASFV virions encoding, for example, the structural protein p54 fused to GFP (B54GFP) (Hernaez et al., 2006).

Maintenance of the ASFV VFs at the MTOC requires the presence of the aforementioned motor proteins as it has been previously reported that microtubule depolymerization with nocodazole prevents the correct localization of the fluorescent recombinant ASFV virions at VFs and subsequently results in a clear dispersion of these structures (Alonso et al., 2001; Carvalho et al., 1988; de Matos and Carvalho, 1993; Heath et al., 2001). It has also been demonstrated that the ASFV structural protein p54 is able to interact directly with the dynein motor protein (Alonso et al., 2001; Hernaez and Alonso, 2010). In fact, repression of the p54-encoding *E183L* gene results in a disruption of ASFV assembly in VFs (Rodríguez et al., 2004). These findings suggest that VFs require an intact microtubule network (Hernaez et al., 2006).

2.6 Comparative study of ASFV Viral Factories (VFs) with aggresomes

It has been previously described that ASFV VF resemble aggresomes (Heath et al., 2001), which are formed at the MTOC in response to the aggregation of misfolded proteins (Johnston et al., 1998). These aggregates are highly toxic and involved in many neuropathological diseases such as Alzheimer's, Huntington's and spongiform encephalopathies. Redirection of protein aggregates to aggresomes isolates them from the cell, reducing toxicity and thus facilitating their degradation either by the proteasome or lysosomes after sequestration by autophagy (Garcia-Mata et al., 2002).

Proteins are often ubiquitinated prior to degradation. In fact, ubiquitinated proteins can be detected in virus factories and also some of these proteins have been demonstrated to have a viral origin (Hingamp et al., 1995). The core particles of many viruses are similar in size (60–100 nm diameter) to protein aggregates and it is therefore conceivable that ASFV viral cores may be recognized as protein aggregates and then delivered to the MTOC (Wileman, 2007).

Furthermore, protein aggregates are surrounded by a collapsed cage made of intermediate filament protein vimentin during aggresome formation. ASFV VFs are also surrounded by a vimentin cage at the MTOC during infection. Vimentin is rearranged at the centrosome into a star-shaped structure that resembles the microtubule aster formed during mitosis (Stefanovic et al., 2005a) and this process can be blocked by overexpression of p50 dynamitin, thus indicating an involvement of the dynein motor protein. The vimentin aster provides the basis for the cage that surrounds the VF following the onset of virus DNA replication and synthesis of late structural proteins (Heath et al., 2001; Monaghan et al., 2003; Stefanovic et al., 2005a).

Aggresomes recruit a variety of different cellular components to facilitate protein folding and/or degradation. Cellular chaperones, such as hsp70 and mitochondria, are also recruited to ASFV factories (Castello et al., 2009; Heath et al., 2001; Rojo et al., 1998a). The chaperones may facilitate folding of viral structural proteins, although ASFV encodes a chaperone that is responsible for folding the major capsid protein p72 (Cobbold et al., 2001).

Therefore, similarities found between factories and aggresomes raise the possibility that ASFV may use the aggresome pathway to facilitate assembly. Microtubules can concentrate viral and cellular proteins needed for replication at the MTOC and vimentin can provide a physical scaffold within the factory, or act as a cage to prevent movement of viral components into the cytoplasm. Alternatively, aggresomes may be part of an innate defense against virus infection. Innate immunity is responsible of recognizing viruses as foreign intruders so that they can be stored in inclusions and removed by autophagy in lysosomes (Wileman, 2006, 2007) and get presented by major histocompatibility complexes (Nimmerjahn et al., 2003; Paludan et al., 2005; Schmid et al., 2007). To date, there are two main pathways in aggresome formation: the first one involves HDAC6 (histone deacetylase 6), while the second one is mediated by BAG3 (Bcl-2-associated athanogene 3).

2.6.1 HDAC6-mediated pathway

HDAC6 has the capacity to bind both polyubiquitinated misfolded proteins and dynein motors. It specifically interacts with dynactin/p150^{Glued}, a component of the dynein motor complex, bridging the ubiquitinated proteins to the dynein motors, and promoting transport

of the cargo towards the microtubule organizing center (MTOC) to enable aggresome formation (Dompierre et al., 2007; Kawaguchi et al., 2003). More specifically, HDAC6 is thought to interact with aggregated proteins through its ZnF-UBP domain (Kawaguchi et al., 2003), a domain typically found in deubiquitinases capable of binding the unanchored ubiquitin C-terminus with high affinity and specificity (Pai et al., 2007; Reyes-Turcu et al., 2006). Indeed, cells deficient in HDAC6 fail to clear misfolded protein aggregates from the cytoplasm, cannot form aggresomes properly and are hypersensitive to the accumulation of misfolded proteins. These findings identify HDAC6 as a crucial player in the cellular management of misfolded protein-induced stress and thus, in aggresome formation.

2.6.2 BAG3-mediated pathway

We have showed previously that specific aggresome targeting is achieved by ubiquitination of degradation-prone proteins. These proteins are then recognized by ubiquitin adaptor proteins that bind to dynein, such as the deacetylase HDAC6 (Kawaguchi et al., 2003; Li et al., 2011). However, since many misfolded proteins in aggresomes are not ubiquitinated (Garcia-Mata et al., 1999), selective loading of cargo onto dynein should also occur independently of ubiquitin signaling, thus BAG3 plays a crucial role.

It has been demonstrated that BAG3 directly associates with the microtubule motor dynein and mediates the selective transport of misfolded proteins to the aggresome (Gamerdinger et al., 2011). Binding of BAG3 to dynein is mediated by its PxxP domain.

Based on these findings, BAG3 may act as a nucleotide-exchange factor and directly stimulates substrate transfer from HSP70 to the dynein motor complex. Therefore, BAG3 directly promotes transport of misfolded proteins to the aggresome.

3. Autophagy

Autophagy can be defined as a catabolic process that maintains cellular homeostasis by degradation of damaged or excess cellular organelles and protein aggregates from the cytoplasm, thereby enabling cell survival. In contrast to proteasomal degradation, that specifically targets ubiquitinated proteins, autophagy is mediated by the lysosome, which serves as an end point degradative organelle. The retrograde transport of substrates along microtubules via the cytoplasmic dynein motor complex constitutes a sequestration of degradation substrates in a special perinuclear compartment: the aggresome (Kopito,

2000). Thus, a link between aggresome formation and the autophagy pathway has been well established (Garcia-Mata et al., 1999; Webb et al., 2004), since selective autophagy of damaged, misfolded and aggregated proteins strongly requires concentration and isolation of degrading substrates away from other cytosolic components.

Cell culture and also *in vivo* studies have revealed the importance of autophagy in numerous diseases, including cancer and neurodegenerative diseases in aging. It has also been reported to have a key role in innate and in adaptive immunities to pathogen infections. Therefore, understanding the molecular basis of the formation and composition of the different structures involved in autophagy, as well as the regulation of the pathway, is an important goal to convert autophagy into a potential therapeutic target for improving human disease conditions and infection (Choi et al., 2013).

In general, autophagy can be broadly classified as microautophagy, chaperone-mediated autophagy (CMA) and macroautophagy. All these three pathways share the same mode of degradation via the lysosome, yet they are mechanistically distinct from one another (Yang and Klionsky, 2010).

Microautophagy was mainly characterized in yeast (Mijaljica et al., 2011). It involves a direct engulfment of the cytoplasm at the lysosomal membrane as it is facilitated by protrusion of arm-like structures. On the other hand, CMA specifically directs translocation of unfolded proteins through an inherent consensus motif (KFERQ) across the limiting membrane of the lysosome for degradation (Yang and Klionsky, 2010).

In contrast, macroautophagy (hereafter referred to as autophagy) occurs when a double-membrane structure known as autophagosome engulfs cytosolic material such as proteins and organelles and then fuses them with the endosomal-lysosomal system, which delivers degradative lysosomal proteases to it, converting it into an autolysosome.

3.1 Brief historical overview

The discovery of autophagy in the late 1950s is attributed to electron microscopy analysis that recognized the unique topological properties of a vesicle containing cytoplasmic organelles. Christian De Duve coined the phrase “autophagy” to explain this process in mammalian cells and recognized the contribution of the lysosome to it (Eskelinen et al., 2011). By the 1970s, improvements in electron microscopy and the development of

cytochemical techniques enabled the concept of autophagy to be firmly established. Subsequently, a discrete membrane called a phagophore was identified with unique morphological properties and as the potential initiating membrane of the autophagosome. This membrane appeared unexpectedly in electron microscopy images as a double-membrane cisterna, often as a curved, cup-shaped structure with a translucent lumen that stained heavily with osmium, thus giving it a darker appearance than other cellular membranes (Reunanen et al., 1985).

The osmophilic properties of the phagophore suggested that its lipid and protein composition is unique and distinct from other cellular membranes, and data obtained using freeze-fracture techniques have shown that it contains low levels of protein (Rez and Meldolesi, 1980). Although the initial electron microscopy studies suggested the phagophore, now also called the isolation membrane, was derived from the ER or the GERL (Golgi–ER–lysosome), some evidence implied that it was assembled *de novo* (Ashford and Porter, 1962). However, the current consensus is that it arises from a subdomain of the ER.

Biochemical approaches developed over the subsequent decades provided data that are the foundation for our current understanding of the molecular control of autophagy. The discovery of the pathway in yeast from electron microscopy analysis (Takeshige et al., 1992) and the identification of the first yeast *ATG* (autophagy-related) genes (Thumm et al., 1994; Tsukada and Ohsumi, 1993) transformed the autophagy field. The molecular analyses of autophagy began in earnest in yeast and soon followed in mammalian cells. The first link between autophagy and human disease was made in 1999 (Liang et al., 1999) with the discovery that a haploinsufficient tumour suppressor gene, Beclin 1, the mammalian homologue of yeast Atg6 (also known as Vps30) is an autophagy gene. Subsequently, the generation of the first ATG-knockout mouse, for ATG5, demonstrated that autophagy was essential for postnatal survival (Kuma et al., 2004).

3.2 Impact of viral infection on autophagy

Induction of autophagy involves the coordinated action of several key factors. Among them, there are members of the Atg8 ubiquitin-like (Ubl) protein family, which includes MAP1LC3A (microtubule-associated protein 1 light chain 3A), MAP1LC3B, MAP1LC3C, GABARAP (γ-aminobutyric acid type A [GABA] receptor-associated protein), GABARAPL1 (GABARAP-like

1), GABARAPL2 and GABARAPL3, all of which are important for phagophore formation and closure in mammals (Behrends et al., 2010). In principle, any of the aforementioned Atg8 family proteins can serve as a marker of autophagosomes in mammalian cells. However, only MAP1LC3B (hereafter referred to as LC3) is conventionally used as a marker of autophagosomes in mammalian cells (Galluzzi et al., 2009; Mizushima et al., 2010). During autophagosome formation and elongation, the cytosolic LC3, termed LC3-I, is proteolytically cleaved and coupled to phosphatidyl ethanolamine (PE) to form LC3-II, which is inserted into the autophagosomal membrane. The two main characteristics of autophagy detection is, first of all, the increase in intracellular levels of LC3-II and, second, the re-localization of evenly distributed cytosolic LC3-I into LC3-II positive punctate structures, representing autophagosomes (Inoue and Klionsky, 2010; Yang and Klionsky, 2010). Based on the importance of LC3 processing for autophagosome formation and function, antibodies to LC3-I and LC3-II are widely used in western blotting techniques to monitor autophagy (Karim et al., 2007; Mizushima and Yoshimori, 2007). LC3-I and LC3-II can be readily distinguished based on their differential mobility in SDS–PAGE.

Despite increased molecular weight than LC3-I, LC3-II migrates more rapidly in SDS–PAGE compared to LC3-I, likely due to higher hydrophobicity associated with the PE group (Tanida et al., 2008). Technically, western blotting for LC3-I and LC3-II is straightforward, with reliable antibodies now available from various commercials sources. It should be noted that LC3 is expressed as three isoforms in mammalian cells, LC3A, LC3B and LC3C, but only LC3B-II correlates with increased levels of autophagic vesicles, and therefore it is recommended to use anti-LC3B antibodies for analysis. Indeed, infections with a wide range of DNA or RNA viruses increase abundance of autophagosomes or autophagic vesicles in infected cells (Ait-Goughoulte et al., 2008; Gannage et al., 2009; Jackson et al., 2005; Nakashima et al., 2006; Takahashi et al., 2009; Taylor and Kirkegaard, 2007, 2008).

However, it is important to remark that increased amounts of autophagosomes in infected cells can either be due to their enhanced formation or to their accumulation due to a block in their maturation or degradation. Therefore, to understand the reason for increased autophagosome numbers in virus-infected cells, it is important to study the impact of viral infection on autophagic activity or autophagic, which is defined as the measurement of the balance between the rate of autophagosome formation and degradation **(Figure I2)**.

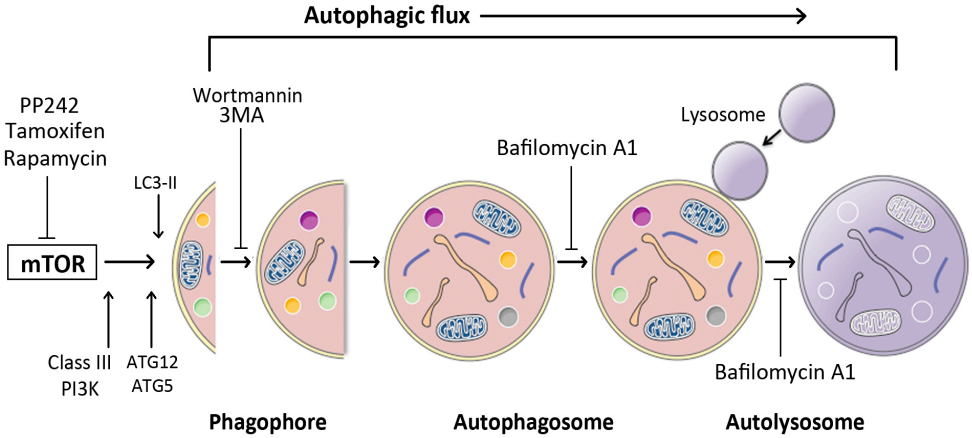

Figure I2. Representative scheme of the autophagic flux. The process of autophagy begins in the cytoplasm by formation of a double-membrane structure, phagophore, that has sequestered or engulfed the targeted portion of the cytoplasm, containing misfolded proteins, damaged macromolecules, and organelles. The autophagic machinery uses Atg proteins for the formation of the phagophore, and its subsequent elongation to mature autophagosome formation. Once the autophagosome is formed, most of the Atg proteins are dissociated, which allows fusion with the lysosome to form the autolysosome. The sequestered contents and the inner membrane of the autolysosome are degraded by the lysosomal hydrolases. Autophagic flux is an indicator that the autophagy process has been completed.

3.2.1 Viral-mediated induction and inhibition of autophagy

Various studies reported the activation of autophagy upon virus infection as inferred from the increased number of autophagic vesicles, the monitoring of LC3-I to LC3-II conversion and the elevated number of LC3-positive punctae in infected cells, (Ait-Goughoulte et al., 2008; Khakpoor et al., 2009; Sir et al., 2008; Takahashi et al., 2009; Taylor and Kirkegaard, 2007). However, considering the dynamic nature of autophagy, it is important to determine the rate of autophagic flux to gain mechanistic insight into how viral infection affects autophagic activity in cells. In fact, recent reports demonstrated that Sindbis virus and hepatitis C virus (HCV) infection increase autophagic flux (Ke and Chen, 2011; Orvedahl et al., 2010). Infection of mouse embryonic fibroblasts (MEFs) expressing GFP-LC3 with Sindbis virus resulted in an increase in the percentage of cells containing GFP-LC3 positive dots concomitant with an increase in LC3-II abundance. In addition, infected cells contained reduced levels of p62 (an accepted marker of autophagic flux), with no significant changes of its mRNA amounts, indicating a complete autophagic response during virus infection (Orvedahl et al., 2010). In case of HCV infection, it has been demonstrated that despite unaltered levels of p62 in infected cells, LC3-II protein levels were increased upon treatment with lysosomal protease inhibitors (E64 and pepstatin A), or chloroquine (a vacuolar ATPase

inhibitor) or Bafilomycin A1 (Baf, an inhibitor of lysosomal acidification), concluding that HCV does not block autophagy (Ke and Chen, 2011).

In line with this conclusion, it also has been shown that treatment of infected cells with chloroquine and Baf resulted in increased LC3-II levels in HCV infected cells as compared to uninfected cells, clearly indicating enhanced autophagic flux. In addition, by employing a tandem-LC3 reporter (mRFP-GFP-LC3), a tool to analyze both autophagosome and autolysosome formation, it has been found that HCV induced autophagosomes that matured into autolysosomes, thus revealing a complete autophagic response in HCV-infected cells.

As opposed to Sindbis virus and HCV, other viruses have evolved strategies to interfere with autophagosome formation or maturation. For instance, Kaposis´s Sarcoma herpesvirus (KSHV), murine γ-herpesvirus 68 (MHV68) and Herpes Simplex virus 1 (HSV-1) target Beclin 1, thereby inhibiting autophagosome formation. These viruses encode proteins that competitively bind to Beclin 1 and thus inhibit its interaction with Vps34. In the case of KSHV, it encodes a viral Bcl-2 homologue, which binds Beclin 1 with much higher affinity than cellular Bcl-2, thereby preventing incorporation of Beclin 1 into Vsp34 complexes (Liang et al., 2008). Furthermore, the viral Bcl-2 homologue encoded by MHV68, M11, also interacts with Beclin 1 and inhibits autophagosome formation (Ku et al., 2008).

3.3 The role of PI3K pathway in autophagy

The regulation of autophagy is a complex process and there are several pathways that are linked to it. Phosphoinositide 3-kinase/protein kinase B/mammalian target of rapamycin (PI3K/Akt/mTOR) pathway is closely related in regulation of autophagy for its role in cell survival, proliferation and differentiation.

The interaction of growth factors (GFs) with GF receptors (GFRs) triggers the phosphatidylinositol 3-kinase (PI3K/Akt/mTOR) signaling cascade, which is involved in controlling cellular macromolecular synthesis, metabolism, growth, and survival and induces rapid activation of their pathways. Such receptors are often activated by viruses (Marsh and Helenius, 2006) and the signals may be used to deceive the host's defenses, allowing safe entrance into the cell.

Activated PI3K induces the conversion of phosphatidylinositol 4,5-bisphosphate (PIP2) to

phosphatidylinositol 3,4,5-trisphosphate (PIP3), which recruits downstream factors to the cell membrane and regulates their activity (Andjelkovic et al., 1997). Akt is a key member of this pathway. PIP3 concentration is tightly controlled and it anchors Akt to the plasma membrane, allowing its activation by phosphorylation. The phosphatase PTEN negatively regulates PIP3 concentration, converting PIP3 to PIP2 and thereby inhibiting PIP3-mediated downstream signaling, including Akt activation. To prolong the infection cycle, viruses attempt to inhibit apoptosis and they have developed several ways to activate Akt by enhancing the functions of the PI3K upstream regulator or by inhibiting negative regulatory phosphatases, or both (Buchkovich et al., 2008; Cooray, 2004).

The downstream effector of Akt, mTOR, is a crucial metabolic sensor. It integrates diverse cellular signals that play critical roles in regulating several pathophysiological processes. This evolutionarily conserved serine/threonine protein kinase functions as a component of two structurally and functionally distinct signaling complexes: mTORC1 and mTORC2 (Populo et al., 2012). mTORC1 is activated by GFs and nutrients, regulates protein translation and cell growth, and plays an important role in the control of lipid synthesis (Porstmann et al., 2008) and mitochondrial metabolism (Schieke et al., 2006).

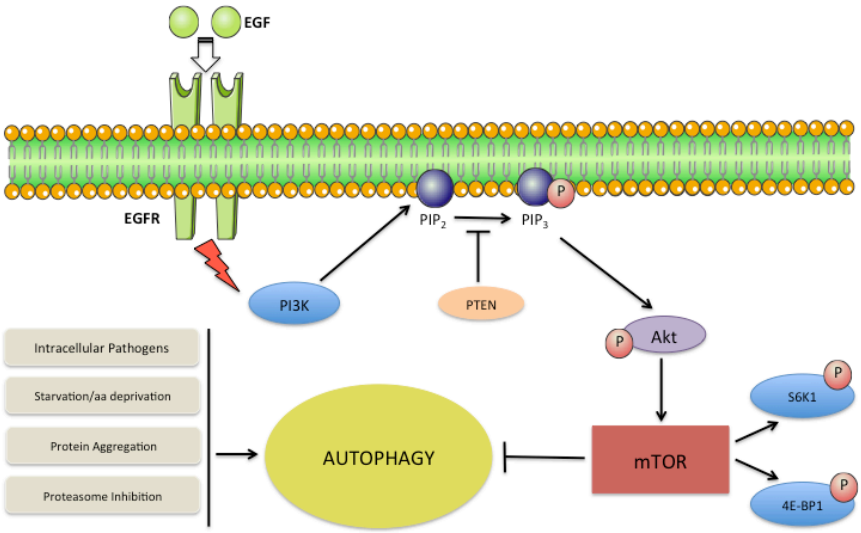

Figure I3. Representative picture of autophagy regulation through the PI3K/Akt/mTOR pathway. Upon growth factors addition, class I PI3K activates Akt, leading to mTORC1 activation and consequently autophagy inhibition. PTEN inhibits formation of PIP_3, activating PI3K/Akt/mTOR signaling, and is therefore an autophagy-promoting signal.

The best-characterized targets of mTORC1 are components of the translation machinery, including eukaryotic initiation factor (eIF)-4E-binding protein 1 (4E-BP1) and 40S ribosomal

protein S6 kinase 1 (S6K1), both of which are important in the control of translation initiation (Hay and Sonenberg, 2004). mTORC1 signaling can be potently inhibited by the naturally occurring antifungal macrolide rapamycin, which acts as an allosteric inhibitor (Petroulakis et al., 2006) but does not completely inhibit mTORC1 activity (Jacinto et al., 2004). For this reason, PP242 and torin, recently discovered specific inhibitors capable of binding the catalytic site of mTORC1, are more widely used (Jacinto et al., 2006). The growth factor-sensitive but nutrient-insensitive mTORC2 phosphorylates Akt, SGK1, and PKC (Jacinto et al., 2004). These also-called "AGC group kinases" control multiple cellular functions, such as the structure of the actin cytoskeleton and cell survival (Alessi et al., 2009; Jacinto et al., 2006; Ma and Blenis, 2009). In contrast to mTORC1, mTORC2 is resistant to acute rapamycin treatment. However, recent studies show that both mTORC1 and mTORC2 are involved in the regulation of autophagy (Fan and Weiss, 2011; Mammucari et al., 2007).

Many DNA viruses are able to regulate the PI3K/Akt/mTOR pathway (Cooray, 2004). For example, HPV early proteins are known to directly activate Akt and mTOR complexes (Jordan and Randall, 2012; Menges et al., 2006; Pim et al., 2005; Spangle and Munger, 2010). In fact, interaction with HPV induces rapid activation of several signaling pathways in host cells (Abban and Meneses, 2010; Payne et al., 2001; Schelhaas et al., 2012), including that of PI3K/Akt potentially via alpha-6 beta-4 integrins (Fothergill and McMillan, 2006). In addition, it has been recently demonstrated that upon HPV16 exposure to keratinocytes, EGFR signals result in rapid Akt activation by phosphorylation and also by inactivation of PTEN. As a result, downstream events of this pathway were initiated: activation of mTOR and its substrates and suppression of autophagy (Surviladze et al., 2013).

However, a possible role of the PI3K/Akt/mTOR pathway to suppress autophagy has never been reported in ASFV infection and therefore, will be studied in the present thesis.

3.4 Autophagy and innate immunity

Intracellular bacteria and viruses must survive the vigorous defense responses of the host. Recent evidence suggests that autophagy is such a host cell response. As we have previously commented, many viruses are vulnerable to autophagic destruction and therefore, they have evolved strategies to circumvent autophagy (Kirkegaard et al., 2004). New evidence

indicates that autophagy not only plays a role in viral degradation but also in both extracellular bacterial pathogens that invade the cell (e.g., group A Streptococcus)(Nakagawa et al., 2004) and true intracellular bacterial pathogens (e.g., *Mycobacterium tuberculosis* and *Shigella flexneri*) (Gutierrez et al., 2004; Ogawa et al., 2005; Xu et al., 2007). Hence, these pathogens have developed methods to evade autophagy. For example, *S. flexneri* encodes a virulence protein, IscB, that blocks bacterial colocalization with the autophagosome. In fact, mutant bacteria lacking IscB display impaired growth in wild type cells but not in $Atg5^{-}/^{-}$ cells deficient in autophagy (Ogawa et al., 2005). These studies indicate that autophagy is involved in innate immunity and that autophagy can be antagonized by pathogen virulence factors.

4. IFN-inducible transmembrane proteins (IFITMs)

4.1 Discovery and structure of IFITMs

IFITM proteins are present across a wide range of species, from amphibians, fish and fowl to mammals. They have been described to play a role in immune cell signaling and adhesion, cancer, germ cell physiology and bone mineralization (Evans et al., 1993; Lange et al., 2008; Lange et al., 2003; Moffatt et al., 2008; Ropolo et al., 2004). Human IFITMs were identified 26 years ago as interferon stimulated genes (ISG) upon both IFN type I (α) and II (γ) induction (Friedman et al., 1984; Lewin et al., 1991). The IFITM1, 2, 3 and 5 genes are clustered on chromosome 11, and they encode for proteins with two transmembrane domains (TM1 and TM2), separated by a conserved intracellular loop (CIL) (Lewin et al., 1991), with both extra-cellular or intra-vesicular termini (Bradbury et al., 1992). TM1 and the CIL are well conserved between the IFITM proteins and a large group of members of the CD225 protein family, which exists from bacteria (125 members) to humans (13 members, with 156 members in chordata). This group of proteins have not been fully studied and functionally characterized so far, with the exception of the IFITM proteins.

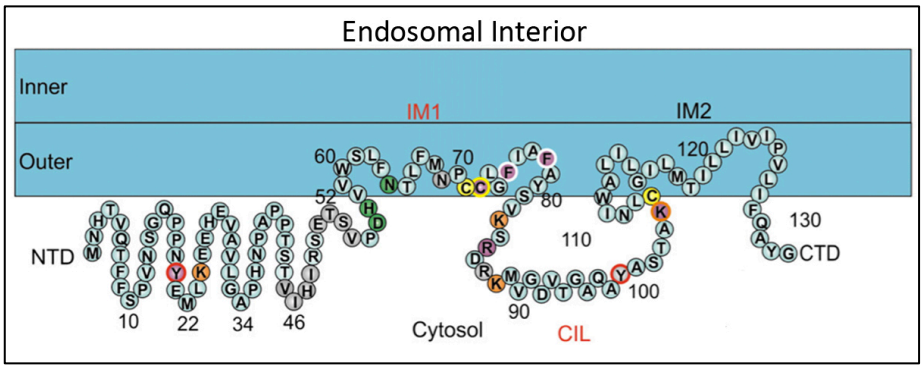

Figure I4. IFITM3 in the endosomal membrane. The N-terminal domain (NTD), the intramembrane domain 1 (IM1), the conserved intracellular loop (CIL) and the intramembrane domain 2 (IM2) are indicated. The outer and inner layers of the endosomal membrane are also noted. Adapted from (Perreira et al., 2013).

4.2 IFITMs exert an antiviral role

Among IFN-stimulated genes (ISG), IFITM 1, 2, and 3, are recently known to inhibit the replication of multiple pathogenic RNA viruses, including influenza A virus (IAV) and influenza B virus, West Nile virus, dengue virus (DENV), severe acute respiratory syndrome coronavirus (SARS CoV), hepatitis C virus (HCV) and the filoviruses, Ebola virus (EBOV) and Marburg virus (MARV)(Brass et al., 2009; Huang et al., 2011b; Wilkins et al., 2013). The antiviral properties of the IFITMs were discovered using orthologous functional genomic strategies (Brass et al., 2009; Jiang et al., 2010; Lu et al., 2011; Schoggins et al., 2011; Shapira et al., 2009). Early work showed that the IFITMs are expressed on the plasma membrane and endosomal membranes and they specifically block viral pseudoparticles bearing the receptors of restricted viruses. (Brass et al., 2009).

Further studies revealed that the IFITMs block viral replication by preventing viral-host membrane fusion subsequent to viral binding and endocytosis (Feeley et al., 2011b; Huang et al., 2011b). These findings demonstrate that they act during early stages of the viral life cycle. Imaging studies of these events revealed that the invading viruses were trapped by the IFITMs, leading to their ultimate destruction in the host cell's lysosomes and autolysosomes, both of which are expanded with IFITM expression (Feeley et al., 2011b). A range of viruses is restricted in a similar way, including ones that exploit the host cell endocytic pathways (Diamond and Farzan, 2013). The kinetics of this entrapment is fast, with viral entry usually occurring between 5 to 30 min, requiring the IFITMs to already be in place or to rapidly mobilize to meet such threats.

Recent studies regarding the IFITMs have been focused on their structure and function as well as on their potential mechanism of action. In addition, new families of IFITM-sensitive RNA viruses have been recently reported. However, to date little is known about the potential role of IFITMs in DNA virus restriction. Therefore, more work will be necessary to compare and contrast the various models proposed for a better understanding of how IFITMs exert their antiviral activity.

OBJECTIVES

1. To study the regulation of autophagy mediated by ASFV.
2. To characterize the possible molecular mechanisms involved in autophagy regulation upon ASFV infection.
3. To develop new tools to monitor the autophagic process in ASFV-infected cells.
4. To determine the origin of ASFV viral factories and their possible link with cellular aggresomes.
5. To validate recombinant tagged ASFV stocks designed and produced in our lab for their use in the study of viral factory formation and other steps of the viral infection.
6. To analyze the possible antiviral role of IFITMs upon ASFV infection, as well as their mechanism of action.

MATERIALS AND METHODS

1. Cell Culture

1.1 Cell lines

In the present work, the following cell lines were used:

Vero (ATCC CCL-81): Very commonly used in mammalian cell culture, they are kidney epithelial cells originating from the African green monkey *Cercopithecus aethiops*. In this study, Vero cells were used in infection assays with the Vero-adapted ASFV strain BA71V.

COS-7 (ATCC CRL-1651): A fibroblast-like cell line derived from the African green monkey *Cercopithecus aethiops*, COS-7 are sensitive to ASFV infection as well. They were obtained from immortalizing CV-1 cells with a modified SV40 virus that can produce large T antigen but has a defect in genomic replication.

HEK 293T/17 (ATCC CRL-11268): Commonly known as 293T cells, they are immortalized human embryonic kidney cells through expression of the SV40 T antigen. These cells are commonly used in lentiviral vector production due to their high transfection rate. They were used in this study to generate stable cell lines expressing different proteins of our interest.

HeLa (ATCC CCL-2): An epithelial-like cell line derived from a sample of human cervix adenocarcinoma. They were chosen to transiently express proteins of our interest due to their high transfection rate.

Primary cultures of swine alveolar macrophages from Large White pigs: They are natural targets of ASFV infection, thus they were used in our infection assays. They are also susceptible of being infected not only by virulent isolates but also by cell culture-adapted isolates, such as the Ba71V.

WSL: A fibroblast-like cell line derived from wild boar lung cells recently developed in Dr. Günther Keil laboratory (Friedrich-Loeffler Institut, Greifswald, Germany). It is widely used in studies of ASFV entry into susceptible cells (Hernaez and Alonso, 2010) and in experiments of infection of sensitive cells to different ASFV isolates (Carrascosa et al., 2011; Portugal et al., 2012).

Vero and COS-7 cell lines were cultured in Dulbecco´s modified Eagle´s medium (DMEM; Biowhittaker) supplemented with 5% and 10% heat-inactivated fetal bovine serum (FBS, Biowhittaker) respectively, 100 IU/ml penicillin (Life Technologies), 100 µg/ml streptomycin

(Life Technologies) and 2mM L-glutamine (Life Technologies). WSL line was grown in Iscove´s medium (Life Technologies), 10% FBS and F-12 nutrient supplement (Life Technologies).

All cells were grown in controlled temperature of 37°C and in a humid atmosphere of 5% CO_2 in air. They were subcultured every two days with trypsin/EDTA (0.25% and 0.025% respectively; Life Technologies).

1.2 Cell transfection

Vero, COS-7 and WSL cells were transfected with Fugene HD (Roche), diluted in DMEM without antibiotics and FBS-free. The used ratio Fugene:DNA was 3:1. The mixture was added to the cell monolayer at 80% of confluence. 6 hours (h) later, the transfection media was replaced with fresh complete medium.

To generate stable cell lines, 293T cells were transfected at 100% confluence with Lipofectamine 2000 (Life Technologies) following manufacturer's protocol. Cells were incubated with the transfection mix for 6 h. The medium was then replaced with fresh DMEM supplemented with 10% FBS.

1.3 Generation of stable cell lines

To generate stable cell lines expressing different proteins of our interest (see table), the commercially available lentiviral expression vector pLVX-Puro (Clontech) was used. 293T cells were transfected at 100% confluency using Lipofectamine 2000 (Life technologies) as described above using Opti-MEM (Life technologies) in 10-cm^2 plates. Plates were previously pretreated with poly-L-lysine (Sigma-Aldrich) at a final concentration of 0.1 mg/ml to avoid cell detachment. Co-transfection of pLVX-puro expression vector, vesicular stomatitis virus glycoprotein (VSV-G) expressing plasmid and the human immunodeficiency virus (HIV) gag-pol expressing plasmid was performed to produce the desired lentiviral pseudoparticles.

Supernatants containing the pseudoparticles were collected twice 48 and 72 h postransfection. Cell debris was removed by brief centrifugation at 1,000 rpm for 5 minutes (min) and cleared supernatants were 0.2 µM-filtered and stored at -80°C until use.

Vero cells were harvested at 40% of confluency and they were transduced with the lentiviral pseudoparticles supplemented with 1 µg/ml of polybrene (EMD Millipore). 24 h later, selective antibiotic treatment was performed using 8 µg/ml of puromycin (Life Technologies) to screen for cells successfully transduced and expressing our proteins of interest. Treatment with puromycin was previously titered in non-transduced cells to determine the optimal working concentration.

Finally, the level of protein expression obtained was determined by Western Blot (WB).

1.3.1 Generation of knock-down stable cell lines

Short hairpin RNA (shRNA) has become a ubiquitous tool in molecular biology to potently and stably silence gene expression for a long term. It is an advantage when compared to other techniques based on the introduction of small interfering RNAs (siRNAs), which have shown to provide effective gene silencing but transiently. In the present work, the lentiviral expression vector pLKO.1-Puro was used to express our shRNA sequences. shRNA lentiviral constructs were obtained by the same methodology described in the section above. They were used to transduce our cells of interest efficiently by integrating the shRNA into their genome to achieve stable gene silencing. A total of 5 shRNAs (Sigma-Aldrich) for each gene to be silenced were tested in order to ensure that at least one of those clones got a yield greater than 70% gene knockdown.

2. Viruses and viral infections

2.1 Viruses

The ASFV isolate **Ba71V**, which is adapted to grow in Vero cells, was used in this current work (Enjuanes et al., 1976a).

The Ba71-54GFP **(B54GFP)** virus was generated using the viral isolate Ba71V as a template. It expresses the structural protein p54 fused to the green fluorescent protein (GFP) in the thymidine kinase locus (K196R).

The Ba71V-12GFP **(B12GFP)** virus was generated using the viral isolate Ba71V as a template. It expresses p12 protein fused to the green fluorescent protein (GFP) in the thymidine kinase locus (K196R).

The Ba71V-54ChFP **(B54ChFP)** virus was generated using the viral isolate Ba71V as a template. It expresses the structural protein p54 fused to red cherry protein (Ch) in the thymidine kinase locus (K196R).

All these recombinant viruses show a viral factory distribution in confocal microscopy, with a predominant accumulation of the structural protein p54 or p12 respectively

2.2 Isolation procedures and viral purification

Preparation of viral stocks, titrations, and infection experiments were performed as previously described (Enjuanes et al., 1976a).

Confluent Vero cell monolayers were infected with ASFV (moi = 0.1 pfu/cell) and incubated at 37°C, 5% CO_2 until cytopathic effect was observed (usually 4-5 days postinfection). Afterwards, cells were harvested and disrupted by sonication on ice at 50% power, 3 times during 30 seconds to free the intracellular virus. Cells were then centrifuged at low speed for 10 min at 4°C and pellet was discarded. Finally, supernatants were centrifuged at 27,000xg for 4 h at 4°C. The obtained pellet containing the virus was resuspended in 5 ml of DMEM with 5% FBS and 125nM of HEPES and stored at -80°C until use.

When a higher quality of the viral stock was required, the ASFV was centrifuged through a sucrose gradient of 40% in PBS at 40,000xg during 20 min at 4°C.

The final step was the viral stock titration, using serial dilutions of the original inoculum following standard plaque assay methods.

2.3 Infections with ASFV

Viral infections were done in Vero and in COS-7 cells. Cells were seeded at the desired density the day before and then infected at different moi depending on the experiment requirements. The viral inoculum was added to the minimal medium volume containing DMEM with 2% FBS, Glutamax (Life Technologies). Viral inoculum was incubated on the cells for 90 min at 37°C. After the incubation, supernatant was removed and new fresh medium (DMEM with 5% FBS) was added. When viral synchronization was required, the adsorption phase took place at 4°C to allow viral attachment to the cell surface but arresting its internalization.

The moi used was different depending on the experiment requirements and it is detailed for each experiment condition.

Experiments in which cells were treated with inhibitors and also viral infected, the cells were pre-treated with the indicated concentration 1 or 2 h prior to infection. Uninfected and infected cells in the absence of drug were used as controls. When synchronization was required for the experiment, virus adsorption was performed for 90 min 4°C to prevent viral internalization. The inhibitor was present throughout the experiment or it was added at different postinfection times. After absorption, cells were washed with fresh medium to discard the unbound virus.

2.4 ASFV titration assays

Viruses were tittered following standard plaque assays in agarose over monolayers of Vero cells (90% confluence). Cells were infected with serial dilutions and viral absorption lasted 90 min in 2% FBS at 37°C.

The viral inoculum was then removed and a 1:1 mix of complete 2X EMEM with 2% low melting agarose was added. After 10-15 days, the plaques produced by ASFV were fixed with 4% paraformaldehyde (PFA), stained with a 1% crystal violet (m/v) solution and then counted to get the corresponding titer.

2.5 Transfections

Vero, COS-7 and WSL cells were transfected with Fugene HD (Roche) following manufacturer´s instructions. Briefly, a total amount of 1 μg/10^6 cells was used with a volume ratio of 3:1 (Fugene: DNA). The transfection mixture was added to a monolayer of cells (80% confluent). 6 h later, the medium was replaced with FBS-containing fresh medium.

293T cells were transfected with Lipofectamine 2000 to generate lentiviral particles that were subsequently used to generate stable-expressing VERO and COS-7 cell lines.

Transfected cells were incubated for 24 h and then cells were washed twice with PBS and fixed with PFA 4% to perform immunofluorescence assays.

3. DNA isolation, quantification and PCR

3.1 Bacterial Strains

The following *Escherichia coli* bacterial strains were used in the present work:

BNN132 (ATCC 47059): This strain expresses Cre-recombinase and allows derivates generation by recombination with vectors based on the bacteriophage λ that contain *lox* sites (Elledge et al., 1991).

DH5α (ATCC 700790): It is commonly used to obtain the different vectors employed (Hanahan, 1983).

BL21 (DE3) pLysS: It constitutively expresses the bacteriophage T7 RNA polymerase under an IPTG inducible promoter. It contains the pLysS plasmid that increases the strain tolerance to vectors that may carry genes which products can be toxic. Furthermore, this strains promotes cellular lysis to purify proteins more easily (Studier, 1991).

All these strains were cultured in lysogenic broth (LB; Sigma-Aldrich) at 37°C with constant agitation until the desired optical density (OD) was reached at a length wave of 600. Strains were conserved in LB medium containing 15% glycerol and stored at -80°C.

3.2 DNA isolation

Isolation of plasmid DNA from transformed DH5α bacteria with the corresponding vector cultures was performed using the commercial kit "Speedtools plasmid DNA purification kit" (Biotools), "Plasmid Midi Kit" (Qiagen), "Plasmid Maxi Kit" or "Plasmid Mega Kit" (Qiagen) depending on the quantity of DNA desired.

Plasmid concentration was quantified with NanoDrop ND-1000 UV-Vis spectrophotometer (Fisher Thermo Scientific), which enables highly accurate DNA quantification analysis using sample volumes as small as 1 µl, measuring absorbance values at 260 and 280 nm.

DNA digestions were done with specific restriction enzymes (Roche, Takara) and ligation reactions were performed with T4 ligase (Roche) following conventional procedures and manufacturer´s instructions.

For DNA electrophoresis, agarose gels were used (Sigma-Aldrich) with concentrations between 0.8% and 1.2% (w/v) and TBE buffer was employed.

To purify DNA fragments either from PCR or agarose bands, the commercial kit "QIAquick Gel Extraction Kit" (Qiagen) was used.

The different genes or fragments of interest were amplified by PCR ("Polymerase Chain Reaction") following conventional methodology. The different primers used are described in Table X. Primers were mixed with the DNA template, deoxynucleotide triphosphates (dNTPs; Roche) and the high fidelity Taq polymerase (Roche) to perform the PCR reaction.

3.3 Detection and quantification of the ASFV genome by quantitative real-time PCR

The quantitation of the number of copies of ASFV genome was achieved by quantitative real-time PCR (qRTPCR) using specific oligonucleotides and Premix Ex Taq PCR Master Mix probe (Takara). The qPCR assay used fluorescent hybridization probes to amplify a region of the p72 viral gene, as described previously (King et al., 2003). .

DNA from mock-infected or infected cells with ASFV BA71V at moi of 1 pfu/cell (or 10 pfu/cell for viral entry assays) was extracted at 16 hpi and purified using the DNAeasy blood and tissue kit (Qiagen). DNA concentration was measured using a Nanodrop spectrophotometer. The amplification mixture was prepared on ice as follows: 300 ng of the DNA template was added to a final reaction mixture of 20 ul containing 50 pmol sense primers, 50 pmol anti-sense primer, 5 pmol of probe and 10ul of TaqMan Fast Universal Master Mix (2x) (Life Technologies).

Positive amplification controls were DNA purified from ASFV purified virions at different concentrations as standards. Negative amplification controls consisted in DNA from mock-infected cells. Each sample was included in triplicates and values were normalized to standard positive controls.

Reactions were performed using the ABI 7500 Fast Real-Time PCR System (Applied Biosystems) with the following parameters: 94ºC for 10min and 45 cycles of 94ºC for 10s and 58ºC for 60s.

4. Chemical Reagents

4.1 Inhibitors

Bafilomycin A1 (Baf): A specific inhibitor of vacuolar type H+-ATPase (V-ATPase) in animal cells, plant cells and microorganisms.

Hanks Balanced Salt Solution (HBBS): Serum-free medium commonly used to induce starvation in cells.

LY294200: Specific inhibitor of PI3K that abolishes AKT phosphorylation on both sites (Thr-308 and Ser-473).

PP242: A recently discovered PI3K inhibitor that fully blocks and binds to the catalytic site of mTORC1.

Rapamycin (*sirolimus*): It is a macrocyclic antibiotic produced by *Streptomyces hygroscopicus*. It specifically blocks the mTORC1 signaling through binding to a specific domain separated from the catalytic site, acting as an allosteric inhibitor (Petroulakis et al., 2006). However, it does not completely inhibit mTORC1 activity (Jacinto et al., 2004).

Tyrphostin AG1478: It is used as a selective inhibitor of epidermal growth factor receptor (EGFR) protein.

Tubacin: A selective inhibitor of histone deacetylase 6 (HDAC6). It is a predominantly cytoplasmic class II histone deacetylase that associates with dynein to facilitate transport of aggresomes through the cytosol to the proteasome for degradation. It selectively inhibits HDAC6-mediated α-tubulin deacetylation (Hubbert et al., 2002; Matsuyama et al., 2002; Zhang et al., 2003).

3-Methyladenine (3MA): It is used to inhibit and study the mechanism of autophagy and apoptosis under various conditions. It inhibits type III PI3K and blocks autophagy by preventing the autophagosome formation.

4.2 Antibiotics

Ampicillin (Roche).

Kanamycin (Roche).

Puromycin (Life technologies).

Penicillyn/Streptomycin (Life technologies).

4.3 Colorants

Crystal violet (Sigma-Aldrich): It is used for plaque assay staining.

Red Ponceau (Sigma-Aldrich): It stains in proteins that are placed in a nitrocellulose membrane in a reversible way.

4.4 Electrophoresis

40% Acrylamide: Bisacrylamide (Biorad).

Conventional Agarose (Conda).

Low melting agarose (Life technologies).

Protein gel markers: Precision Plus Protein WesternC (BioRad) that was revealed with **Precision Protein StrepTactin-HRP Conjugate** (BioRad).

TEMED: N,N,N´,N´-tetramethilethilendiamine (Sigma-Aldrich).

β-mercaptoethanol (Sigma-Aldrich).

Ammonium Persulfate (BioRad).

Laemmli Buffer (BioRad).

4.5 Other Reagents

Lysotracker Red DND-99 (Molecular probes): Fluorescent reagent to stain acid organelles.

Mitotracker CMXRos: Red-fluorescent dye that stains mitochondria in live cells and its accumulation is dependent upon membrane potential.

Puromycin: Aminonucleoside antibiotic produced by the bacterium *Streptomyces alboniger*. It is normally used at a concentrations ranging from 1 to 10 μg/ml. In the present work, puromycin has been used to select for stable Vero cells containing the pLVX vector at a concentration of 8 μg/ml.

Polybrene: Transfection reagent that enables gene transfer into mammalian cells when they become infected with retroviral vectors. The efficiency of retroviral infection is enhanced significantly, between 100- and 1,000-fold, depending on the cell type in the presence polybrene during the infection.

Filipin: Mixture of chemical compounds that were originally isolated from the mycelium of the actinomycete *Streptomyces filipinensis*. It is highly fluorescent and binds specifically to cholesterol, hence it is used as a histochemical stain for cholesterol. This method of detecting cholesterol in cell membranes is used clinically in the study and in the diagnosis of Type C Niemann-Pick disease.

Human epidermal growth factor (hEGF): It is a 53-amino acid (aa) protein that stimulates cell growth, proliferation and differentiation. In the present work, it is used as a PI3K pathway inducer through the binding to EGFR.

5. Antibodies and chromogens

Primary Antibodies	Origin	Usage	Dilution	Manufacturer
α-acetylated tubulin	Mouse	IF	1:1000	Sigma-Aldrich
α-Vimentin-Cy3	Mouse	IF	1:200	Sigma-Aldrich
AKT	Rabbit	WB	1:1000	Cell Signaling
BAG3	Rabbit	IF	1:50	Proteintech
		WB	1:500	
CD63 (H5C6)	Mouse	IF	1:200	Developmental studies H.B.
EEA1 (EEA1/14)	Mouse	IF	1:50	BD biosciences
Flag	Mouse	IF	1:100	Sigma-Aldrich
HA	Mouse	WB	1:100	Sigma-Aldrich
HDAC6	Rabbit	IF	1:100	Santa Cruz Biotechnology
IFITM1	Rabbit	IF	1:200	Proteintech
		WB	1:2000	
IFITM2	Rabbit	IF	1:200	Proteintech
		WB	1:2000	

IFITM3	Rabbit	IF	1:200	Proteintech
Lamp1	Rabbit	IF	1:50	Abcam
		WB	1:2000	
LC3	Rabbit	IF	1:100	Sigma-Aldrich
		WB	1:1000	
AKT (Total)	Rabbit	WB	1:1000	Cell Signalling
P-AKT (Ser473)	Rabbit	WB	1:1000	Cell Signaling
P-AKT (Thr308)	Rabbit	WB	1:1000	Cell Signaling
p30	Mouse	Flow Cytometry	1:50	Dr. Escribano (INIA,Madrid)
		IF	1:100	
		WB	1:500	
p72 (1BC11)	Mouse	IF	1:1000	Ingenasa
p72 (18BG3)	Mouse	WB	1:2000	Ingenasa
p150 (17AH2)	Rabbit	IF	1:1	Ingenasa
Rab7 (D95F2)	Rabbit	IF	1:200	Cell Signaling
Tubulin	Mouse	WB	1:2000	Sigma-Aldrich

Secondary Antibodies	Origin	Usage	Dilution	Manufacturer
Alexa Fluor™ 488	Mouse	IF	1:300	Molecular Probes

Alexa Fluor™ 594	Mouse	IF	1:200	Molecular Probes
Alexa Fluor™ 488	Rabbit	IF	1:200	Molecular Probes
Alexa Fluor™ 594	Rabbit	IF	1:500	Molecular Probes
IgG-HRP	Rabbit	IF	1:2000	Amersham
IgG-HRP	Mouse	WB	1:5000	Amersham
PE	Mouse	WB	1:50	Dako

Chromogens	Usage	Dilution	Manufacturer
Mitotracker CMXRos	IF	75 nM	Life technologies
Alexa Fluor™ 594 - Phalloidin	IF	1:200	Life technologies
Topro-3	IF	1:1000	Life technologies

6. Western Blot (WB)

Cells were washed in PBS and collected at different time points in Laemmli buffer (BioRad) or RIPA buffer if phosphorylated proteins were being detected.

Cell lysates were obtained by sonication and boiled at 100°C for 5 min. Proteins were separated by polyacrylamide gel electrophoresis (10%) in their native state (SDS-PAGE).

Once the proteins were separated, they were transferred to a 0.45-µm nitrocellulose membrane (BioRad) at 100V during 90 min and blocked with PBS supplemented with 0.05%

Tween-20 (Sigma-Aldrich) and 5% non-fat milk. If phosphorylated proteins were going to be detected, membranes were blocked with PBS-Tween 5% BSA. For protein detection, a modified version of Bakkali's protocol was used (Bakkali et al., 1994). Antibodies were used following manufacturer´s instructions. Secondary antibodies, conjugated with horseradish peroxidase (GE Healthcare), were diluted 1:2,000. The protein marker **Precision Plus Protein WesternC** (BioRad) and the **Precision Protein StrepTactin-HRP Conjugate** (Biorad) were used for developing. To expose the proteins, an ECL detection kit (Amersham) was employed following manufacturer´s instructions. The protein expression was analyzed in the molecular imager **Chemidoc XRSplus Imaging System**. Bands were quantified by densitometry and data were normalized using the **Image Lab** software (BioRad).

7. Immunofluorescence Assay (IF)

Cells were seeded at a variable density over 13mm coverslips. Infected, transfected or mock-infected cells were fixed using either 4% of formaldehyde or paraformaldehyde for 15 min. Then, cells were permeabilized with 0.1% Triton X-100 in PBS during 10 min and blocked with 2% bovine serum albumin (BSA) in PBS for 1 hour at room temperature (RT) to avoid unspecific unions.

Cells were incubated with the according primary antibody dilution either 1 hour at 37°C inside a wet chamber or overnight at 4°C.

Secondary antibodies were normally incubated for 45 min at RT. To stain DNA, the reagent Topro-3 (Life technologies) was used at a 1:1,000 dilution in PBS during 5 min.

Finally, coverslips were mounted with Prolong Antifade Reagent (Life technologies).

Cells were always washed twice between each step.

8. Microscopy

8.1 Conventional fluorescent microscopy

A photomicroscope coupled to a Leica camera equipped with the appropriate filters was employed to detect the different fluorophores and chromogens described in this work.

8.2 Confocal microscopy

A Leica TCS SPE microscope was used with a 63X oil immersion objective. The image acquisition was performed with **Leica Application Suite Advanced Fluorescence** software (LAS AF).

All the images were taken with a 512 x 512 pixel resolution but when higher zoom was required, the resolution was switched to 1024 x 1024 pixels. Images were processed with either Adobe Photoshop CS6 (Adobe Systems Inc.) or Image J.

9. Flow Cytometry

Cells were seeded either in MW12 or MW24 plates (depending on the experiment), they were trypsinized and washed with PBS and FACS buffer (containing PBS, 0.01% sodium azide and 0.1% BSA). Cells were then analyzed by flow cytometry either without fixation (in the case of using a recombinant GFP virus) or fixed and permeabilized with Perm2 (BD science) for 10 min at RT. In order to detect fixed-infected cells, they were incubated with monoclonal p30 monoclonal diluted 1:50 in FACS buffer for 30 min at 4°C. The secondary antibody used was phycoerythrin (PE) conjugated (DAKO) 1:50 diluted in FACS buffer for 30 min at 4°C. After repeated washes, 10,000 cells/tube were analyzed in the FACSCalibur flow cytometer (BD Science) and always in duplicate or triplicates.

The obtained infection rates were always normalized to the corresponding control.

10. Cytotoxicity analysis

Cellular viability in the presence of the different reagents used were determined with the commercially available **Cell Titer 96 aqueous Non-Radioactive Cell Proliferation Assay** kit (Promega) following manufacturer´s protocol. The concentrations used in all cases did not exert 20% of cell toxicity. All reagents were prepared either in DMSO or MilliQ H_2O in order to generate the stock solution. Subsequently, they were finally diluted in DMEM with 2% FBS to the working concentration in order to perform the experiment.

11. Alveolar Macrophage Library Screening

11.1 λ-ACT2 Library

λ-ACT2 Library ($3.6x10^6$) clones was a kindly gift from Dr. Dixon (Pirtbright, United Kingdom). The library represents a collection of coding DNA sequences from swine alveolar

macrophages: the main host cells of ASFV. These DNA sequences are fused to the transcription factor GAL4 activation domain (AD) and then cloned into the bacteriophage λ (Miskin et al., 1998).

11.2 Conversion of the λ-ACT2 Library into its plasmidic form

Converting the library into its plasmid form (pACT2), in order to use it for the yeast two-hybrid assay, was performed following the instructions compiled in the **Matchmaker Library User Manual** (Clontech**).** Briefly, it consists on a subcloning technique that occurs between *lox* sites by specific recombination. This specific recombination is induced by a temperature alteration during the fague λ infection in the bacterial strain BNN132. To ensure that the new library obtained is well represented, the total number of plasmidic clones was quantified and its number was analyzed to be at least 2 or 3 times the number of clones of the original library.

11.3 Yeast Two-hybrid assay

The yeast-two-hybrid (YTH) assay is a sensitive *in vivo* method used to identify genes encoding proteins that interact with a protein of interest, and it is well suited for detecting transient or even weak interactions (Guarente, 1993). In fact, many specific previously unknown protein-protein interactions were discovered by screening mammalian and yeast fusion libraries (Bulimo et al., 2000; Hernaez et al., 2008).

The screening procedure is based on growth selection and it consists on reconstituting a functional GAL4 transcriptional activator and consequent activation of a nutritional reporter gene (HIS3) under the control of a GAL4-responsive promoter (Chien et al., 1991).

In the present work, the ASFV gene I215L has been cloned into a DNA-BD vector (pGBT9) such that a fusion between the target protein and the GAL4 DNA-BD is generated. The alveolar macrophage library was constructed in an AD vector (pACT2) to generate fusions between proteins encoded by the library cDNAs and the GAL4 AD as described before. The two types of hybrid plasmids were sequentially co-transformed into *Saccharomyces cerevisiae* Y190 reporter yeast host strain with the lithium acetate (LiAc) procedure (Gietz et al., 1992).

Firstly, Y190 yeast were transformed with 50ng of pGBT9 plasmid containing the bait gene sequence and were selected in SC-agar medium (Gibco) without tryptofan (-Trp).

Selected yeasts were then transformed again with 200ng pACT2 library and harvested in 200x200 mm plates (Nunc). Co-transformants were plated on synthetic defined broth (SD)/-His/-Leu/-Trp to select the colonies expressing the interacting proteins and also contained 33 mM of 3AT (3-Amino-1,2,4-triazole) (Sigma-Aldrich). Y190 yeast is very leaky for HIS3 expression and grows normally on SD/-His in the absence of 3AT so it is required in the medium to suppress background growth of Y190. If the target protein finally interacts with a library-encoded protein, a functional GAL4 activator is reconstituted and the expression of the *HIS3* reporter gene is activated.

Furthermore, to confirm the protein interaction, primary His^+ transformants were tested for expression of the second reporter gene lacZ using a β-galactosidase assay over Hybond-C-super membranes (Amersham). All positives transformants were then tested and segregated three times to eliminate false positives. The coding sequence in fusion to the AD (pACT2) contained in the clones that were considered as positives was amplified with specific primers (pACT2FWD and pACT2 REV), sequenced and matched in the NCBI database.

The same methodology was used to delimit the regions or domains that were important for protein-protein interactions but in this case it consisted on a one to one yeast two-hybrid assay where the different fragments were cloned in fusion to AD or BD into either pGBT9 or pACT2 vectors respectively.

12. Pull-Down Assays

GST and GST-DP71L were expressed in *E. coli* BL21 (DE3) cells, previously transformed with pGEX- 4T3 plasmid and induced with 0.1 M IPTG for 2 h at 37°C. However, GST-A179L was obtained using a recombinant Vaccinia virus expressing GST fused to the N-terminus of the *A179L* protein (Galindo et al., 2008). To express and purify Beclin 1, the baculovirus system was chosen because of its efficiency to produce His-tagged Beclin 1. GST, GST-DP71L and GST-A179L were purified from cleared lysates by mixing with glutathione-Sepharose 4B beads (GE HealthCare). After extensive washing, GST, GST- DP71L and GST-A179L beads were incubated in binding buffer (50 mM HEPES, pH 7.5, 50 mM NaCl, 0.1% Nonidet P-40) with protease inhibitor mixture (Roche Molecular Biochemical) at 4°C for 1 hour with infected insect cell extracts containing overexpressed His-tagged Beclin 1. Beads were then

washed four times with 10 volumes of binding buffer, subjected to SDS-PAGE and analyzed by immunoblot assay with the anti-Beclin 1 antibody and the corresponding secondary antibody.

13. Statistical Analysis

The experimental data were analyzed by one-way ANOVA by GraphPad Prism 5 software. For multiple comparisons, Bonferroni´s correction was applied. Values were expressed in graph bars as mean ± SD of at least three independent experiments unless otherwise noted. The *P* value < 0.05 was considered statistically significant.

RESULTS

1. Construction and characterization of an LC3 stable cell line

In this study, a Vero cell line stably expressing the LC3 protein (hereinafter referred to as Vero-LC3) was generated as a reliable cell platform to assess the dynamic process of autophagy. We found that preliminary experiments transfecting pEGFP-LC3 with liposomes had two shortcomings: unstable efficiency of transfection, leading to a reduction in the number of cells effectively expressing pEGFP-LC3; and degradation of the recombinant plasmid, resulting in a reduction in GFP-LC3 autophagy puncta. Therefore, we decided to create a Vero cell line that stably expressed LC3 by using the pLVX-puro system. Once screened, this cell line could express the LC3 protein at high levels for more than 30 cell passages and as it is explained below, it turned into a useful tool to study autophagosome formation.

1.1 Successful construction of pLVX-LC3 vector

The 426-bp long cDNA sequence of the *Rattus norvegicus* LC3 protein was obtained by PCR amplification using the pEGFP-LC3 plasmid (kindly given by T. Yoshimori) as a template with specific primers containing BglII and EcoRI restriction sites. It was then subcloned into the lentiviral pLVX vector.

To determine whether the pLVX-LC3 vector was successfully constructed, the recombinant plasmids were digested by restriction enzymes and analyzed by agarose gel electrophoresis. We identified bands of the target gene with the correct size (not shown) and sequencing results confirmed a positive match of the recombinant gene.

1.2 Generation of Vero LC3 stable cell line

1.2.1 Lentiviral particles production and Vero cells transduction

A 293T confluent monolayer was co-transfected with pLVX-LC3, gag-pol and VSVg plasmids to generate lentiviral particles (as described in Material and methods section). Supernatants containing the aforementioned particles were collected at 48h and 72h post-transfection and they were subsequently used to transduce our cells of interest (**Figure R1**). Cells stably expressing LC3 were positively selected by treating the whole population with puromycin. We used a high dose of puromycin (8 μg/ml) to select the population of cells that were expressing stable levels of LC3, thus removing the non-transduced cells.

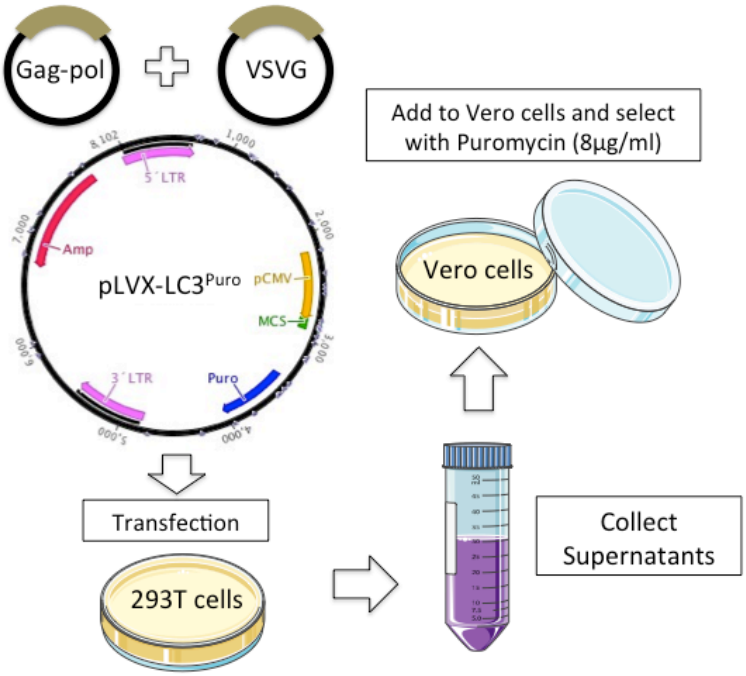

Figure R1. Establishment of Vero-LC3 cells protein. 293T cells were transfected with Gag-pol, VSVG and pLVX-LC3 vectors. 48 hours post-transfection, supernatants were collected and used to transduce target Vero cells. 24 h later, cells expressing the vector were selected with 8 µg/ml of puromycin.

1.3 LC3 expression in Vero-LC3 cells

Expression and cellular distribution of LC3 were analyzed using an immunofluorescence (IF) assay. Protein expression of LC3 was increased in LC3-Vero cells compared to the control cells (expressing the empty vector). The expression was mainly cytoplasmic (**Figure R2A**). Furthermore, as it is explained below, the LC3 protein, which exists homogeneously distributed in the nucleus and in the cytoplasm, becomes aggregated to form bright autophagy puncta after induction of starvation. Increased protein expression of LC3 was confirmed by WB analysis. Two different commercial antibodies were tested using different lysis buffers (RIPA or Laemmli, respectively) to determine the optimal conditions for LC3 detection. We found no significant differences between both RIPA and Laemmli buffers. However, the LC3 antibody from Sigma was more efficient than the one available from Novus Biologicals (**Figure R2B and R2C**).

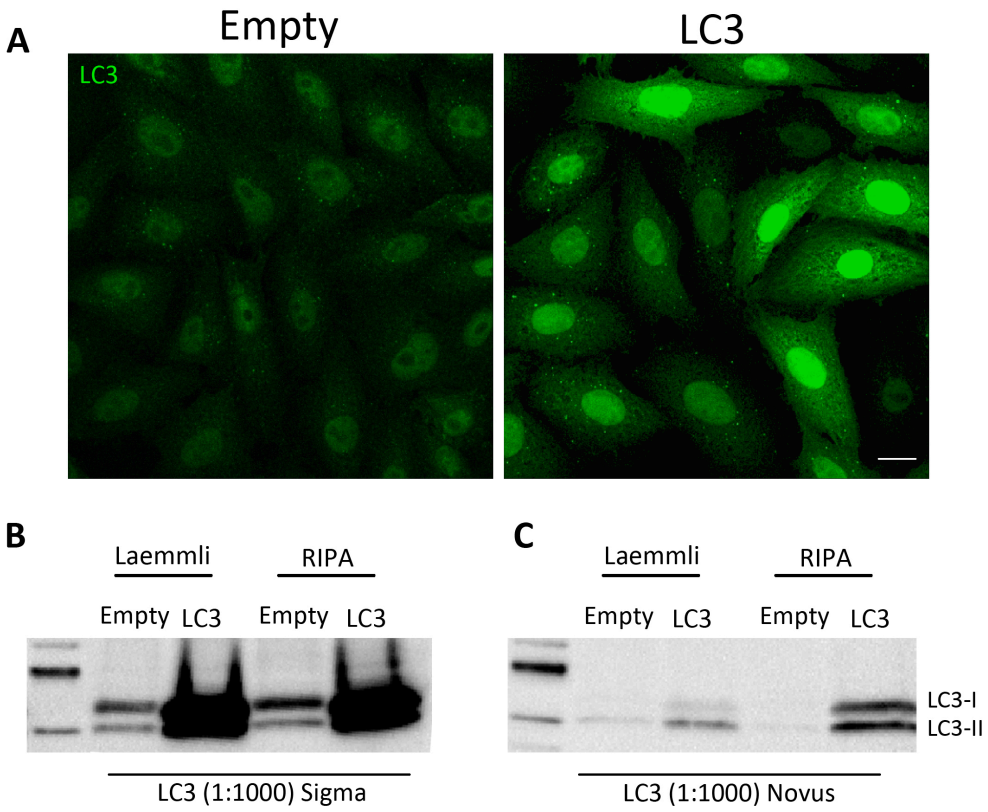

Figure R2. LC3 expression in Vero LC3-stable cell line. (A) Representative confocal images of Vero cells stably expressing either empty vector (left panel) or LC3 protein (right panel). **(B, C)** Analysis of LC3 protein expression in Vero cells stably expressing empty vector or LC3 protein. Protein extracts were collected either with Laemmli or with RIPA buffer and tested with different LC3 antibodies. Bar=10 µm.

1.4 Vero-LC3 cells are susceptible to ASFV infection

We sought to study the effects of ASFV infection in the context of LC3 overexpression. LC3-expressing Vero cells were infected with B54GFP viral stock (moi=5 pfu/cell). The number of infected cells was quantified by monitoring cells that are expressing viral protein p54GFP at 16 hours postinfection (hpi) using flow cytometry analysis. **Figure R3** shows the percentage of infected cells in LC3-expressing stable cells compared and relativized to control cells expressing the empty vector. Each experiment was performed in triplicates for each condition in living cells. We found that overexpression of LC3 did not confer protection of Vero cells to ASFV infection. Statistical analysis revealed no significant differences in the level of infection between both cell lines.

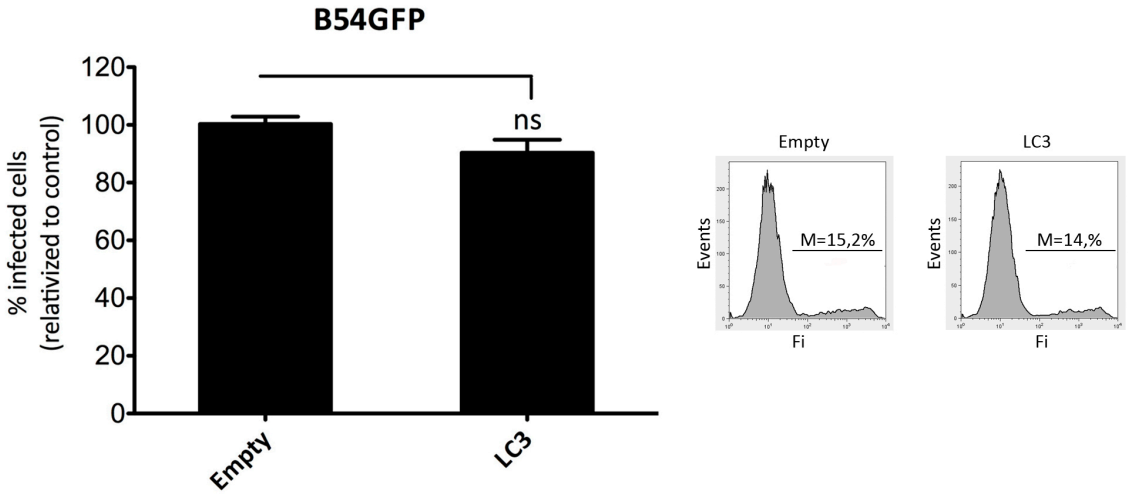

Figure R3. Vero-LC3 cells are susceptible to ASFV infection. Levels of ASFV infection were analyzed in Vero-LC3 cells and relativized to control cells expressing the empty vector (16 hpi) by flow cytometry. Cells were infected with recombinant viral stock B54GFP (moi=5pfu/cell). Experiments were performed in triplicates. Statistical analysis revealed non-significant (ns) differences between Vero-LC3 and control cells.

1.5 Vero-LC3 cells are susceptible to autophagy inducers

The fact that LC3 is stably expressed does not result in constitutively induced autophagy. To verify this, we decided to measure autophagy rates in these cells upon autophagy inducers.

Vero-LC3 cells were incubated with rapamycin (1µM), Hanks balanced salt solution (HBSS) supplemented with rapamycin (1µM), PP242 (0,5µM) or tamoxifen (10µM) (starved), supplemented with autophagy inhibitor 3MA (5mM) or incubated in complete DMEM with 5% FBS or DMSO (controls) for 2 hours (h). After this time period, cells were collected in Laemmli buffer and a WB was performed (**Figure R4B**). Upon starvation, cellular response to autophagy induction was determined by measuring the LC3-II/LC3-I ratio (**Figure R4A**). This ratio was significantly increased in the presence of the different autophagy inducers, when compared to those incubated in complete DMEM with 5% FBS medium (control) or in the presence of the autophagy inhibitor 3MA. However, rapamycin treatment alone did not significantly increase autophagy rate.

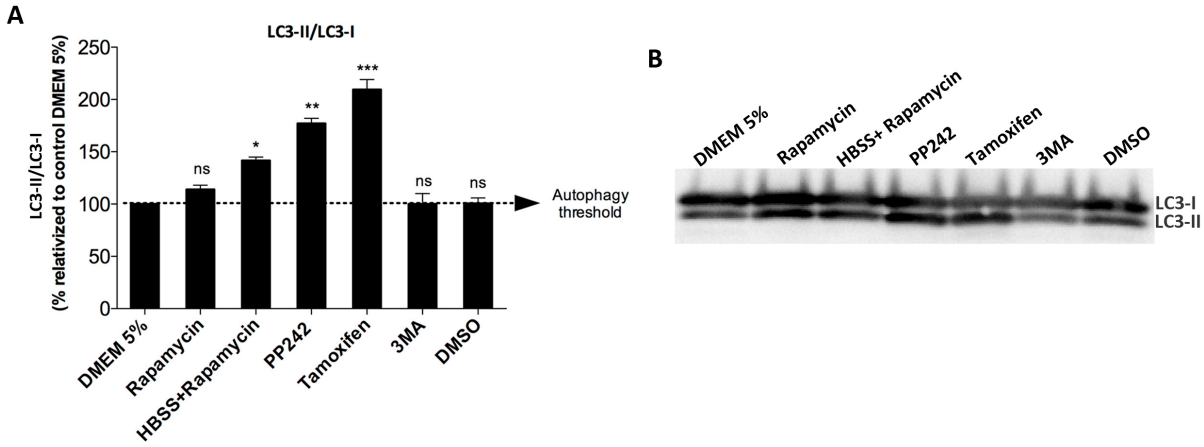

Figure R4. Vero-LC3 cells are susceptible to autophagy inducers. (A) LC3-II/LC3-I protein ratio was measured in Vero-LC3 cells upon treatment with autophagy inducers rapamycin (1µM), HBSS supplemented with rapamycin (1µM), PP242 (0,5uM) or tamoxifen (10µm) or autophagy inhibitor 3MA (5mM) by WB. Dotted line represents the autophagy activation threshold. Data are expressed as the mean and the standard deviation (SD) of three independent experiments. Asterisks denote statistically significant differences (*=P<0.05; **=P<0.01; ***=P<0.001; ns=no significant. **(B)** WB analysis depicting levels of LC3-I and LC3-II proteins. Bands were quantified, normalized to the control treatment and graphically represented in (A).

These results demonstrate that Vero-LC3 cells are sensitive to the different autophagy stimuli.

2. Effect of autophagy inducers and inhibitors in ASFV infection

We also wanted to test the effect of the different autophagy inducers and inhibitors in ASFV infection. To this end, we performed flow cytometry analysis to detect early viral protein p30 at 6 hpi in fixed cells or p54 viral protein in live cells infected with recombinant B54GFP at 16 hpi.

Autophagy inducers rapamycin+HBSS, PP242 and tamoxifen reduced the number of cells expressing p30 and p54, thus inhibiting ASFV infection in a dose dependent manner at 6 hpi and 16 hpi respectively **(Figure R5A, B)**. A similar trend was shown upon treatment with autophagy inhibitor 3MA. In contrast, rapamycin alone did not affect ASFV infection at early postinfection times and only revealed a modestly decrease at late postinfection times. WB analysis of early viral protein p30 and late protein p72 confirmed the flow cytometry results (not shown).

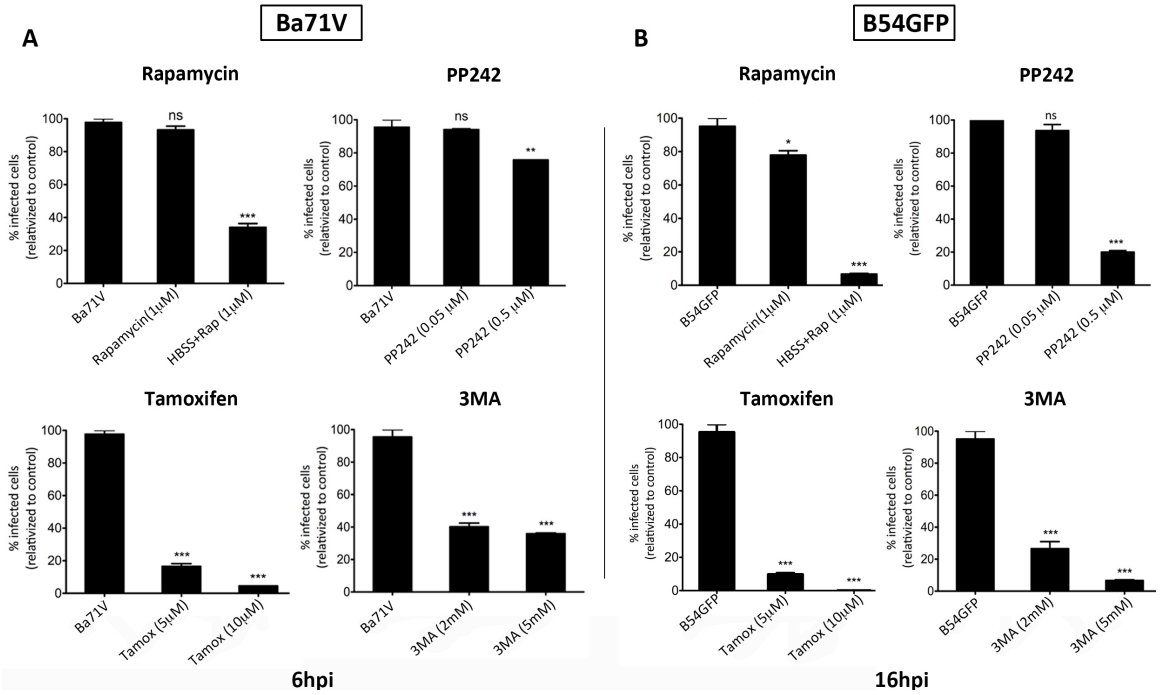

Figure R5. Effect of the different autophagy inductors or inhibitors on ASFV infection. Vero cells were infected either with ASFV or recombinant B54GFP and a flow cytometry analysis was performed at 6 hpi or 16 hpi, respectively. Vero cells were incubated with drugs 2 h prior to infection and treatment was continued until the end of the experiment. The number of infected cells were relativized to infected controls and expressed in percentages. Data are expressed as the mean and the standard deviation (SD). Asterisks denote statistically significant differences (*=P<0.05; **=P<0.01; ***=P<0.001; ns=no significant).

These results show that both autophagy inducers and inhibitors decrease ASFV infectivity.

3. Analysis of autophagy in the context of ASFV infection

Taking into consideration the aforementioned data in which ASFV infection was negatively regulated upon treatment with either autophagy inducers or inhibitors, we decided to

further characterize the role of autophagy in the context of ASFV infection, focusing on early and late postinfection times.

3.1 Analysis of autophagy at early postinfection times

3.1.1 ASFV induces rapid activation of AKT in Vero cells

It has been recently described that viruses can stimulate the PI3K/AKT/mTOR pathway to inhibit autophagy, thus benefiting virus infection (Surviladze et al., 2013). Our goal was to study this pathway upon ASFV infection.

AKT activation requires its translocation to the plasma membrane and dual phosphorylation of two distant segments of the polypeptide. AKT phosphorylation occurs in Thr-308 by PDPK1 and in Ser-473 by mTORC2 (Alessi et al., 2009; Sarbassov et al., 2005). We tested whether ASFV induced AKT activation upon infecting Vero cells. To this end, Vero cells at 70% of confluence were serum-starved for 3 h. Cells were infected with purified ASFV at high moi (10 pfu/cell) and viral entry was previously synchronized at 4°C during 90 min. Then, cells were incubated at 37°C to allow viral entry. Protein extracts were subsequently harvested at 5, 15, 30, 45 and 60 min postinfection (mpi) in RIPA buffer.

WB analysis was performed to detect rapid phosphorylation of AKT in both Thr-308 and Ser-473 residues upon infection **(Figure R6).** Although mock-infected controls had basal AKT phosphorylation in both sites **(lane 1)**, exposure to ASFV led to increased AKT phosphorylation, with levels reaching those achieved by EGF stimulation at 60 mpi **(lanes 2 and 9, respectively)**. The EGFR-specific inhibitor AG1478 (10μM), used as a negative control, markedly reduced the AKT phosphorylation levels, indicating that Thr-308 and, to a lesser extent, Ser-473 phosphorylation were a consequence of EGFR pathway activation **(lane 3)**. Also, specific inhibitor of PI3K, LY294002 (50μM) abolished phosphorylation of both sites on AKT **(lane 4)**.

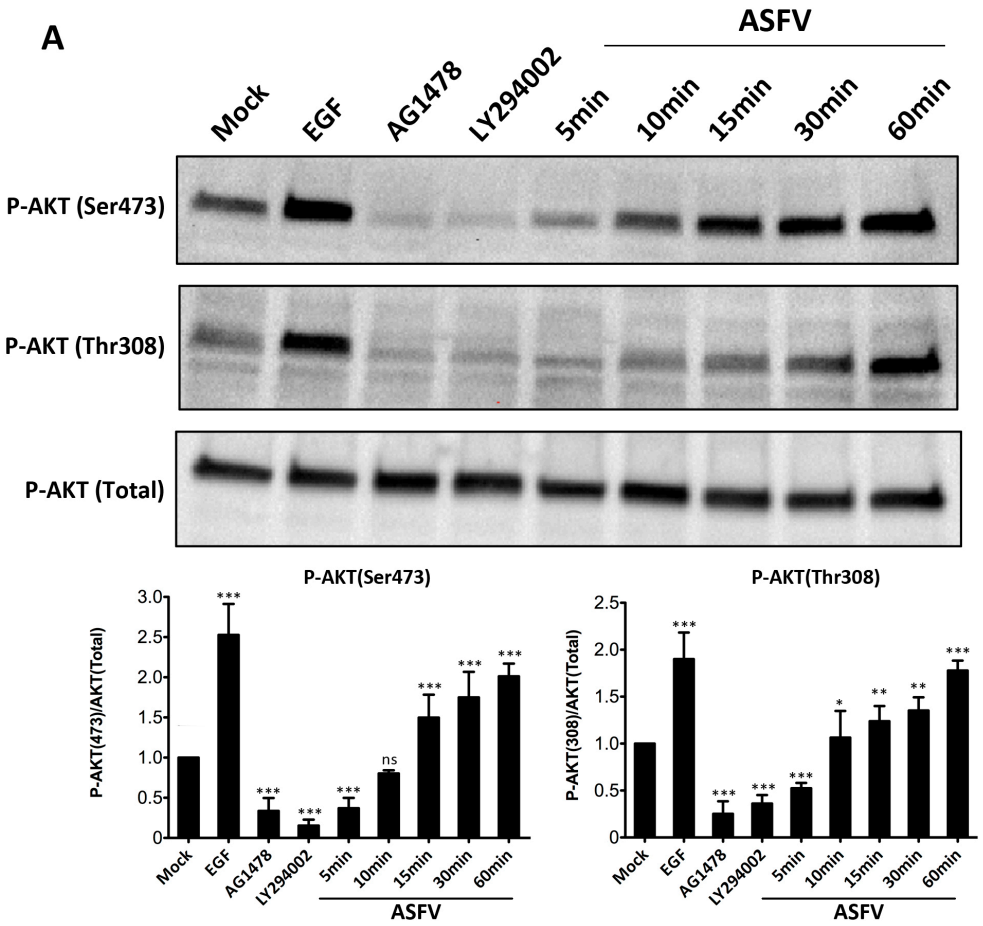

Figure R6. ASFV infection induces AKT phosphorylation in Vero cells. Level of AKT-P in in both Thr-308 and Ser-473 residues was analyzed at different early post infection times and relativized to total AKT by WB . Cells were serum-starved prior to infection. Human EGF was used as a positive control while the EGFR-specific inhibitor AG1478 (10µM) and PI3K-specific inhibitor, LY294002 (50µM) were used as negative controls. Mean±standard deviation (SD) plotted in graphs are shown in lower panels. Asterisks denote statistically significant differences (***p<0.001; **p<0.01; *p<0.05).

These findings show that ASFV infection leads to a rapid AKT activation by phosphorylating residues Thr-308 and Ser-473, which might indicate an activation of EGFR. Also, ASFV might induce the PI3K/AKT signaling pathway in a rapid manner upon cell contact.

3.1.2 ASFV induces autophagy within the first 5 min after infection

As a result of AKT activation, downstream events of the PI3K/AKT pathway are initiated leading to a suppression of autophagy. Interestingly, AKT phosphorylation was suppressed at 5 min postinfection, since levels of P-AKT were lower in both residues in infected cells than in mock-infected controls. Thus, we next wanted to confirm whether this decreased

phosphorylation of AKT was coincident with an induction of autophagy that could be detectable by measuring the ratio between LC3-II/LC3-I **(Figure R7)**.

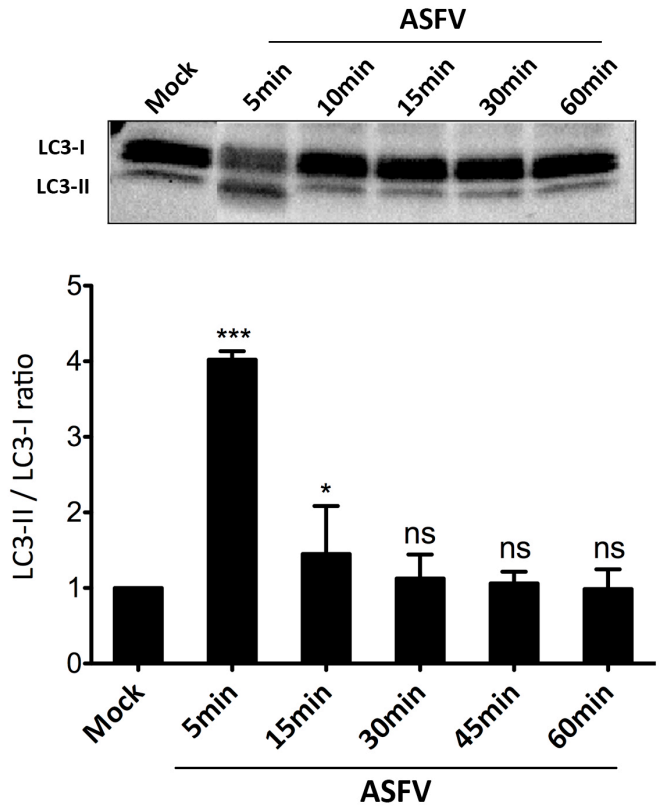

Figure R7. ASFV induces autophagy within the first 5 min after infection. Changes in LC3-II/LC3-I ratio were analyzed to measure the autophagy levels at different time points during the first hour post infection. Cells were serum-starved prior to infection. The lower panel represents the WB quantification for each condition expressed as mean±SD. Asterisks denote statistically significant differences (*=P<0.05; **=P<0.01; ***=P<0.001; ns=non significant).

Vero cells at 70% of confluency were serum-starved for 3 h and then were mock-infected or infected with purified ASFV (moi=10 pfu/cell). Viral entry was previously synchronized at 4°C during 90 min. Then, cells were incubated at 37°C to allow viral entry and they were subsequently harvested at 5, 15, 30, 45 and 60 min postinfection (mpi) in RIPA buffer. WB analysis was performed and the LC3-II/LC3-I ratio was analyzed to measure the autophagy levels for each condition. As shown in **Figure R7**, there was a strong autophagy induction at 5 mpi. This result is consistent with previous data in which AKT-P was severely decreased in both residues (Ser 473 and Thr308) at this time after infection, thus leading to an early activation of the autophagy pathway.

This finding suggests that ASFV quickly induces autophagy within the first 5 min after infection, followed by inhibition of autophagy at later postinfection times.

3.1.3 Effect of AG1478 and LY294002 in viral infection

We also tested the effect of PI3K inhibitor (LY294002) and EGFR specific inhibitor (AG1478) in ASFV infection by measuring viral protein p30 at 6 hpi **(Figure R8A)** and GFP signal by using recombinant B54GFP at 16 hpi **(Figure R8B)**. The number of infected cells was analyzed by flow cytometry analysis. Treatment with LY294002 reduced the number of infected cells not only at early (6 hpi) but also at late postinfection times (16 hpi) in a dose dependent manner. However, AG1478 did not significantly affect the percentage of infected cells at any of the time points tested.

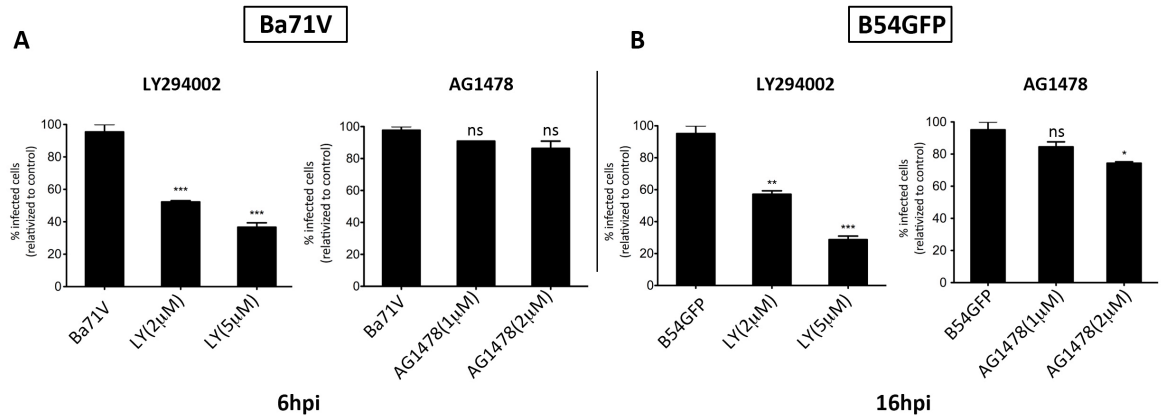

Figure R8. Effect of LY294002 and AG1478 in ASFV infection. Treatment with LY294002 reduced the number of infected cells at early (6 hpi) and late postinfection times (16 hpi) in a dose dependent manner. AG1478 did not significantly affect the percentage of infected cells at any of the time points tested. Vero cells were incubated with drugs 2 h prior to infection and treatment was continued until the end of the experiment. The number of infected cells were relativized to infected controls and expressed in percentages. Data are expressed as mean±SD and depicted in graphs. Asterisks denote statistically significant differences (*=P<0.05; **=P<0.01; ***=P<0.001; ns=non significant).

3.2 Analysis of autophagy at late postinfection times

3.2.1 ASFV infection does not promote autophagy

Lipidation of the microtubule-associate protein 1 light chain 3 (LC3) is a hallmark of autophagy induction. When autophagy is induced, the mainly cytoplasmic form LC3-I is conjugated to phosphatidylethanolamine, then targeted to autophagic membranes and finally transformed into the conjugated form of LC3, LC3-II. Lipidated LC3 is subsequently incorporated to double membranes during autophagosome elongation and maturation (Kabeya et al., 2004).

As the amount of LC3-II correlates with the number of autophagosomes, immunoblotting of endogenous LC3 can be a useful tool to measure autophagic activity (Kabeya et al., 2000). We monitored LC3-I conversion to LC3-II to examine the impact of ASFV infection on cell autophagy. LC3-Vero cells were mock infected or infected with ASFV at a range of different postinfection times (0, 16, 24 and 48 hpi). The LC3-II/LC3-I protein ratio was then measured. We observed that the LC3-II/LC3-I ratio was not increased throughout infection when compared to uninfected cells at the time points analyzed. **(Figure R9A)**. However, an increased LC3-II/LC3-I ratio was observed in all positive control samples in which cells had been treated with HBSS + rapamycin (1µM), PP242 (0,05 µM) or tamoxifen (10 µM). These findings indicate that autophagy was correctly induced in the context of LC3 overexpression.

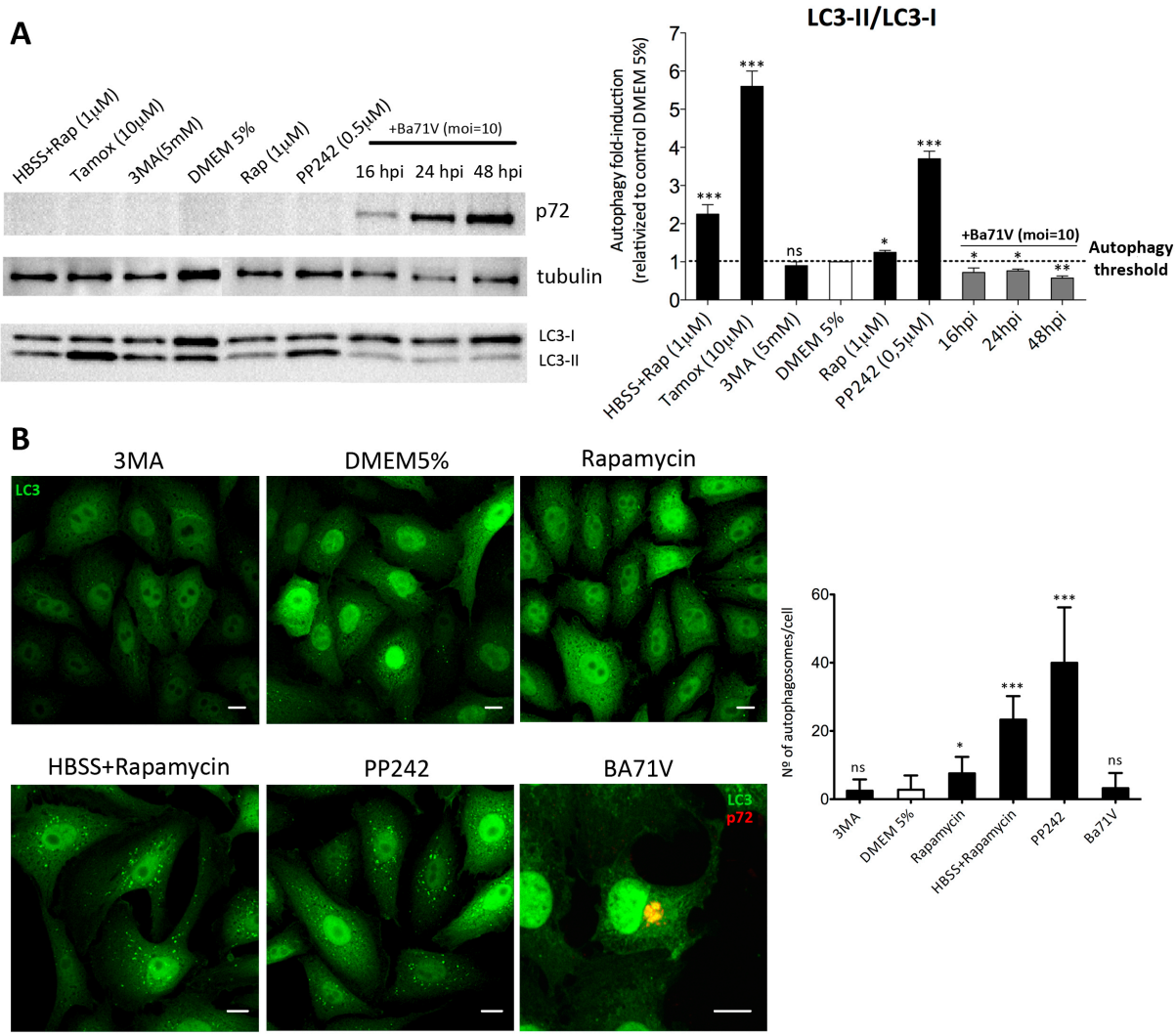

Figure R9. ASFV Infection inhibits autophagy at late post-infection times. (A) Analysis of endogenous LC3 protein expression to measure autophagic activity. LC3-Vero cells were mock infected or infected with ASFV at different time points. **(B)** Changes in the number of autophagosomes upon treatment with autophagy inducers

rapamycin (1μM), HBSS+rapamycin (1μM), PP242 (0,5μM) and tamoxifen (10μM) or autophagy inhibitor 3MA (5mM). These were compared to the number of autophagosomes upon ASFV infection at 16 hpi. The number of autophagosomes was not increased after ASFV infection and similar numbers were counted in uninfected cells or controls in complete DMEM with 5% FBS or with 3MA. The results are presented as the average number of puncta per cell. Asterisks denote statistically significant differences (*=P<0.05; **=P<0.01; ***=P<0.001; ns=non significant).

Interestingly, Vero cells were scarcely sensitive to autophagy induction upon rapamycin treatment alone, as the levels of LC3-II/LC3-I were quite similar to mock-infected cells or cells treated with autophagy inhibitor 3MA.

The redistribution of the autophagy marker LC3 from a diffuse cytoplasmic pattern to a punctate pattern, coincident with autophagosomes, is another hallmark of autophagy induction. To monitor the incorporation of LC3-II to the autophagosome membrane we used the Vero LC3 stable cell line.

Vero stable LC3 cells were infected with ASFV (>1 pfu/cell) for 16 h and then stained with an LC3 specific antibody. We observed a clear redistribution of LC3, from a diffuse to a bright green fluorescent punctate pattern only in cells that had been incubated with autophagy inducers HBSS+rapamycin (1μM), PP242 (0,05μM), or tamoxifen (10μM) but not in infected cells or cells treated with the autophagy inhibitor 3MA (5mM). LC3 puncta were also detectable but to a lesser extent upon rapamycin treatment.

Moreover, the average number of autophagosomes per cell was not increased after ASFV infection and similar numbers of autophagosomes were observed in uninfected cells or controls in complete DMEM with 5% FBS or with 3MA **(Figure R9B)**. Each single puncta was regarded as equal to one autophagosome. The results are presented as the average number of puncta per cell.

Collectively, these results indicate that ASFV did not promote autophagy, since there was no enhancement of autophagosome formation during infection.

3.2.2 LC3 is recruited into ASFV viral factory

Our experiments have shown absence of typical autophagosomes and any detectable increase of autophagosome-associated LC3-II form upon ASFV infection. However, we noticed that ASFV infection led to the formation of coarse LC3 puncta. It is important to mention that the morphology of these puncta is not exactly the same as the puncta formed

in response to amino acid deprivation **(Figure R10)**. These puncta likely reflect the massive accumulation of LC3 in form of aggregates. To verify this, Vero LC3 stable cells were ASFV-infected (moi=1 pfu/cell) for 16 h, followed by analysis of the localization of both viral protein p72 and LC3. As seen in **Figure R10**, there was a massive accumulation of LC3 in the nuclear periphery that corresponds to the ASFV viral factories (VF), as it perfectly and completely co-localizes with the p72 viral protein. VFs are the ASFV replication sites. As expected, no LC3 accumulation was visible in mock-infected cells.

In conclusion, all these studies showed a very early activation of the AKT–EGF pathway without autophagy induction upon ASFV infection. This will be followed by a stable and strong autophagy inhibition that would persist during the whole infective cycle to ensure the viral replication site formation. In fact, autophagosomes seemed to be part of the viral factory and lipidated LC3 membranes form part of this structure. This suggests that autophagy is a highly regulated process upon ASFV infection.

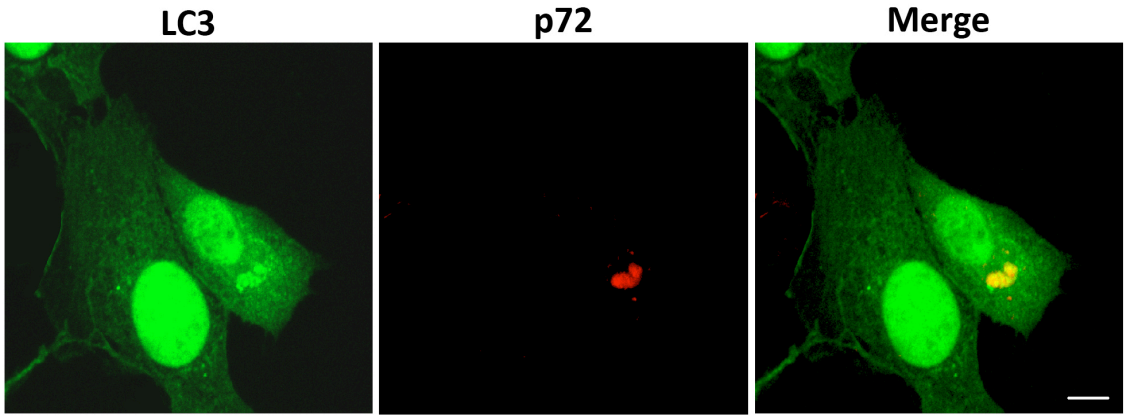

Figure R10. LC3 is recruited into ASFV viral factories. Colocalization of LC3 and viral protein p72 at VFs. Vero LC3 stable cells were ASFV-infected and at 16 hpi an IF assay was performed against LC3 (green) and viral protein p72 (red). Bar=10µm.

3.2.3 Inhibition of autophagy through the interaction of *A179L* with Beclin 1

In our goal to discover putative interactors of ASFV with autophagy-related genes, we established different strategies to generate a list of candidates. We based our plan of approach through the yeast two-hybrid assay. Initially, we screened a swine alveolar macrophage cDNA library (Miskin et al., 1998) for interactors of the ASFV protein UBCv1, which to date is the only known ubiquitin-conjugating E2 enzyme reported to be encoded

by the virus and it may have a role in ubiquitin-mediated selective autophagy.

The following table shows the list of UBCv1-interacting proteins found in the cDNA library screening:

Bait Protein (pACT2 plasmid)	Captured Protein (pGBT9 plamid)	Protein size (aa)	Interacting Region (aa)	Organism	Times found
UBCv1	rps23 (40S ribosomal protein S23)	143	29-143	*Sus scrofa*	2
UBCv1	GLYR1 (Glyoxylate reductase 1)	553	29-91	*Sus scrofa*	1
UBCv1	TFIID (Transcription initiation factor TFIID subunit 1)	1872	1312-1401	*Sus scrofa*	2

Among the list of putative candidates, 40s ribosomal subunit protein S23 (rps23) interaction with UBCv1 was confirmed using a GST pull-down experiment **(Figure R11A)**. In the presence of GST-UBCv1, rps23 was specifically retained, since the band did not appear in the presence of GST alone, indicating specific interaction of UBCv1 with rps23 and not with GST. This interaction was further confirmed in COS-7 cells by IF assay **(Figure R11B)**.

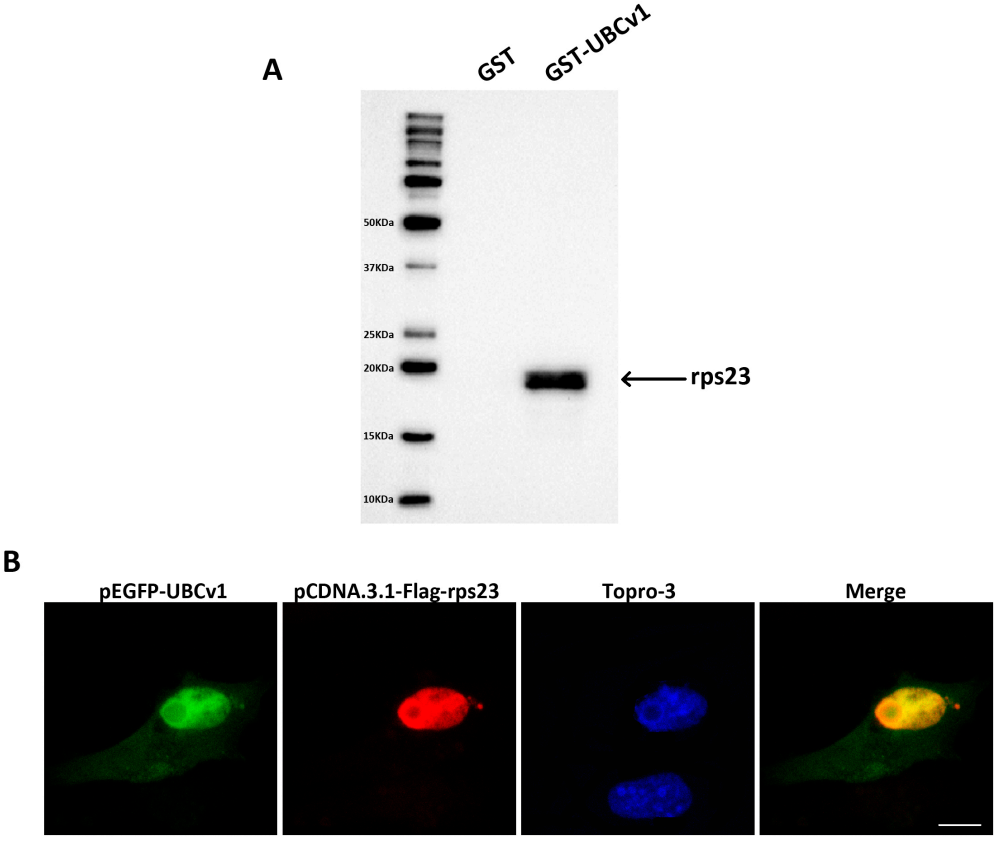

Figure R11. Interaction of UBCv1 protein with rps23. (A) Equal amounts of GST-UBCv1 fusion protein and the control GST protein were bound to glutathione-sepharose beads and incubated overnight at 4°C in binding buffer with bacterial extracts containing rps23-His protein..An specific band was retained for rps23. **(B)** Colocalization of UBCv1 protein (green) and rps23 (red) in the cell nucleus at 24 h. Cell nuclei were stained with Topro-3. Bar=10µm.

Although we successfully managed to characterize a set of UBCv1 interactors, efforts to further analyze their function were unsuccessful, due to their weak expression, long sequences and lack of specificity from the commercially available antibodies. Therefore, we established a one-to-one YTH approach to elucidate other interactions between ASFV and the autophagy-related genes.

Beclin 1 was initially described as a Bcl2-interacting protein in a yeast two-hybrid assay (Liang et al., 1998) and this interaction was found to have an anti-autophagic role for Bcl2. In fact, cellular Bcl2 (cBcl2) has a dual role as it inhibits both apoptosis and autophagy processes.

Given that the ASFV genome encodes a viral Bcl2 homolog (vBcl2; *A179L*) with full anti-apoptotic functions, we explored whether *A179L* is involved in the regulation of the autophagic cellular pathway. To this end, we used a yeast two-hybrid assay in which strain *Y190* was sequentially transformed with pGBT9-A179L and pACT2-Beclin 1 plasmids. The presence of *A179L* and Beclin 1 coding sequences were confirmed by PCR in double transformants obtained after auxotrophic selection. The blue clones obtained when tested for β-galactosidase activity, indicated interaction with Beclin 1.

ASFV also encodes for the *DP71L* gene, a homolog of herpes simplex virus 1 (HSV1) *ICP34.5*, which has been recently shown to interact with Beclin 1 in order to counteract autophagy (Orvedahl et al., 2007). However double transformants for pGBT9-DP71L and pACT2-Beclin 1 did not exhibit β-galactosidase activity so this finding indicates that there is no demonstrable interaction between both proteins. As expected, single transformants with pGBT9-A179L or pACT2-Beclin 1 and also double transformants for pACT2-Beclin 1 and pGBT9-p54, an unrelated ASFV protein used as negative control, were negative in the β–galactosidase assay **(Figure R12A)**.

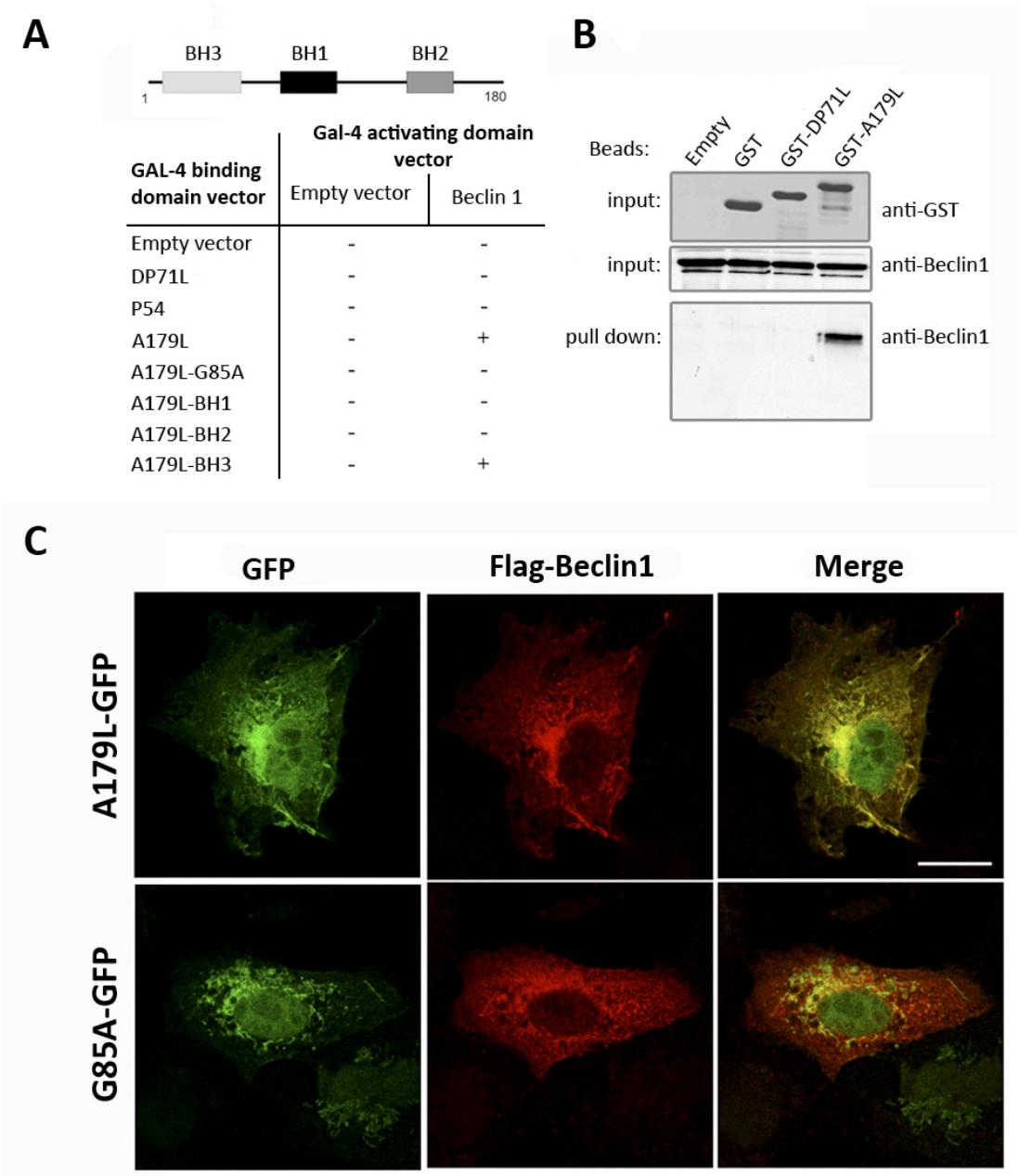

Figure R12. Viral Bcl2 *A179L* interaction with Beclin 1. (**A**) Analysis of the interaction of A179L and Beclin 1. The summary results from the β-galactosidase activity assay, are shown as positive (+) for reporter gene activity within 6 h or negative (-), lack of reporter gene activity after 24 h. A schematic representation of BH domains in *A179L* is shown. (**B**) Positive interaction between *A179L* and Beclin 1 as determined by GST pull-down assay of Beclin 1 with GST-A179L. Baculovirus-expressed and affinity-purified Beclin 1 was incubated with empty, GST, GST-DP71L or GST-A179L beads. GST fusion proteins from supernatants containing Beclin 1 in the assay are shown in the upper and middle panel, as analyzed by WB using an anti-Beclin 1 antibody (lower panel). **(C)** Colocalization analysis of A179L, G85A mutant A179L (green) and Beclin 1 (red) after 24 h transient expression in Vero cells (red). Representative images of 0.1-µm confocal sections. Bar=18 µm.

To further confirm yeast two-hybrid assay results we also performed pull down assays. To that end we used an *in vitro* GST binding assay using recombinant proteins expressed in heterologous systems. GST-A179L and GST-DP71L fusion proteins and GST alone were

obtained and purified as previously described (Galindo et al., 2008; Rivera et al., 2007b). For efficiency, reasons we used the baculovirus expression system to produce Beclin 1. A recombinant baculovirus was constructed as described in (Hernaez et al., 2013) to express His-tagged Beclin 1, which could be affinity-purified from infected cell extracts. Equal amounts of GST-A179L, GST-DP71L and GST, as judged by Coomassie blue staining, were immobilized on glutathione-sepharose beads and incubated with His-tagged Beclin 1. After extensive washing, the proteins bound to the beads were separated by SDS-PAGE and detected by WB with a specific antibody against Beclin 1. His-tagged Beclin 1 was retained only in the presence of GST-A179L and it showed a band of appropriate size (55-60 kDa) corresponding to Beclin 1 in WB analysis. However, this did not happen with GST-DP71L or GST alone, **(Figure R12B)**.

Taking together all these findings, we can conclude that ASFV-mediated autophagy inhibition is a consequence of the interaction between cBcl2 homolog A179L and Beclin 1.

3.2.4 Relevance of vBcl2 BH domains in the interaction with Beclin 1

Viral encoded *A179L* protein contains BH1, BH2 and BH3 homology domains from Bcl2-related proteins but lacks the characteristic Bcl2 transmembrane domain. Anti-apoptotic Bcl2 proteins are structurally characterized by a hydrophobic surface groove that can accommodate the BH3 domain of either pro- apoptotic members or Beclin 1.

Hence, we explored the relevance of BH domains from *A179L* in the Beclin 1 interaction by using a yeast two-hybrid assay, as described above. Thus, yeast strain *Y190* was sequentially transformed with pACT2-Beclin 1 and then with corresponding pGBT9 plasmids encoding BH1 (residues 50 to 125), BH2 (residues 95 to 180), or BH3 (residues 1 to 75) **(Figure R13A)**. Results showed that vBcl2 BH3 maintains the capacity of complete A179L to interact with Beclin 1. Interestingly, the point mutation G85A in BH1 that abolishes the anti-apoptotic function of vBcl2 *A179L* failed to interact with Beclin 1 in the yeast two-hybrid assay, as it was previously described for cellular Bcl2 (Pattingre et al., 2005).

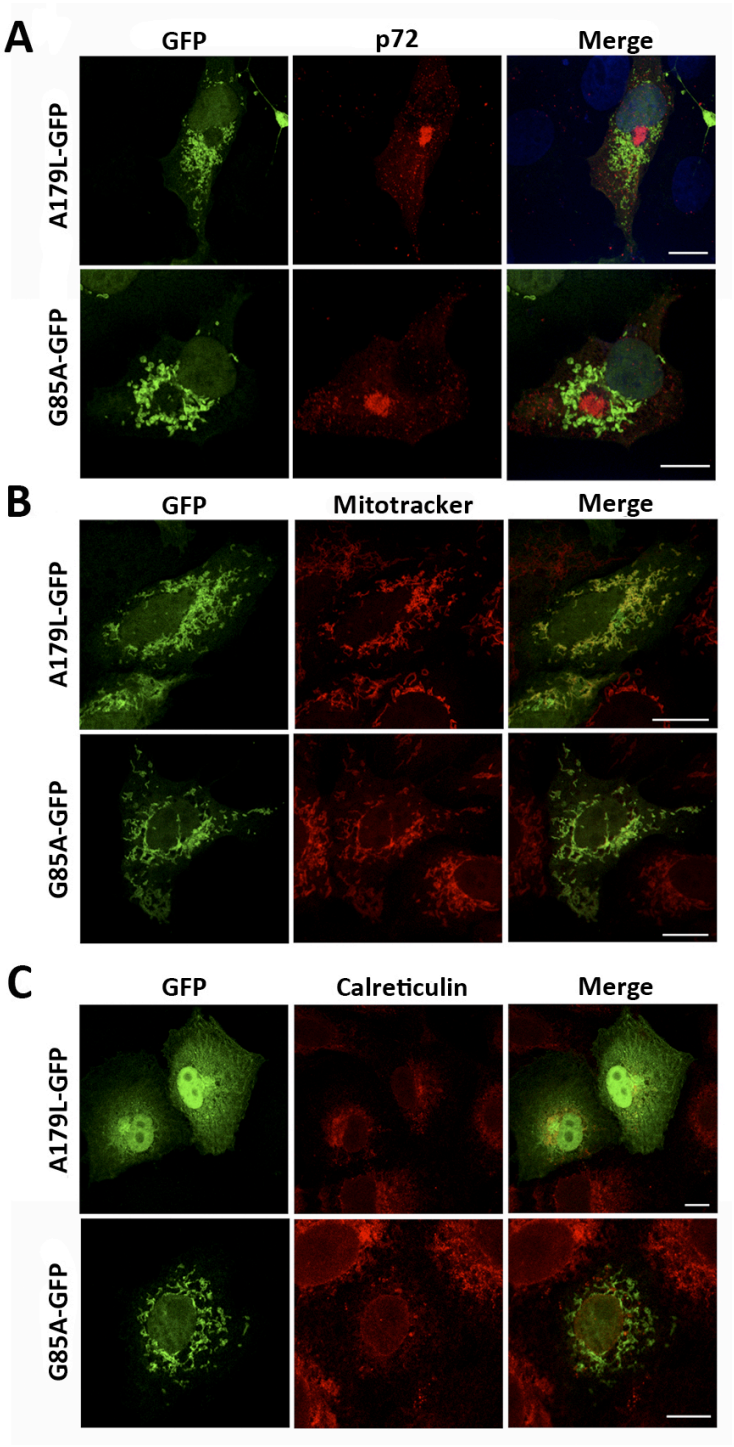

Figure R13. Analysis of the subcellular distribution of A179L-GFP. (**A**) Vero cells transiently expressing A179L-GFP or G85A-GFP mutant were infected with ASFV. At 16 hpi, the distribution of A179L-GFP and mutant G85A-GFP in infected cells was examined together with the viral factory, detected with an anti-viral capsid p72 protein antibody (red). Similarly, in uninfected Vero cells, previously transfected with corresponding vectors, A179L-GFP and G85A-GFP localization at mitochondria (**B**), detected with Mitotracker (red), or at endoplasmic reticulum (**C**), detected by incubation with an anti-calreticulin antibody (red), was analyzed. Merged images of representative confocal sections in each case are shown. Bar= 18µm.

Using confocal microscopy, we also examined the A179L-GFP association with Flag-Beclin 1 in cotransfected Vero cells **(Figure R13C)**. Flag-Beclin 1 invariably displayed an identical pattern to that of A179L-GFP. In addition, A179L-GFP colocalized with Flag-Beclin 1 at higher rates than G85A-GFP.

3.2.5 Subcellular localization of transiently overexpressed A179L-GFP

Previous studies have shown that vBcl2 *A179L* is mainly associated with the cytoplasmic virus factory in infected cells at late times postinfection (Granja et al., 2004). However, cBcl2 is known to associate with the outer mitochondrial membrane, the ER and perinuclear membranes (Park and Hockenbery, 1996). Given the fact that *A179L* lacks the cBcl2 transmembrane domain, this localization could be absent for the viral Bcl2.

In order to explore the *A179L* association with cellular compartments that are relevant in autophagy, we analyzed A179L-GFP distribution in transfected and infected cells at 12 hpi. A179L-GFP was found around virus factories, indicating that fusion to GFP did not alter original *A179L* localization **(Figure R13A)**.

In transfected cells, A179L-GFP colocalized mainly with mitochondria but also with the ER **(Figure R13B and C)**. In contrast, the subcellular distribution of A179L BH1 region mutant G85A-GFP exhibited a mitochondrial pattern and colocalization with ER markers was much lower than that observed for A179L-GFP wild type.

3.2.6 *A179L* inhibits autophagosome formation under starvation conditions

Beclin 1 is required during autophagosome initiation and maturation under starvation conditions. Therefore, the capacity of *A179L* to interact with Beclin 1 led us to study a specific role for *A179L* in the inhibition of autophagosome formation. HeLa cells were used due to their autophagic competence and because they offered acceptable transfection efficiency. These cells were transfected with vectors encoding GFP, A179L-GFP or G85A-GFP. 24 h after transfection, cells were incubated or not with starvation media for 4 h and the autophagosomes were counted in 100 transfected cells. Previously, the specificity of LC3 antibody was confirmed by detecting autophagosomes simultaneously with anti-LC3 antibody and LC3-GFP in cells transfected with pEGFP-LC3 **(Figure R14A)**. After the induction of autophagy, cells expressing A179L-GFP exhibited a reduction in the number of autophagosomes when compared to control cells ($P<0.001$). In order to clearly identify

induced autophagy, only those cells containing 20 or more LC3 dots were considered as autophagy-positive cells. The percentage of cells showing this autophagy LC3 pattern under starvation conditions decreased in cells expressing A179L-GFP (28%; *P*<0.001) when compared to those expressing GFP alone (66%). Nevertheless, expression of mutant G85A-GFP resulted in 53% of autophagic cells **(Figure R14B)**. A reduction of autophagosome number suggests that the overexpression of vBcl2 *A179L* counteracts the effect of starvation conditions thus preventing autophagosome formation.

In conclusion, autophagy is highly regulated upon ASFV infection by means of the interaction of the viral Bcl2 homolog with Beclin1.

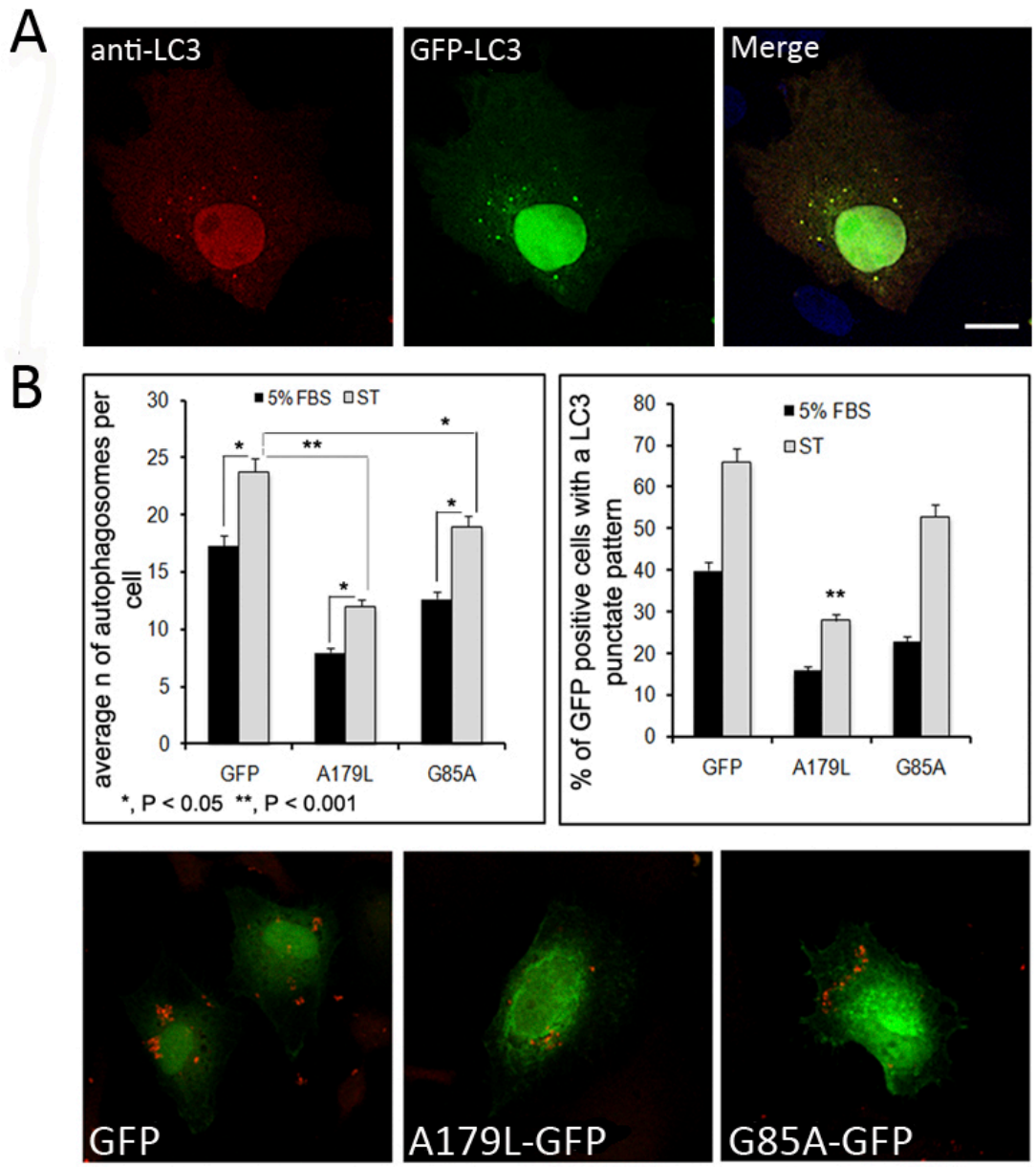

Figure R14. Overexpression of *A179L* impairs autophagosome formation. (**A**) Autophagosomes were simultaneously detected with an anti-LC3 antibody (red) or GFP direct emission (green) in HeLa transfected cells with pGFP-LC3. (**B**) Average number (plus SE, error bars) of autophagosomes from 100 GFP-positive HeLa cells transfected with indicated vectors, detected with an anti-LC3 antibody (left-hand side histogram). Statistically significant values are indicated (* *P* <0.05 or ** *P* <0.001). Average number of GFP-positive cells exhibiting an LC3 punctate pattern (more than 20 dots) for each vector (right-hand side histogram). ** *P*<0.001 versus correspondent GFP control cells. Representative images, obtained by confocal microscopy of autophagosome formation in cells expressing control GFP, A179L-GFP or mutant G85A-GFP under starvation conditions are shown below.

3.2.7 Autophagy induction negatively affects ASFV infection

The results described above suggest that ASFV *A179L* modulates autophagic cellular response through a mechanism involving the *A179L* interaction with Beclin 1 as its cellular counterpart. Therefore, we performed "time of addition" experiments to examine how a pre- or a post-autophagy induction affects ASFV infection. In that manner, it was possible to elucidate in which time intervals the autophagy inhibition remained more crucial to achieve a successful infection.

Vero cells were starved with two different autophagy inducers, HBSS+Rapamycin or tamoxifen, at different timepoints: 2 h prior to infection, at the time of viral adsorption and at different postinfection times **(Figure R15A)**. Vero cells infected with ASFV B54GFP were used as a control. Under these conditions, the number of infected cells was scored by flow cytometry analysis at 16 hpi. Infected cells were detected by direct fluorescence emission of the recombinant B54GFP viral stock **(Figure R15B)**.

A dramatic decrease in ASFV infection was detected when cells were starved 2 h prior to infection, at the viral adsorption time and also at 1 hpi **(Figure R15B)**. There was a correlation between inducing autophagy at later postinfection times and reducing the inhibition upon viral infection, thus suggesting that the autophagy inhibition plays an important role especially in the first steps of viral infection. Furthermore, both autophagy inducers that were tested displayed a similar trend. These results correlate with the percentage of infected cells (counted as the total number of viral factories stained with p72) observed at 16 hpi for the same different time points by confocal microscopy (data not shown).

We next wanted to analyze whether morphology of the VFs was affected upon autophagy induction. After treatment with HBSS+Rapamycin (1μM), morphology of VFs was not altered

(not shown). Analysis of autophagosome marker LC3 and p72 in ASFV-infected cells at 16 hpi revealed a clear compact area of colocalization coincident with the VF **(Figure R15C)**. However, we found that VFs formed in the presence of tamoxifen (5μM) were highly disaggregated when the drug was added either at 6 hpi or at 9 hpi, increasing 60% and 50% respectively compared to control cells **(Figure R15C)**. A total of 100 VFs were counted in control cells at 16 hpi or when tamoxifen was added at 6 hpi or 9 hpi.

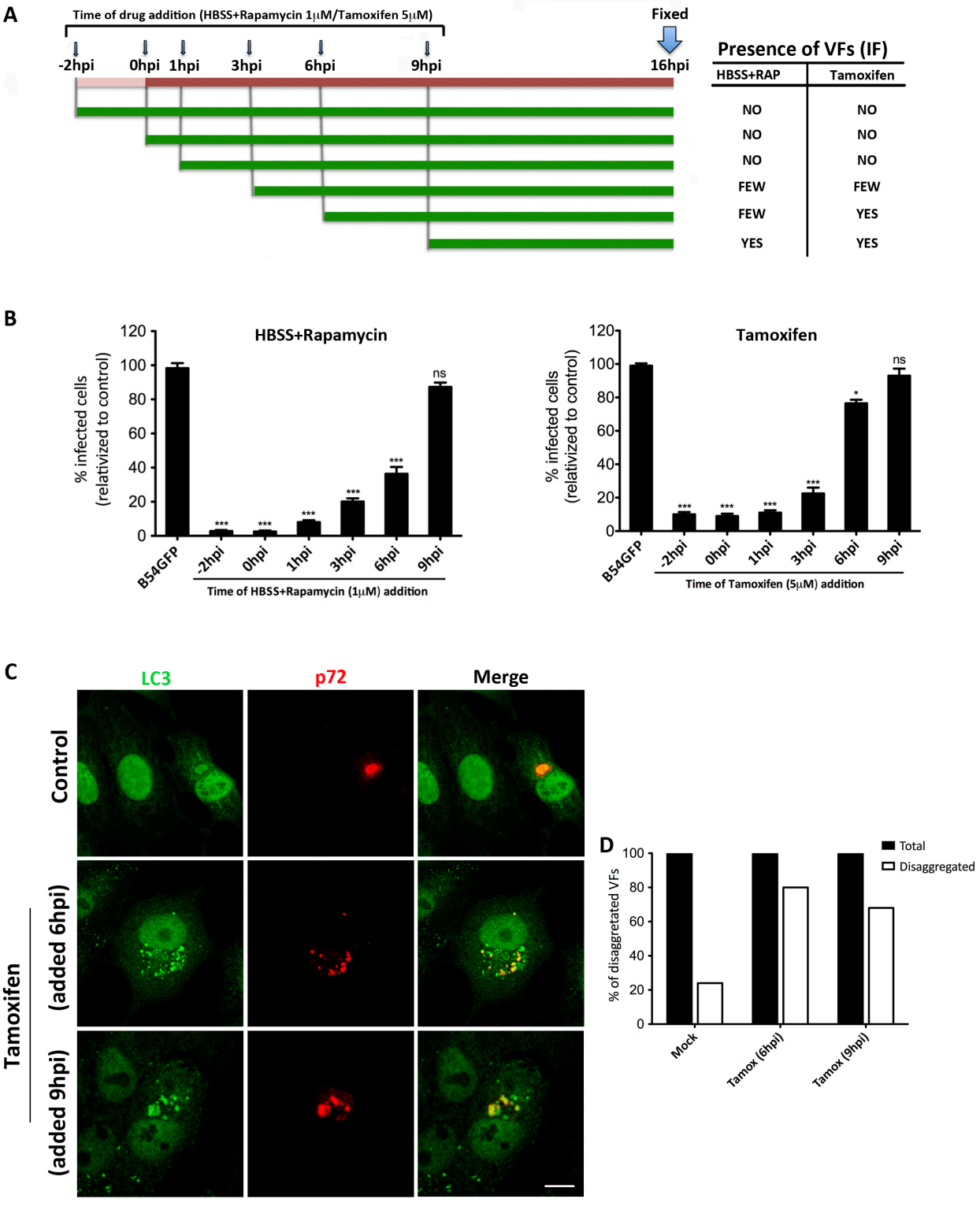

Figure R15. Autophagy induction negatively affects ASFV infection. (A) Diagram of the treatments performed in Vero cells with two different autophagy inducers, HBSS+Rapamycin or tamoxifen, at different timepoints. Presence of VFs was checked for every time point tested. **(B)** Effects in ASFV infection upon autophagy induction with HBSS+Rapamycin or with Tamoxifen at different pre or postinfection times. Infection with ASFV B54GFP without any drug treatment was used as a control. Infected cells were detected by direct fluorescence emission of the recombinant B54GFP. **(C)** Analysis of viral factory morphology in ASFV-infected cells upon autophagy induction with tamoxifen (5μM) at 16 hpi. **(D)** Graphical representation of (C). Asterisks denote statistically significant differences (*=P<0.05; ***=P<0.001; ns=non significant).

These results show that inhibition of autophagy is crucial in early steps of ASFV infection and illustrates the requirement for a tightly regulated process.

3.2.8 Infection of ASFV confers resistance to autophagy induction

Our data indicate that ASFV can significantly reduce basal levels of autophagy in untreated cells. To elucidate whether ASFV infection also antagonizes the autophagy induced by rapamycin (1μM), HBSS+rapamycin (1μM), PP242 (1μM) or tamoxifen (10μM) treatment, we used Vero-LC3 cells, previously infected for 6 h with ASFV (moi=1pfu/cell) and then treated with the different inducers at the indicated concentrations for 2 h. Autophagosome formation was analyzed by visualizing punctate staining of LC3 in control cells treated with HBSS+rapamycin, PP242 or tamoxifen to find that these treatments readily enhanced autophagosome formation **(Figure R16)**. In contrast in ASFV-infected cells formation of the autophagosome was totally blocked. Interestingly, presence of ASFV could not revert the autophagic induction upon tamoxifen treatment, probably because the stimulus was too strong to be counteracted by ASFV itself.

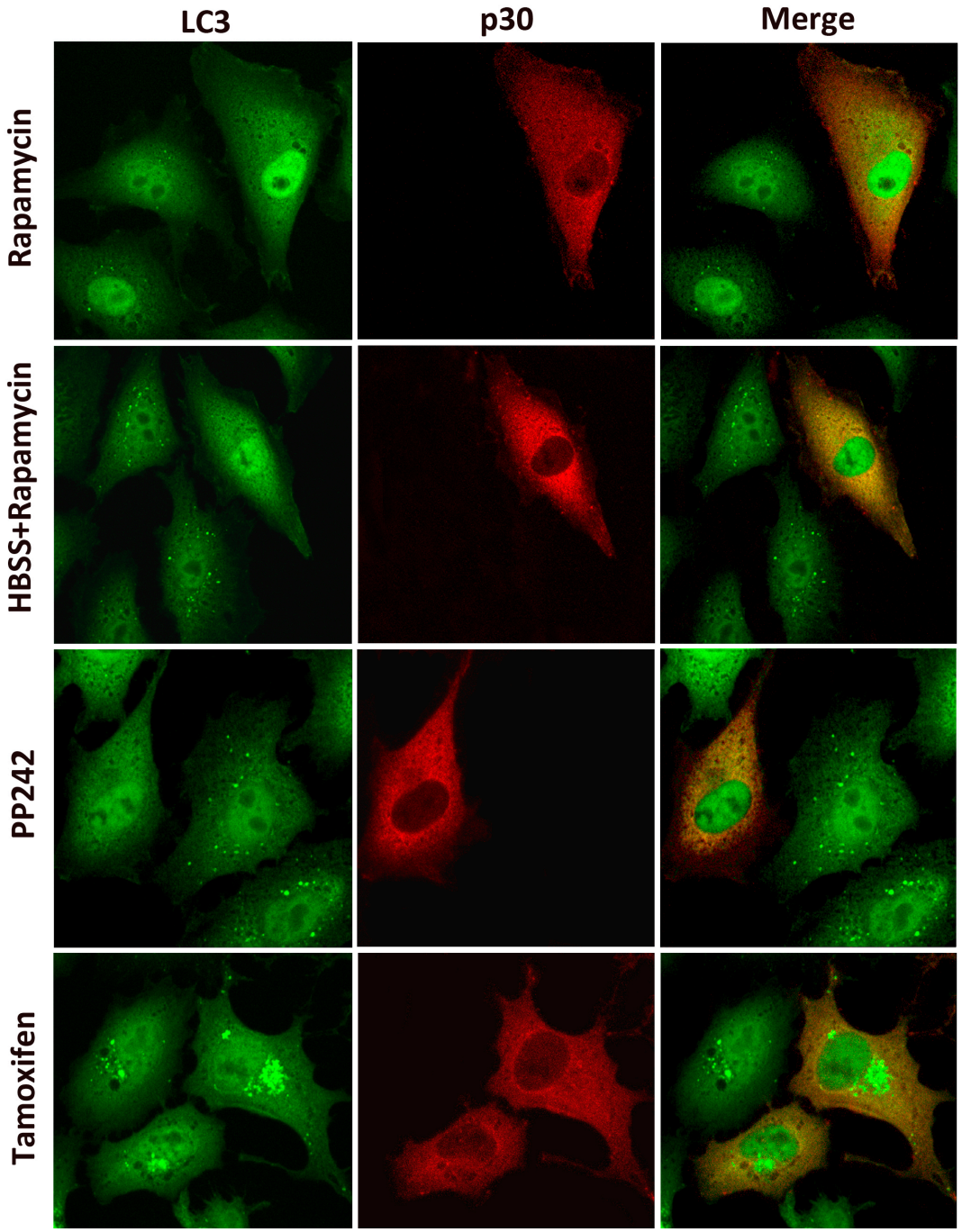

Figure R16. ASFV-infected cells become resistant to autophagic inducers. Autophagosome formation under autophagic inducers is antagonized by ASFV infection except for tamoxifen. IF against LC3 was performed to analyze LC3 punctate staining after treatment with autophagy inducers. Vero-LC3 cells were previously infected with ASFV (moi=1pfu/cell) for 6 h and they were then treated with the different inductors: rapamycin (1µM), HBSS+rapamycin (1µM), PP242 (1µM) or tamoxifen (10µM). Confocal images show LC3 staining (green) and viral protein p30 (red). Bar=10µm.

This finding corroborates that the autophagy inhibition induced by ASFV is able to counteract a previous autophagic stimulus.

3.2.9 Autophagy flux is inhibited in ASFV-infected cells

Measuring autophagy in a meaningful way requires an analysis of the autophagic flux rate. Autophagic flux is the rate at which cellular material is cleared from the cell by autophagy. To better interpret changes in levels of processed LC3-II, it is now *de rigueur* in the field to perform WB on control extracts harvested from cells treated with lysosomal pump inhibitors, such as Bafilomycin A1 (Baf). Baf inhibits degradation of autolysosome content by blocking the $Na^{+}H^{+}$ pump at the lysosome (Rubinsztein et al., 2009). In the presence of Baf inhibitor, accumulation of LC3-II-positive autophagosomes would be a sign of efficient autophagic flux, while failure of LC3-II protein to increase in the presence of such inhibitors would indicate an early defect or delay in the process, prior to degradation at the autophagolysosome.

To differentiate these two possibilities, we determined the effect of ASFV virus infection in the context of autophagy flux. As shown in **Figure R17**, treatment of uninfected wild type Vero cells with Baf for 3 h inhibited the fusion between autophagosomes and lysosomes, thus leading to an increased accumulation of LC3-II due to lack of lysosomal degradation. In contrast, when wild type cells were infected with ASFV for 12 hpi and Baf was added for 3 h, there was a severe decrease in LC3-II levels, which became more evident as the moi was increased.

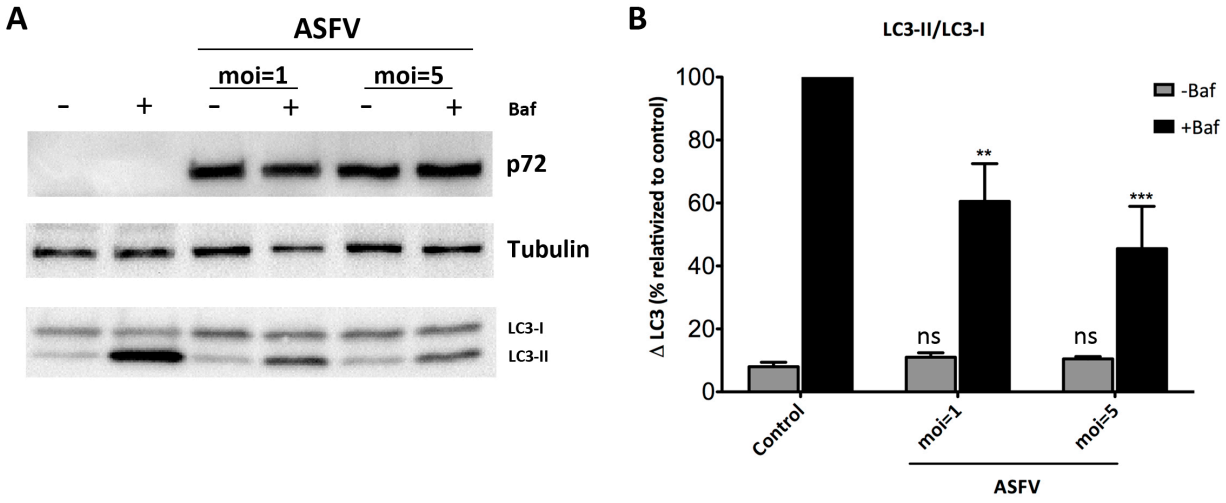

Figure R17. Autophagy flux is inhibited in ASFV-infected cells. (A) Analysis of LC3-II accumulation in ASFV-infected cells upon inhibition of the fusion between autophagosomes and lysosomes, induced by treatment with Baf for 3 h. **(B)** Graphical representation of (A). Data are expressed as mean±SD and asterisks denote statistically significant differences (**=P<0.01; ***=P<0.001; ns=non significant).

Taken together these results, they strongly support that ASFV virus actively disrupts the normal cellular autophagy machinery that is required for autophagosome formation. As we will see below, the lysosome is a very relevant organelle, an intersection were endocytosis meets both autophagy and innate immunity against virus infections.

3.2.10 ATG5 silencing negatively affects ASFV infection

Previous results in this study described the autophagy inhibitor 3MA as a negative regulator of ASFV infection. Since treatment with 3MA has been shown to affect not only the autophagic pathway but also other cellular processes such as glycogen metabolism, lysosomal acidification, endocytosis and mitochondrial permeability transition (Caro et al., 1988; Punnonen et al., 1994; Xue et al., 2002), we proceeded to use a more specific autophagy negative regulator to test its effect in ASFV infection.

To that end, we silenced ATG5 expression on Vero cells by shRNA lentiviral transduction (as described in material and methods section). Five different clones encoding shRNA for ATG5 (Sigma) were tested. Once Vero cells were selected with 8 µg/ml of puromycin, we confirmed ATG5 silencing by analyzing autophagosome formation in ATG5 knockdown cells upon autophagic stimuli compared to control cells **(Figure R18A)**. Immunofluorescence assay revealed that the formation of anti-LC3-labeled autophagosome-like dots was increased after 2 h treatment with HBSS+Rapamycin or with PP242 in Vero scrambled (Scr) control cells while it was almost completely suppressed in ATG5 knockdown (shATG5-Vero) cells. Hence, it was an effective autophagy inhibition.

The next step was to determine the effect of ATG5 depletion in the context of ASFV infection. Scrambled (Scr) control cells and shATG5-Vero cells were infected either with ASFV (moi=1 pfu/cell) or with recombinant stock B54GFP (moi=5 pfu/cell) at 6 or 16 hpi respectively. Then, the number of infected cells was quantified by flow cytometry. As shown in **Figure R18B**, the number of infected shATG5-Vero cells was decreased a 40% in early infection steps and a 60% in late infection steps when compared to control cells. Hence, autophagy inhibition by ATG5 silencing seemed to impair ASFV infection.

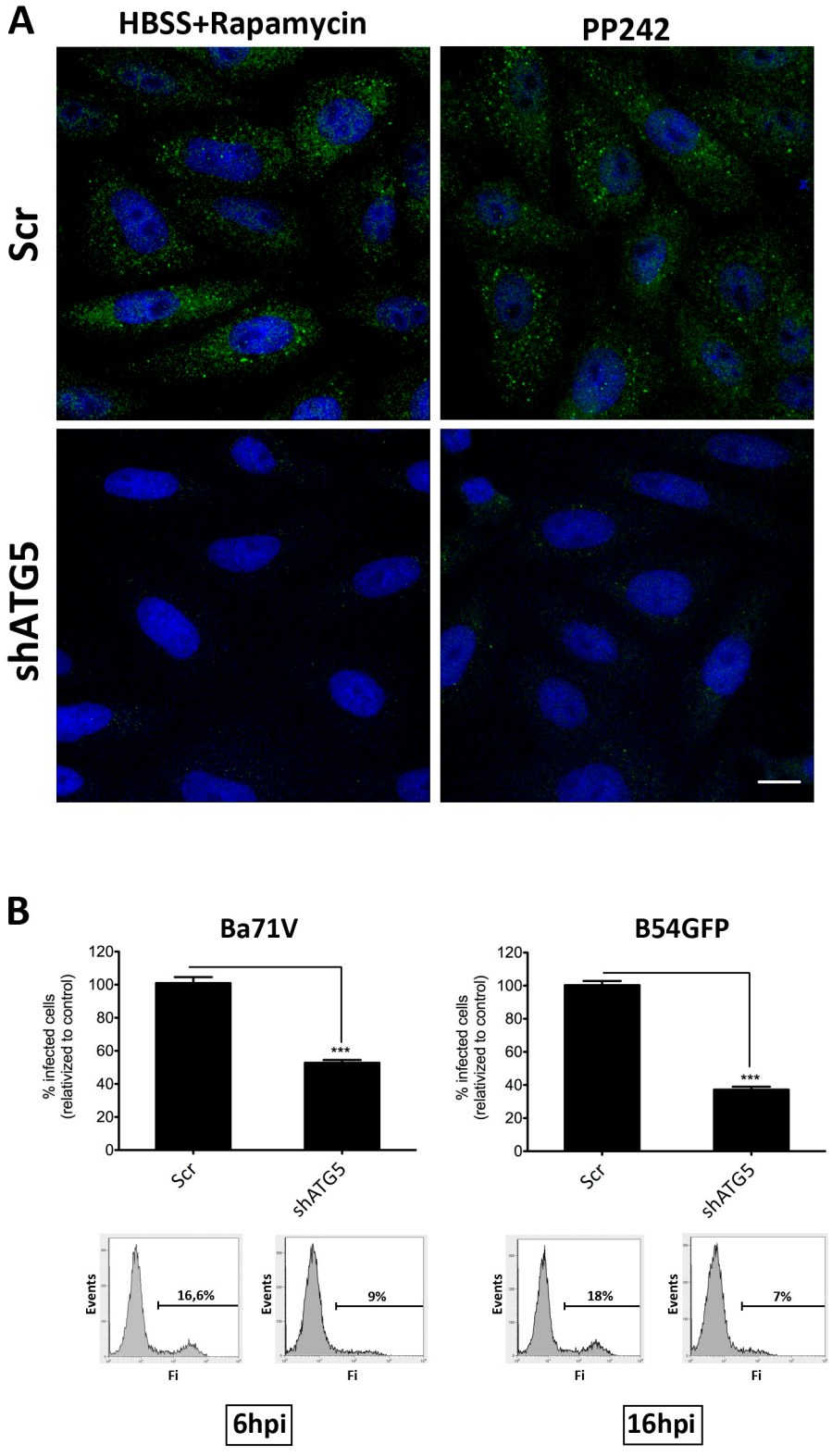

Figure R18. ATG5 silencing negatively affects ASFV infection. (A) Analysis of the inhibition of LC3-autophagosome formation (green) upon expression of shATG5 and treatment with autophagy inducers HBSS+Rapamycin (1µM) or PP242 (0.5µM) for 2 h. **(B)** Inhibition of ASFV infection at 6 and 16 hpi upon knockdown of ATG5. Data are depicted in graphs as mean±SD. Asterisks denote statistically significant differences (***=P<0.001). Bar=10µm.

This finding suggests that autophagy inhibition negatively affects ASFV infection upon specific prevention of autophagosome formation, not only at early but also at late postinfection times.

4. Morphometric analysis of the ASFV viral factories and the pathways involved in aggresome formation

Above results would reinforce the notion that autophagy could be necessary for the virus to pursue replication. In fact, we showed that lipidated form of LC3 form part of the viral factory. Then, we further analyzed the origin of the viral replication organelle or viral factory.

Recent studies have postulated that ASFV VFs share many similarities with aggresome structures (Wileman, 2006). However, solid evidence is necessary to confirm if ASFV-mediated inhibition of autophagy allows the virus to recruit aggresome formation for the generation of its own replication sites, the VFs.

In this current work, we wanted to study the nature of the ASFV VFs in terms of their morphology and cellular distribution, and their possible relationship with the aggresome pathway formation.

4.1 Recombinant fluorescent viruses as tools for the study of ASFV VFs

Making use of two recombinant fluorescent ASFV stocks generated in our laboratory (B54GFP and B12GFP), we performed an extensively study of location, morphology and size of VFs to establish a comparison between Vero and WSL cells. As shown in **Figure R19A**, no significant differences were found in the size of the VF in cells infected with the different recombinant viruses in either cell line (N_{Vero}=140, N_{WSL}=50; p>0,05).

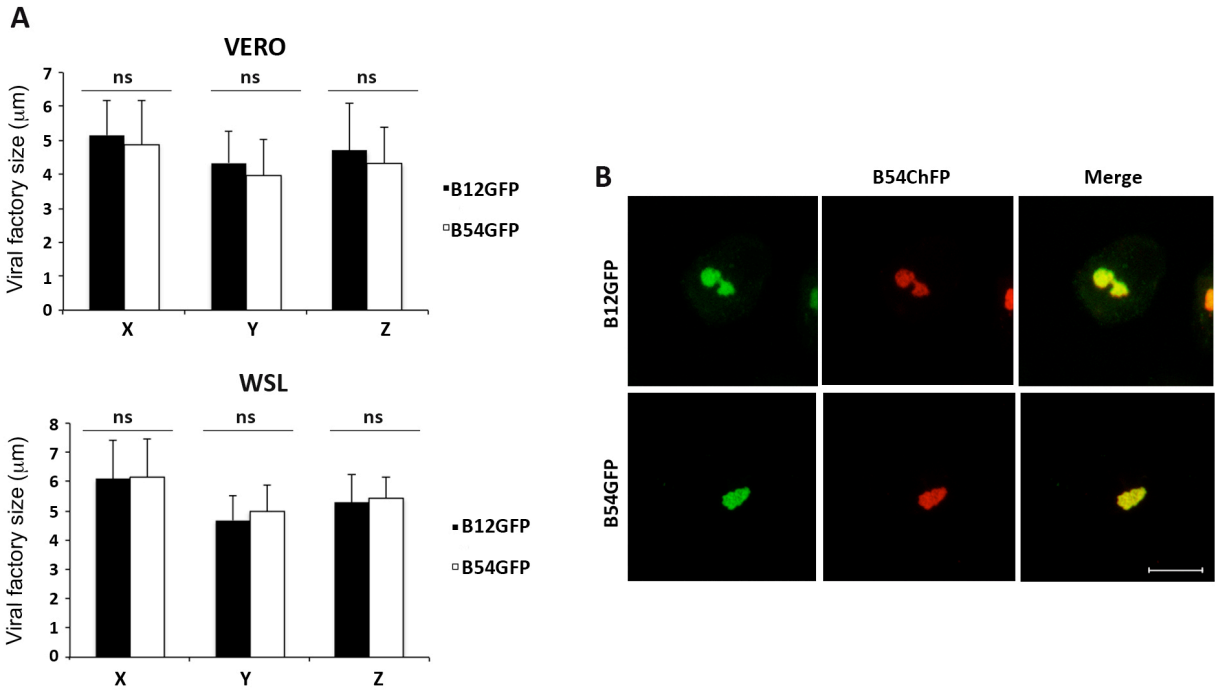

Figure R19. Recombinant ASFV expressing fluorescent proteins. (A) Comparison of the size of the virus factories in Vero and WSL cells infected with recombinant viruses B12GFP and B54GFP (N_{Vero}= 140, N_{WSL}= 50; ns $p > 0.05$). **(B)** Representative confocal micrographs of Vero cells infected with the recombinant viruses in (A) and B54ChFP. The merged images show almost complete superposition of these fusion proteins at the viral factories. Bar=10μm.

Moreover, those recombinant viruses showed almost a complete and perfect superposition in their distribution at the VF **(Figure R19B).** VFs also showed an intense fluorescence as a result of the high amount of proteins that are accumulated in this perinuclear replication and assembly areas (**Figures 19B and 20A-C).** However, viral DNA stained with Topro-3 did not show a complete superposition in VFs.

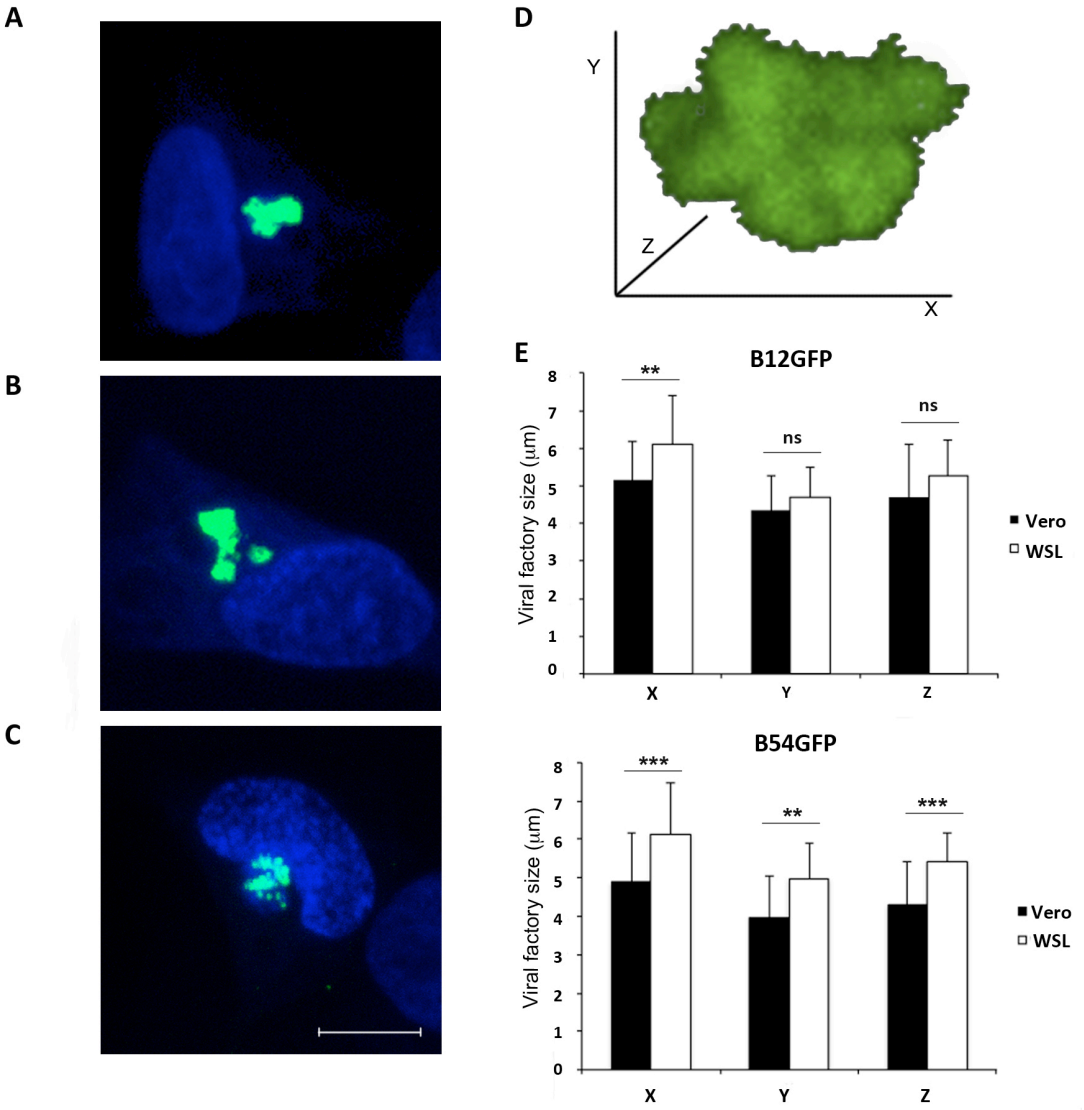

Figure R20. Morphology of the ASFV viral factory. (A)-(C) are representative confocal micrographs of viral factories; as atypical single compact fluorescent spot **(A)** or as multiple viral factories **(B)** and **(C).** Bar 10 µm. **(D)** Three-axis dimensions of the viral factories in Vero and WSL cells infected with recombinant viruses B12GFP and B54GFP at 16 hpi were analyzed. Image acquisition of 13 Z-stacks per viral factory from N_{Vero}=140 and N_{WSL}=50 cells infected with these recombinant viruses was performed by confocal laser scanning microscope (Leica) and tridimensional reconstruction, and image analysis was done with the Leica Application Suite Advanced software. **(E)** Graphics show mean±SD of X, Y and Z axis in µm. Major axis (X) was significantly larger in WSL cells when compared to Vero cells. Asterisks denote statistically significant differences (**=P<0.01; ***=P<0.001; ns=non significant).

As shown in **Figure R20E**, VFs are well-defined structures with a major axis size (X) *ca.* 5 µm at 16 hpi in Vero cells and *ca.* 6 µm in WSL cells. The only differences found between these two cell lines were in the size of VFs, in fact, the major axis of the factories was significantly larger in WSL than in Vero cells as displayed in **Figure R20E.** Furthermore, at this time point (16 hpi), 34 and 39% of Vero and WSL cells respectively, presented a marked cytophatic

effect. In addition, in 25% of infected Vero and 12% of WSL cells, multiple VFs as several independent organelle-shaped fluorescent spots prior to coalescence were found **(Figure R20B and C)**. Those infected cells bearing multiple VFs did not show a marked cytophatic effect in 83% of infected Vero cells or in 87,5% of WSL cells.

4.2 VFs, cellular organelles and cytoskeleton disposition in ASFV-infected cells

We also addressed organelle organization in Vero cells infected with recombinant viruses B12GFP and B54GFP at 16 hpi **(Figure R21)**. VFs were characteristically devoid of organelle markers. ER staining in infected cells was disperse in the cytoplasm, and sometimes maintained an empty halo around the factory. Consistent with previous reports, mitochondria were organized around the VFs and the Golgi complex disassembled following microtubules (Netherton et al., 2006; Rojo et al., 1998b) until the signal almost disappeared.

With respect to cytoskeleton organization, intermediate filaments stained with anti-vimentin antibody proliferated in the cytoplasm forming a robust vimentin cage around the factories (Stefanovic et al., 2005b). Acetylated tubulin filaments were reduced, and actin cytoskeleton was progressively disassembled, as shown by the faint staining of the few remaining polymerized actin filaments.

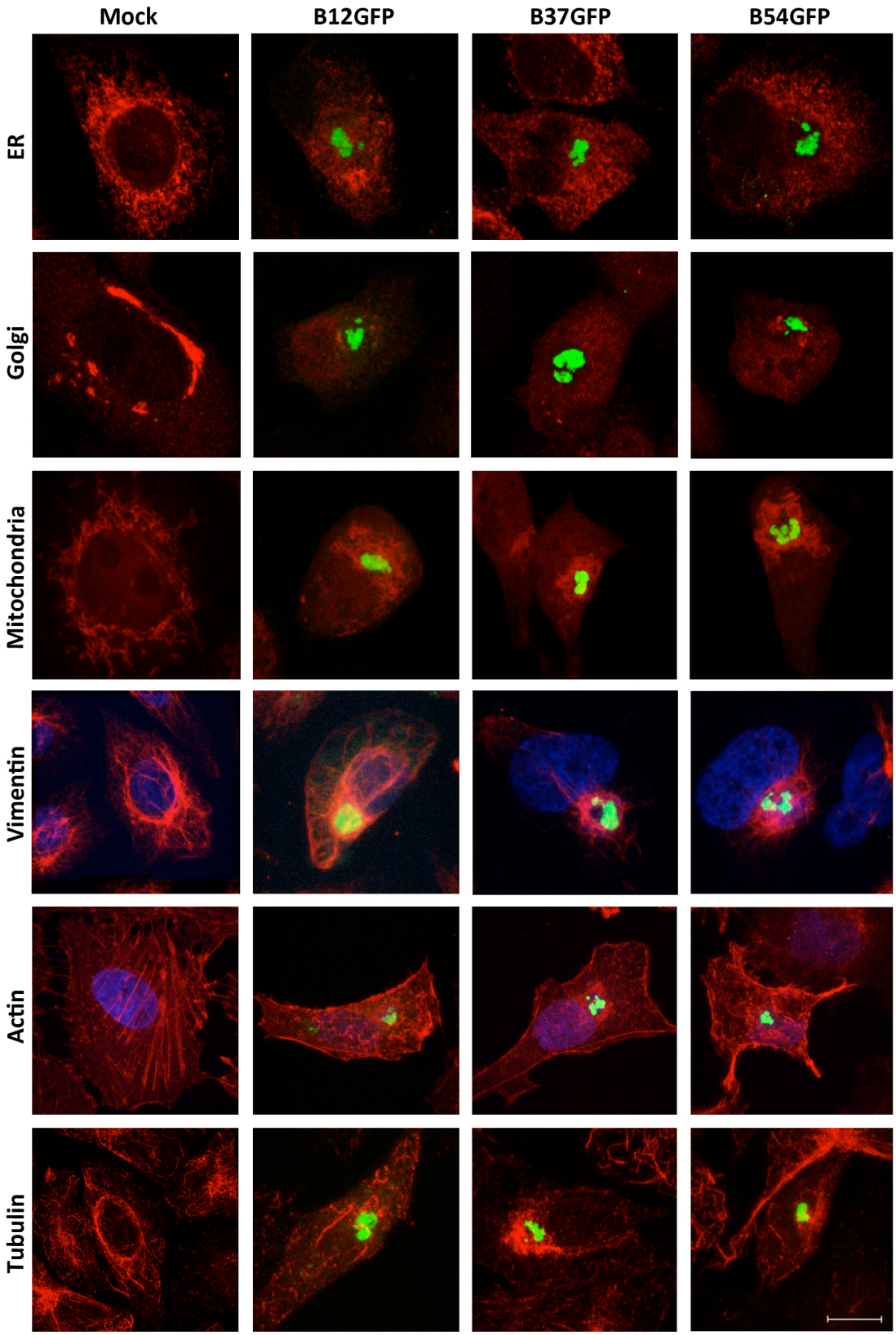

Figure R21. Viral factories, cellular organelles and cytoskeleton. Intracellular structures in Vero cells infected with ASFV recombinant viruses B12GFP and B54GFP (moi=1pfu/cell) at 16 hpi and stained for ER (α-PDI), Golgi (α-TGN46), mitochondria (Mitotracker CMXRos), α-Vimentin-Cy3, AF594 phalloidin for actin and α-acetylated tubulin AF594. Bar=10 µm.

4.3 Analysis of pathways involved in aggresome formation

We next wanted to further investigate the aggresome formation pathways to unveil any possible exploits by the ASFV in the formation of the VFs.

Cytoplasmic histone deacetylase 6 (HDAC6) is a key element that mediates the disposal of protein aggregates and cytotoxic misfolded proteins by sequestering activity in cellular "storage bins" that are called aggresomes. HDAC6 exerts this function through its simultaneous interaction with ubiquitinated proteins and dynein motors.

On the other hand, the Bcl2-associated athanogene 3 (BAG3) is involved in the active transport of protein substrates within the cell and plays a selective role by loading the cargo onto dynein to carry misfolded proteins that are not ubiquitinated into the aggresome (Garcia-Mata et al., 1999). Therefore, we wanted to analyze the possible role of Bag3 in viral factory formation as we previously did for HDAC6.

4.3.1 HDAC6 inhibition does not affect ASFV infectivity

To test the role of HDAC6 in ASFV infection, the reversible inhibitor tubacin (tubulin acetylation inducer), which impedes the specific interaction of HDAC6 with dynein (Hideshima et al., 2005), was used.

Vero cells were pretreated for 3 h with tubacin at the indicated concentrations in DMEM with 5% FBS at 37°C, followed by cold synchronized infections with ASFV or with the recombinant B54GFP (moi=1 pfu/cell) (Hernaez et al., 2006). The inhibitor was present in the medium throughout the experiment. Posteriorly, at 24 hpi, cells were either trypsinized for FACs analysis or lysed with Laemmli buffer to perform a WB. Concentrations of 1-2 µM tubacin (Ding et al., 2008) leads to increased acetylated tubulin levels in Vero cells (over 4-fold starting 1 hour after addition and reaching its maximum level at 16 hpi, as detected by WB and confocal laser scanning microscopy **(Figure R22, A and B)**. This finding demonstrates that tubacin is exerting its function at the selected working concentrations. Nevertheless, at the same doses that tubacin increased microtubule acetylation, tubacin did not modify infected cell percentages, as shown by immunostaining at 6 hpi and 16 hpi with specific ASFV viral proteins p30 or p72 respectively **(Figure R22C)**. Nor did tubacin alter the detection of infected cells with recombinant virus B54GFP by flow cytometry **(Figure R22E)**. Moreover, the inhibitor did not change early or late protein expression (p30 or p72) as

shown by WB analysis **(Figure R22D)**. Furthermore, viral production was not modified under tubacin-induced HDAC6 inhibition (data not shown).

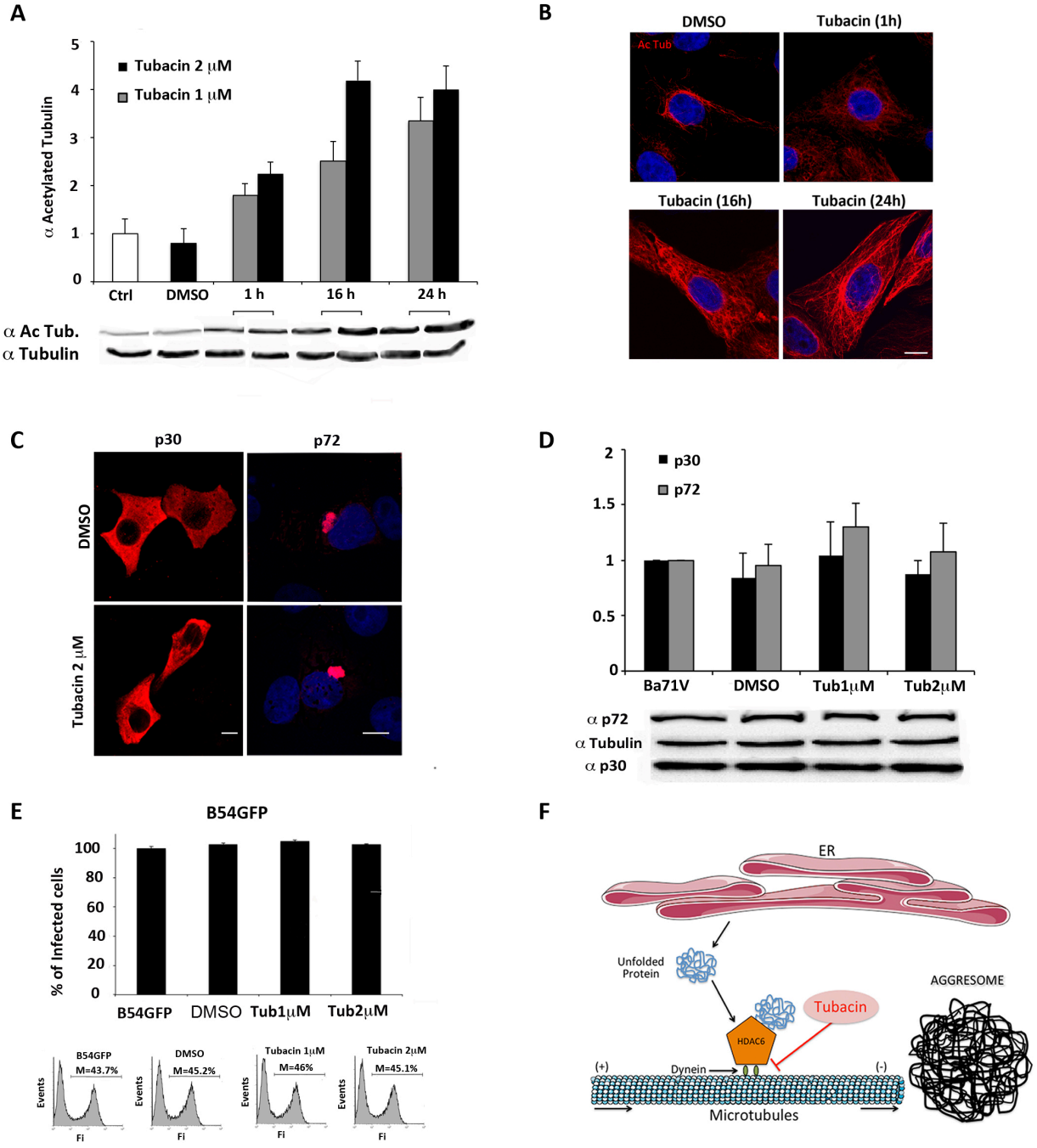

Figure R22. HDAC6 participation in the viral factory formation. (A) Acetylated tubulin levels in Vero cells treated with HDAC6 inhibitor tubacin, as shown by WB. **(B)** Confocal microscopy images of acetylated tubulin levels in Vero cells treated with HDAC6 inhibitor tubacin (2μM) at different times. **(C)** Infectivity was analyzed by IF using antibodies against ASFV proteins p30 and p72 to evaluate infected cell numbers. Representative micrographs of p30 (6 hpi) or p72 (16 hpi) in Vero cells infected with ASFV (moi=1 pfu/cell) and treated with tubacin. **(D)** WB analysis of p30 and p72 viral protein expression of tubacin-treated infected cells or controls. **(E)** Flow cytometry analysis of infectivity in Vero cells infected with recombinant B54GFP (moi=5 pfu/cell) and

treated with tubacin. WB analysis of p30 and p72 viral protein expression of tubacin-treated infected cells or controls. **(F)** Role of HDAC6 in the canonical pathway of aggresome formation. Bar=10 µm.

4.3.2 Vimentin cages and VFs are formed in the presence of HDAC6 inhibitor tubacin

Next, we wanted to test whether vimentin cages and VFs are still formed when HDAC6 is inhibited. To that end, Vero cells were infected with recombinant viral stock B54GFP or treated with tubacin (2µM) previously to infection **(Figure R23)**. Confocal microscopy revealed that inhibition of HDAC6 with specific inhibitor tubacin (2µM) did not alter the formation of VFs and their number, morphology and location was preserved under these conditions. Furthermore, the characteristic vimentin cage was formed around the viral factory**.**

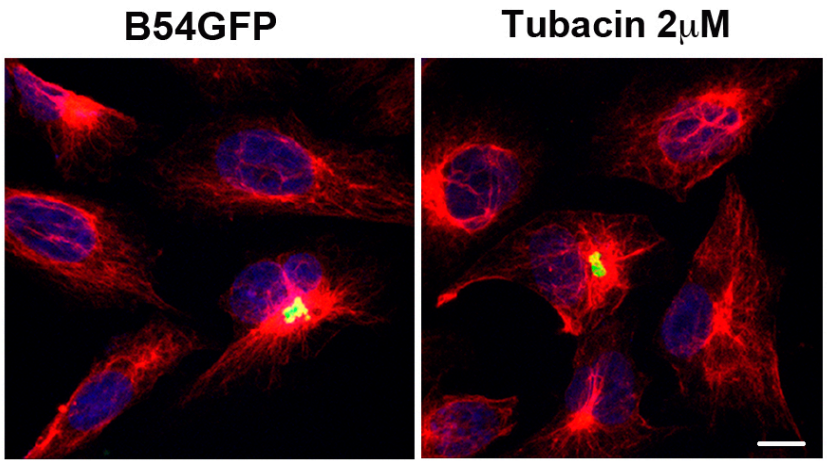

Figure R23. Vimentin cages and VFs are formed in the presence of HDAC6 inhibitor tubacin. Vimentin cage formation around the viral factories. Vimentin staining of Vero cells (red) treated with tubacin and infected with B54GFP (green) in control cells (left panel) or in cell treated with tubacin (2µM). Bar=10µm.

Therefore, although the viral factories formed by ASFV are morphologically very similar to aggresomes, the mechanism of viral factory formation for this virus is apparently not related with the canonical aggresome pathway mediated by HDAC6.

4.3.3 HDAC6 does not colocalize with ASFV VFs

Vero cells were treated with proteasome inhibitor MG132 (5mM) for 16 h and an immunofluorescence against HDAC6 was performed. As shown in **Figure R24A**, upon proteasome inhibition, HDAC6 was accumulated in a perinuclear area: the aggresome. However, when Vero cells were infected (moi=5 pfu/cell) and stained against p72 (that is accumulated in VFs) and HDAC6 simultaneously, no colocalization between both proteins was found, adding to the notion that AFSV factories are not true aggresomes **(Figure R24B)**.

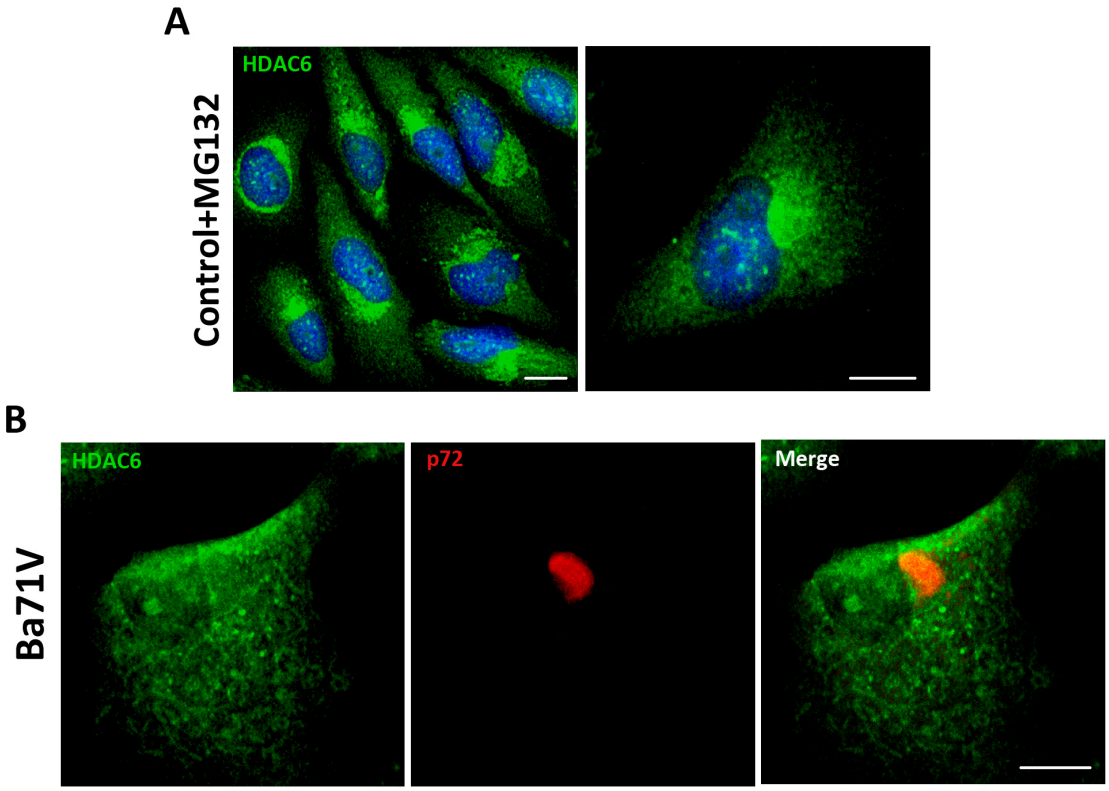

Figure R24. HDAC6 does not colocalize with ASFV VFs. (A) Analysis of HDAC6 expression in Vero cells treated with proteasome inhibitor MG132 (5mM) for 16 h. **(B)** Cellular localization of p72-expressing VFs (red) and HDAC6 (green) in ASFV-infected Vero cells (moi=5 pfu/cell). Bar=10µm.

4.3.4 Analysis of BAG3 in VF formation

As no specific BAG3 inhibitors were available, BAG3 was knocked down in Vero cells following shRNA lentiviral transduction methods, described in the materials and methods section. As 5 clones for shBAG3 (Sigma) were tested (Table X), a WB analysis was performed to screen for the stable cell line with the highest silencing level. As seen in **Figure R25A**, the stable cell line that showed the highest BAG3 knockdown was clone 3, BAG3(3). It thus became our selected candidate to perform further experiments while the others were

discarded. In parallel, IF of shBAG3 Vero cells were performed to ensure that BAG3 levels were also lower when compared to scrambled (Scr) control **(Figure R25B)**.

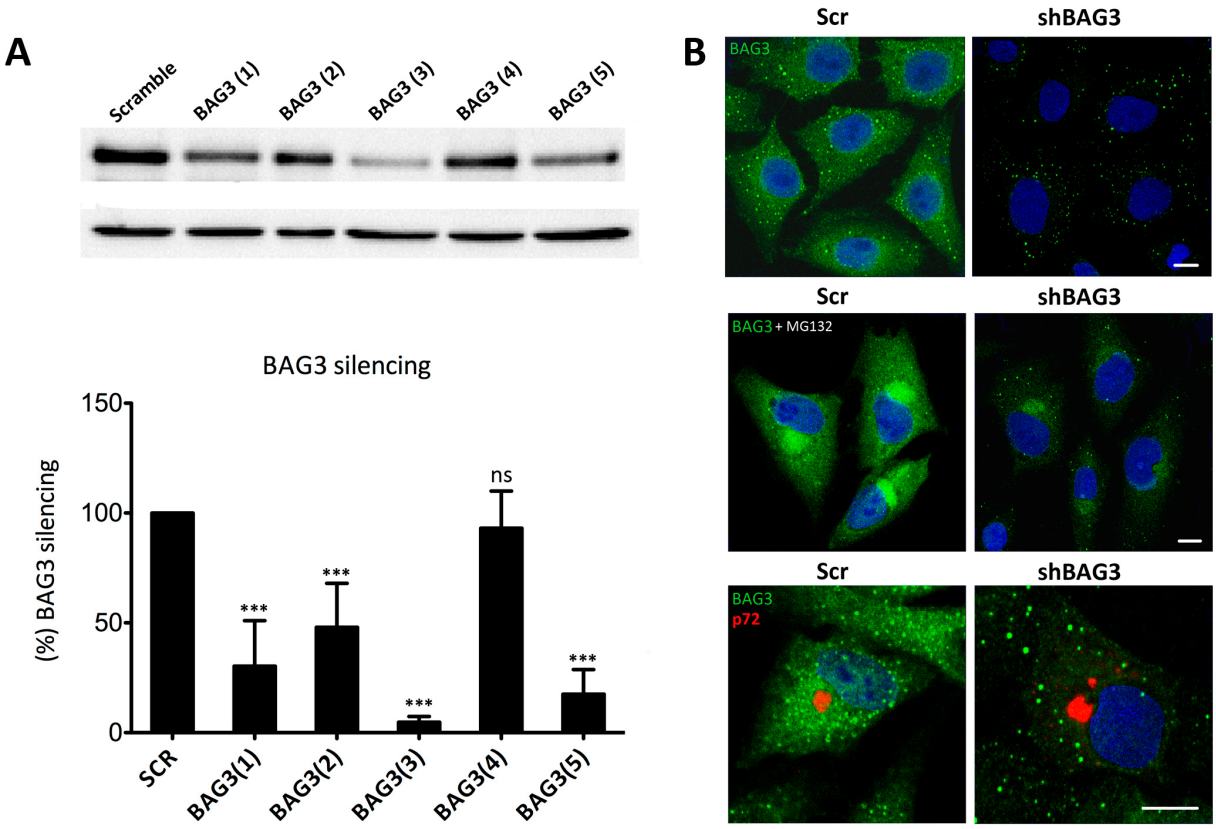

Figure R25. Analysis of Bag3 in VF formation (A) Different levels of BAG3 silencing among five clones obtained from shBAG3 transduction in Vero. BAG3 clone 3 (BAG3(3)) was the selected candidate for further experiments. Graphics in the lower panel show mean±SD of WB quantification. **(B)** BAG3 expression in shBAG3-Vero cells either with proteasome inhibitor MG132 treatment (5mM) for 16 h or infected with ASFV (moi=1 pfu/cell). Capsid viral protein p72 (red) was used to detect VFs. Asterisks denote statistically significant differences (***=P<0.001; ns=non significant). Bar=10µm.

To further confirm shBAG3 Vero cells were properly silenced, they were pretreated overnight with proteasome inhibitor MG132 (5mM). As shown in **Figure R25B**, control cells displayed perinuclear aggresomes by IF when stained with a specific antibody against BAG3. In contrast, majority of shBAG3 cells either did not exhibit aggresome formation or there were smaller in size under the same antibody conditions. Once Vero shBAG3 cells were well characterized, we analyzed the effect of BAG3 knockdown in VF formation. To that end we infected Vero shBAG3 cells (moi=1 pfu/cell) and then an IF against BAG3 and viral protein p72 was performed. As seen in **Figure R25B**, confocal microscopy revealed that VF was still formed in Vero shBAG3 cells and BAG3 did not colocalize with p72. The same disposition of VF was found in Vero Scr control cells.

In conclusion, following our results, none of the aggresome pathways seemed to be involved involved in the formation of the ASFV viral factory.

5. Viral clearance *versus* establishment of infection. Role of interferon-induced family of IFITMs.

Autophagy seems to play a role in the clearance of some viral agents. This process has been called xenophagy (Levine and Deretic, 2007). Moreover, we hypothesized that the complex autophagy regulation found after ASFV infection, mainly based in a rapid induction followed by later inhibition, could be related with its maintenance of the viral replication site and avoiding viral clearance. This is closely related with innate immunity against the virus. Then, we proceed to analyze some unknown aspects of innate immunity related with ASFV infection. It has been recently described that the interferon-induced family of proteins (IFITMs) inhibit a wide range of enveloped viruses (Brass et al., 2009). Then, our initial objective was to analyze whether IFITMs could affect ASFV infection.

5.1 Induction of the IFN pathway abrogates ASFV infection

The relationship between IFN and ASFV infection has been previously reported (Correia et al., 2013). To determine whether the interferon pathway inhibits ASFV infection, Vero cells were pretreated with universal type I IFN for 24 h and they were then infected with recombinant ASFV B54GFP (moi=5 pfu/cell). Viral infection was quantified by analyzing the number of GFP-positive cells by flow cytometry. As shown in **Figure R26**, pretreatment of Vero cells with universal type I IFN at both concentrations tested (1,000 and 10,000 U/ml), completely abrogated ASFV infection when compared to control cells.

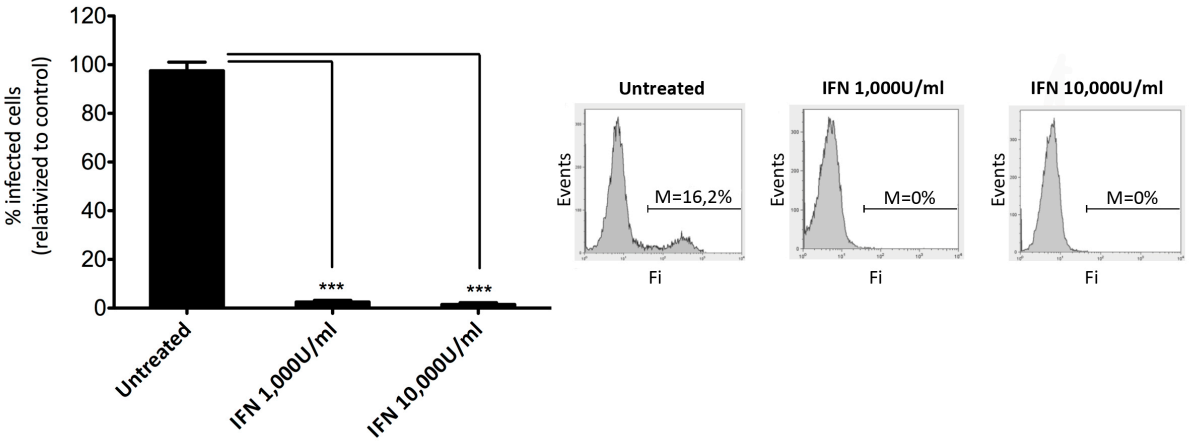

Figure R26. Universal Type I IFN inhibits ASFV infection. Analysis of the number of ASFV-infected cells upon treatment with IFN at 1.000U/ml or 10.000U/ml 24h before the infection. Vero cells were infected with recombinant ASFV B54GFP (moi=5 pfu/cell). Data are expressed as mean±SD and asterisks denote statistically significant differences (***=P<0.001).

To exclude the possibility that the observed effect of universal type I IFN on ASFV infection might reflect cytotoxicity rather than inhibiting infection, we measured in parallel cell viability using the commercially available "Cell titer 96 Aqueous Non-Radioactive Cell Proliferation Assay" kit (Promega), following manufacturer´s protocol. No significant effect on Vero cell viability was observed at any of the tested concentrations (see material and methods section).

5.2 IFN treatment induces expression of IFITM proteins

Once we have demonstrated that pre-treating Vero cells with universal type I IFN completely abrogates ASFV infection, we decided to analyze the induction of IFITM1, 2 and 3 upon this treatment in Vero and in 293T cells.

Cells were incubated with either 1,000 or 10,000 U/ml of universal type I IFN for 24 h. Protein lysates were then collected in Laemmli buffer for WB analysis. As shown in **Figure R27**, expression of IFITM1, 2 and 3 were detected after IFN treatment. We concluded that IFITM3 induction was higher than IFITM1 and IFITM2 in both cell lines.

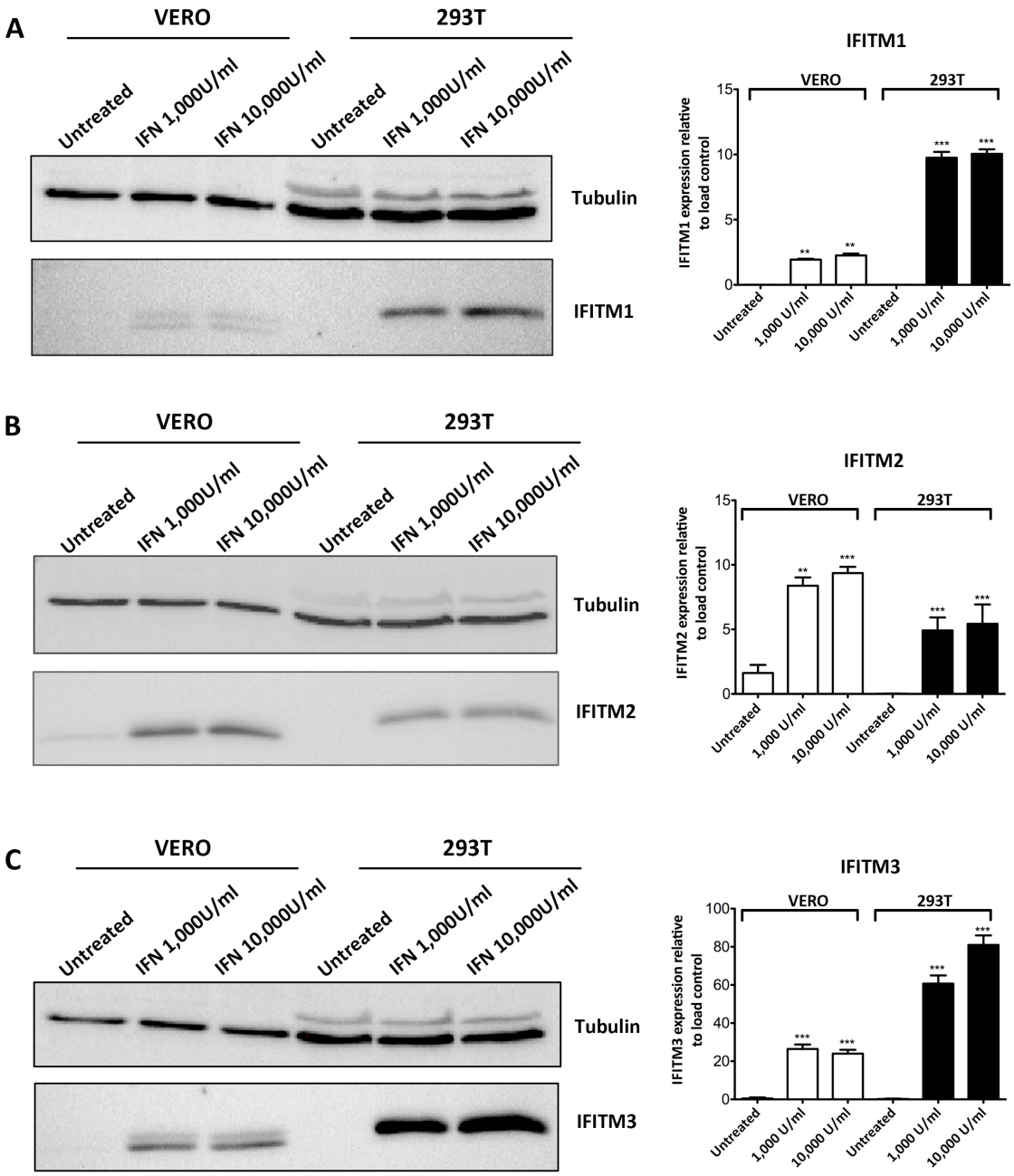

Figure R27. Interferon treatment induces expression of IFITM proteins. Expression of IFITM proteins was analyzed after treatment with Universal type I IFN. Vero and 293T cells were left untreated or pretreated with Universal type I IFN at concentrations of 1.000U/ml or 10.000U/ml respectively for 16 h. Cell extracts were incubated with antibodies against IFITM1 **(A)**, IFITM2 **(B)** and IFITM3 **(C)**. Right side panels represent WB quantification for each case. Data are expressed as mean±SD and asterisks denote statistically significant differences (**=P<0.01; ***=P<0.001; ns=non significant).

5.3 Generation and validation of IFITM-expressing cell lines

To further study and further understand the possible role of IFITMs in ASFV infection, we generated Vero cells stably expressing the human IFITM1, 2, 3 or the empty vector. Again, the method used to generate the stable cell lines was the lentiviral transduction system. Our proteins of interest were cloned into the pLVX vector (see material and methods section for more detailed experimental procedures). Positive transduced Vero stable cells were selected with 8 µg/ml of puromycin. Once these cells were established, expression of different IFITM proteins was confirmed by WB analysis. **Figure R28** shows levels of expression of IFITM 1, 2 and 3 of Vero stable cell lines respectively. The highest expression within the IFITM family members corresponded to IFITM3, followed by IFITM2 and IFITM1, which were expressed at significant lower levels. These findings confirmed previous results showing that IFITM3 is the most expressed protein of the IFITM family upon universal type I IFN in Vero cells.

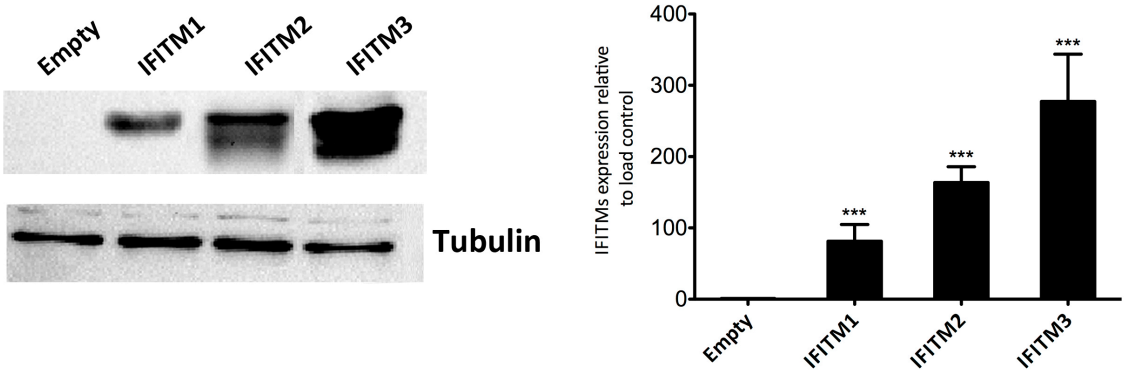

Figure R28. Generation and validation of IFITM-expressing cell lines. Analysis of IFITM1, 2 or 3 expression levels in Vero cells after lentiviral transduction. Data are expressed as mean±SD and statistically significant differences are marked with asterisks (***=P<0.001).

After assessing the expression levels of the different IFITMs in stable cell lines, we next wanted to ascertain their subcellular distribution. To that end, specific antibodies against each IFITM were used to detect protein expression in Vero cells by means of an IF assay. Expression of IFITM1, 2 and 3 in Vero stable cell lines was compared with the distribution of IFITMs in Vero cells with the empty vector.

Confocal microscopy revealed that upon overexpression, IFITM1 distributed mainly to the plasma membrane and, to a lesser extent, in perinuclear compartments resembling endosomal structures **(Figure R29A).** In contrast, endogenous IFITM1 was barely detected in Vero cells expressing the empty vector **(Figure R29A).**

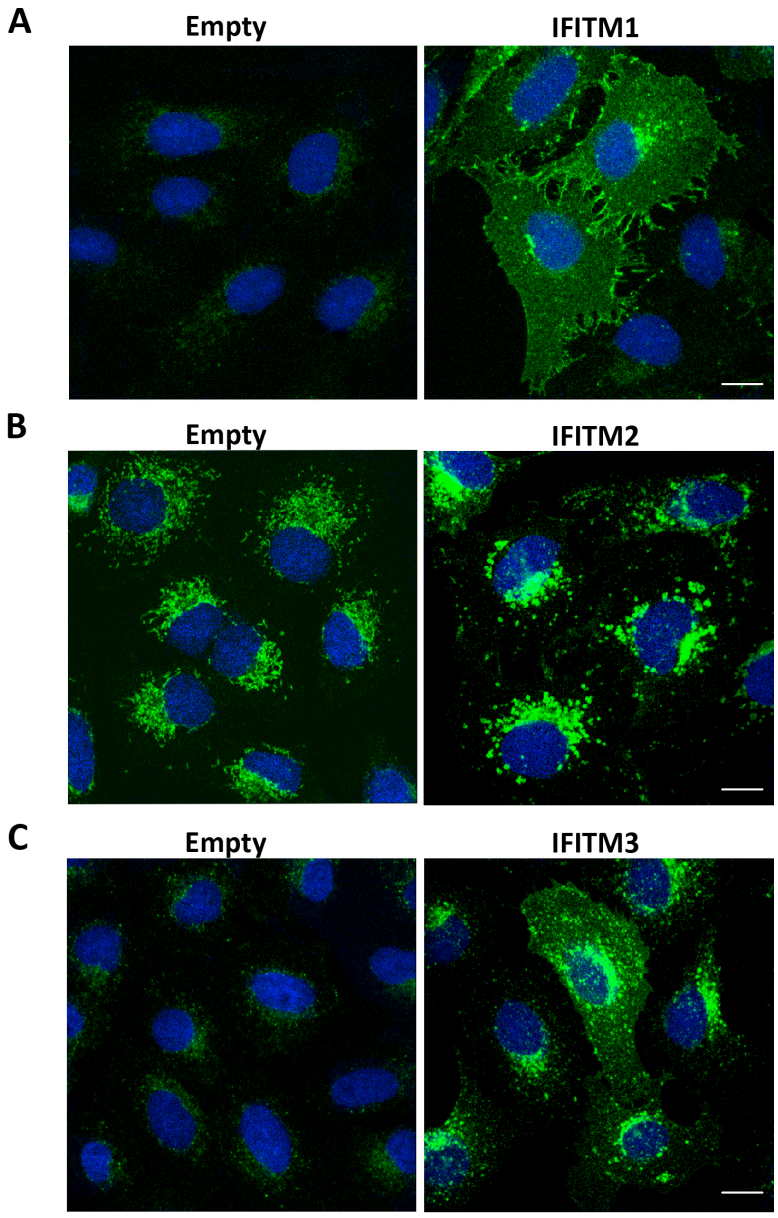

Figure R29. Generation and validation of IFITM-expressing cell lines. Cellular distribution of IFITMs, depicting different distribution patterns for each of protein: IFITM1 at the plasma membrane and at a perinuclear location **(A)**, IFITM2 in a perinuclear location resembling endosomal compartments **(B)** and IFITM3 in the cytoplasm, in perinuclear aggregates resembling endosomes and to a lesser extent at the plasma membrane **(C)**. Bar= 10 µm.

In the case of IFITM2, its overexpression led to a high accumulation in the perinuclear region, co-localizing with the contour of spherical structures that resemble endosomal compartments **(Figure R29B).** Intriguingly, in Vero cells expressing the empty vector, endogenous IFITM2 was also detected. **(Figure R29B).**

Finally, overexpressed IFITM3 was found highly accumulated in the perinuclear region, co-localizing with the aforementioned endosomal structures. IFITM3 was also detected in the plasma membrane to a lesser extent **(Figure R29C).** Endogenous IFITM3 was barely detected in Vero cells expressing the empty vector **(Figure R29C).**

5.4 IFITM2 and IFITM3 proteins restrict ASFV entry

In the section above, we characterized the distribution of IFITMs in Vero cells upon overexpression. Thus, we wanted to investigate whether overexpression of IFITMs could restrict ASFV infection, which is known to require acidic compartments for entry into host cells. We recently published that ASFV entry and egress from endosomal compartments depends on low pH in Vero cells (Cuesta-Geijo et al., 2012). Previous experiments in the laboratory revealed that under bafilomycin (Baf) treatment, viral decapsidation is stopped in Rab7-positive late endosomes, thus blocking viral infection progression (Cuesta-Geijo et al., 2012). Given that IFITM restriction is mediated along the endocytic pathway (Diamond and Farzan, 2013; Perreira et al., 2013), we hypothesized that IFITM overexpression may affect the virus entry processes and subsequent ASFV infection.

Then, we first analyzed the possible role of overexpressed IFITMs in viral entry. Viral entry steps include virus attachment to the host cell, internalization and decapsidation through the endocytic pathway until the virus is released into the cytoplasm to start replication.

Vero cells stably expressing IFITM1, 2, or 3 or with empty vector were infected with ASFVASFV (moi=5 pfu/cell). Infections were cold synchronized at 4°C for 90 min to enable virus attachment to the cell but restricting viral entry. Then, we allowed the infection proceed for 1 h and after this period, cells were treated with trypsin for 10 min to eliminate attached virions that finally did not enter into the cells as described in (Petersen et al., 2014). DNA from mock-infected cells or cells infected with ASFV was extracted and purified with the “DNAeasy blood and tissue kit” (Qiagen). Then, qPCR was performed to quantify the number of copies of the ASFV genome corresponding to the viral particles that had entered Vero cells stably expressing IFITM1, IFITM2, IFITM3 or the empty vector. The number of copies of the ASFV viral genome was quantified by amplifying a specific region of the p72 viral gene. As shown in **Figure R30,** IFITM2 and IFITM3 restricted ASFV entry and

subsequent viral replication. IFITM1, however, did not have any effect in viral entry, as levels of p72 vDNA were comparable to those obtained in the control cells.

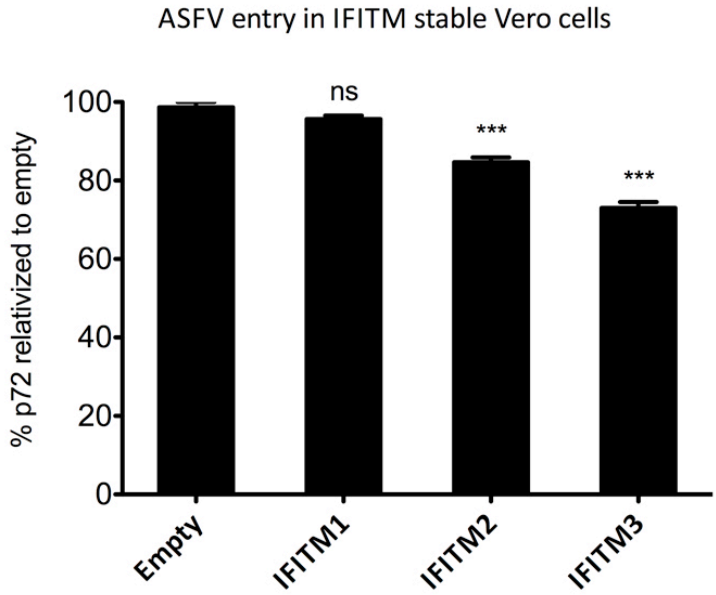

Figure R30. IFITM2 and IFITM3 restrict ASFV entry. Analysis of ASFV entry inhibition in cells stably expressing IFITM1, 2, or 3. Viral genome copy number was quantified by p72 levels. Graphics depict qPCR values normalized to control empty vector expressed as mean±SD. Statistically significant differences are marked with asterisks (***=P<0.001; ns=non significant).

5.5 IFITM2 and IFITM3 prevent ASFV uncoating

Once we determined that IFITMs restricted ASFV entry, our next goal was to ascertain which stage of the process was impaired. We investigated whether overexpression of IFITMs was affecting ASFV uncoating inside endosomal compartments. This was achieved by quantifying the number of p150 viral core particles that corresponds to decapsidated virions in these conditions.

Vero cells stably expressing IFITM1, 2, 3 and the empty vector were infected with ASFV as above described (moi=10 pfu/cell). Infection was cold synchronized at 4°C during 90 minutes. Then, cells were washed, and infection proceeded for 45 minutes. Presence of virions was quantified by IF assay, by labeling ASFV virions with an antibody against the viral inner core protein p150, which correspond to uncoated virions. Confocal microscopy revealed that the number of viral cores was severely decreased in cells stably expressing IFITM2 and IFITM3 respectively while in IFITM1 cells the amount of decapsidated virions was similar to control cells expressing the empty vector **(Figure R31)**.

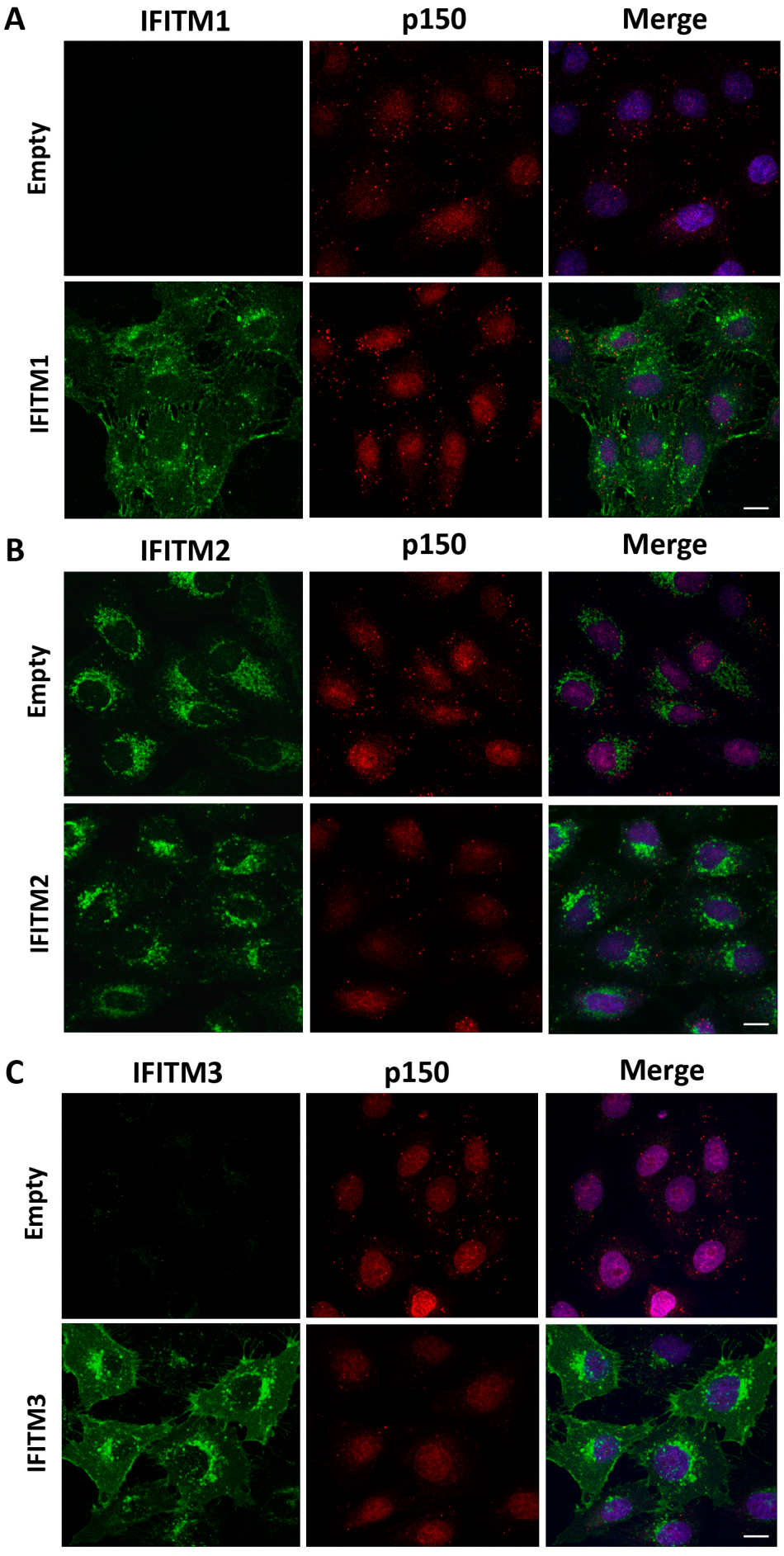
A
IFITM1
p150
Merge
Empty
IFITM1
B
IFITM2
p150
Merge
Empty
IFITM2
C
IFITM3
p150
Merge
Empty
IFITM3

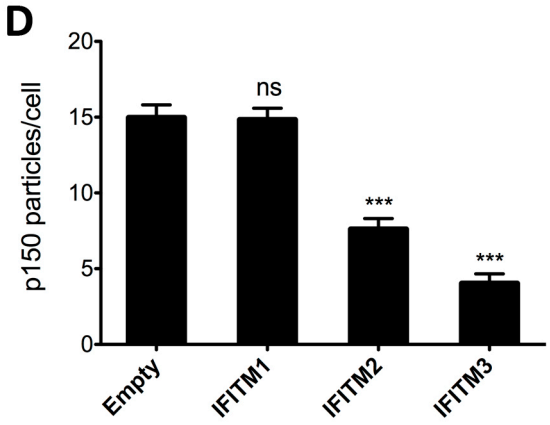

Figure R31. IFITM2 and IFITM3 impair ASFV uncoating. Analysis of uncoating of virions with ASFV inner core protein p150 (red) upon expression of IFITM1 **(A)**, IFITM2 **(B)** and IFITM3 **(C)**. **(D)** Graphical representation of p150 viral cores detected per cell for each condition. Data are expressed as mean±SD statistically significant differences are marked with asterisks (***=P<0.001; ns=non significant). Bar=10μm.

In conclusion, these data show that viral uncoating was the rate-limiting step in cells stably expressing IFITM2 and IFITM3 for ASFV.

5.6 IFITM2 and IFITM3 alter distribution of endosomal compartments

After concluding that IFITM2 and IFITM3 could be restricting ASFV entry and uncoating, we investigated the mechanism underlying this restriction. First, we searched for an alteration of the endosomal compartments in which viral decapsidation takes place (Cuesta-Geijo et al., 2012). To that end, we analyzed expression of endosomal markers EEA1 (early endosomes), CD63 (MVB), Rab7 (late endosomes, LE) and Lamp1 (lysosomes) in the different stable cells expressing IFITMs or the control empty vector **(Figure R32)**. This shows the normal distribution of the different maturation stages of endosomes and lysosomes with EEA1, CD63, Rab7 and Lamp1 dispersed throughout the cytoplasm in controls and also in IFITM1-expressing cells. However, in cells expressing IFITM2 and IFITM3, this distribution was lost showing perinuclear accumulation. This endosome relocation was analyzed in 3D (x, y, z) planes by measuring the mean distance between these endosomal markers and the cell nucleus, using the "Distance Measure" ImageJ plug-in **(Figure R32B)**. A total of 20 cells were analyzed for each condition.

We can conclude that IFITM2 and IFITM3 acted altering normal endosome distribution by accumulating these vesicles to the perinuclear region. This change in localization frequently reflects an alteration in endo-lysosomal maturation and function as it is shown below.

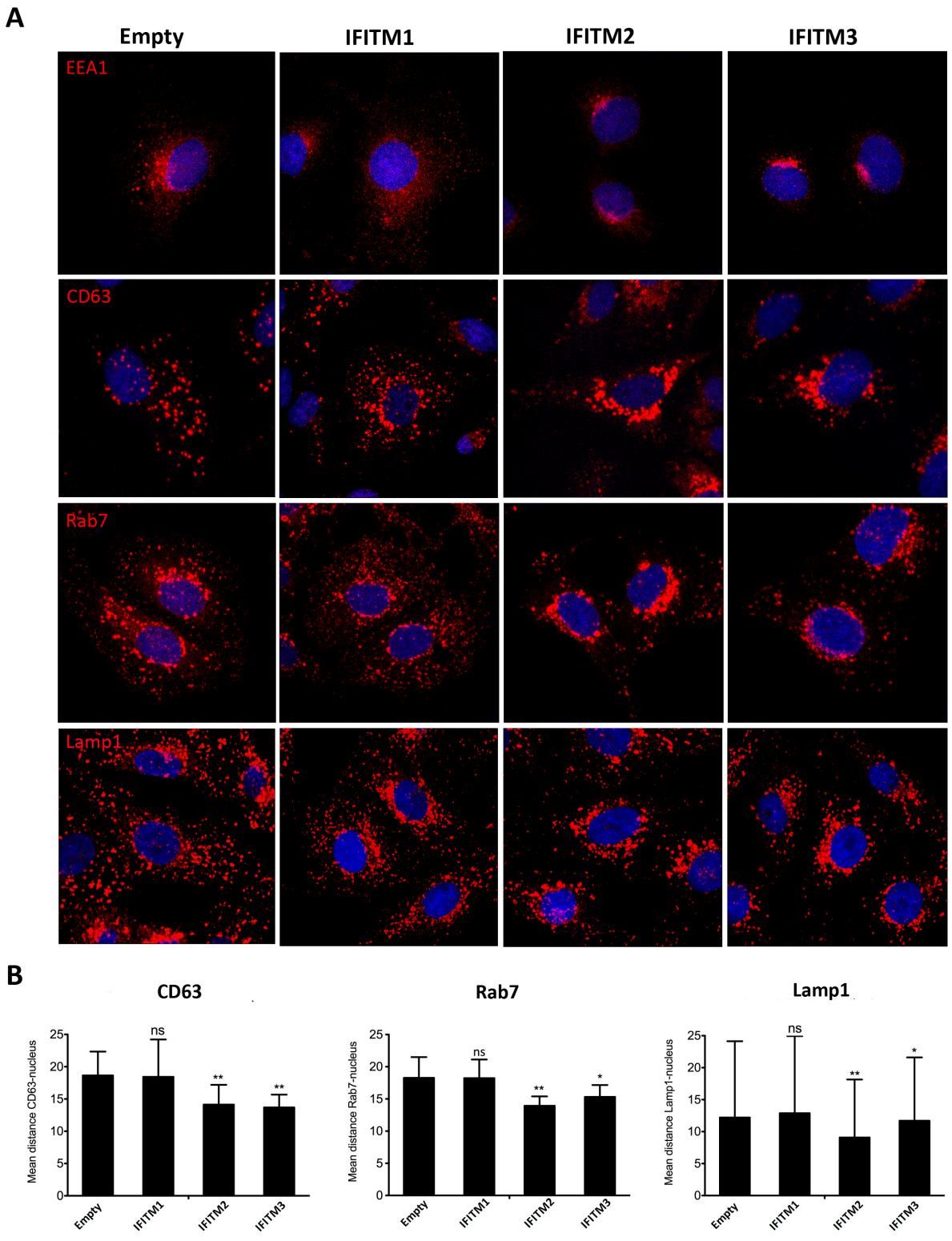

Figure R32. IFITM2 and IFITM3 alter distribution of endosomal compartments. (A) Analysis of distribution and accumulation of late endosomes with markers EEA1, CD63, Rab7 and Lamp1 (red) upon expression of IFITM1, 2 and 3.. Bar=10µm. **(B)** Endosomal relocalization was analyzed by measuring the mean distance between CD63, Rab7 and Lamp1 and the cell nucleus respectively in x, y and z planes using Distance Measure ImageJ plug-in. A total of 20 cells were analyzed for each condition. Plotted data are expressed as mean±SD and statistically significant differences are depicted with asterisks (*=P<0.05; **=P<0.01; ***=P<0.001; ns=non significant).

5.7 Colocalization of IFITMs with endosomal compartments

We have previously demonstrated that IFITM2 and IFITM3 alter the normal endosome compartments distribution. We next analyzed the colocalization rate between IFITMs and these endosomal structures. CD63 remains mainly associated with intracellular vesicular membranes and it is particularly abundant in endosomal structures called multivesicular Bodies (MVBs), which constitute a late and acidic endosomal compartment with a very relevant function in endosomal physiology for late endosome maturation.

Co-staining of IFITMs and CD63 by IF assay revealed a clear colocalization of IFITMs and CD63 in stable Vero cells **(Figure R33)**. The colocalization rate was analyzed with the "Leica Application Suite Advanced Fluorescence" software (LAS AF). Analysis revealed a colocalization rate of 75% in the case of IFITM2 and up to 40% in IFITM1 and IFITM3.

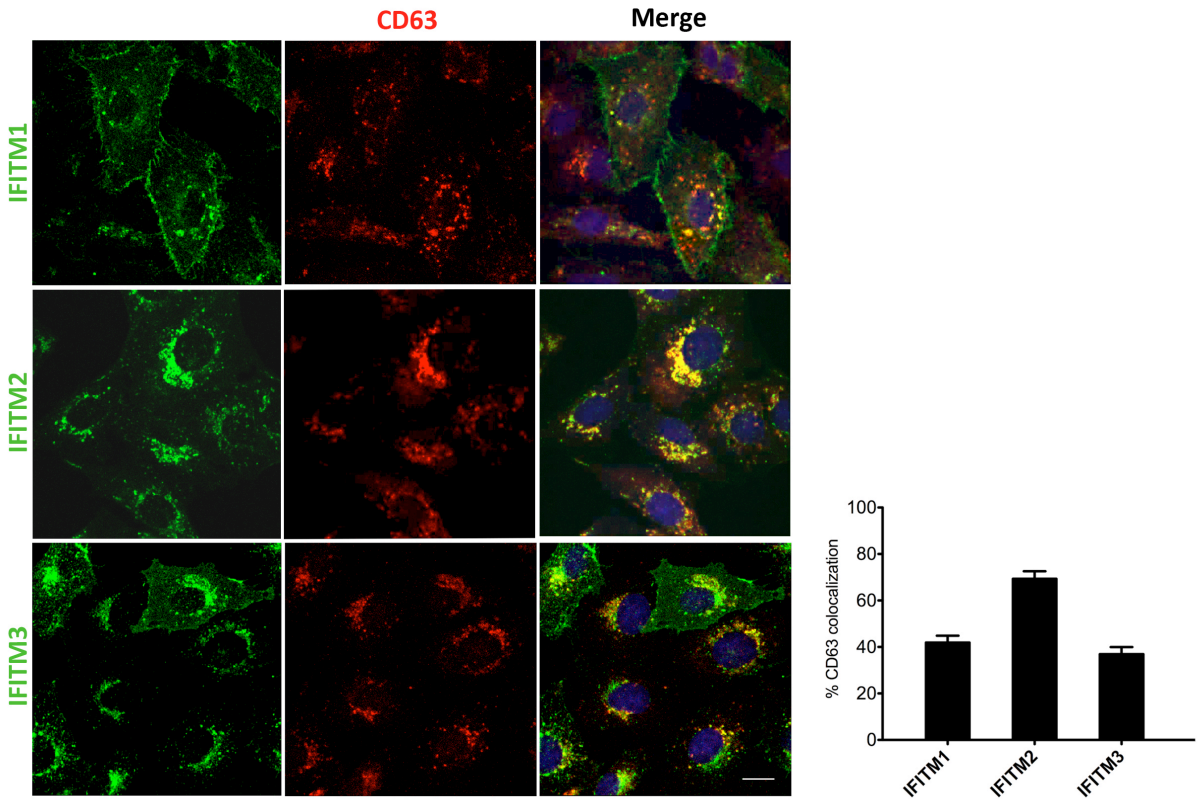

Figure R33. Colocalization of IFITMs with endosomal compartments. Expression of IFITM1, 2 and 3 proteins (green) and CD63-positive late endosomes (red). Data were plotted on graphics on the right side representing the colocalization rate values in each condition. Bar= 10µm.

5.8 IFITM2 and IFITM3 induce accumulation of cholesterol in endosomal compartments

IFITM2 was located primarily in endosomal compartments as indicated by its high colocalization with endosomal marker CD63. Colocalization was also visible but to a lesser

extent in IFITM 1 and 3 stably expressing cells. Furthermore, we demonstrated that overexpression of these proteins not only colocalize with late endosomal compartments, but also alter their normal distribution.

This alteration in endosomal distribution is similar to altered cholesterol efflux phenotype. In fact, a normal endosomal cholesterol efflux has been shown to be required for a correct endosomal function. Hence we analyzed intracellular and intraendosomal cholesterol in cells by using the histochemical cholesterol marker filipin. As shown in **Figure R34**, Vero cells stably expressing IFITM2 and IFITM3 showed much higher intracellular cholesterol levels than those expressing the empty vector. This cholesterol accumulation also colocalized with the IFITM-enriched endosomal vesicles. In contrast, in Vero cells stably expressing IFITM1, only discrete colocalization areas between IFITM1 and cholesterol were found at the plasma membrane.

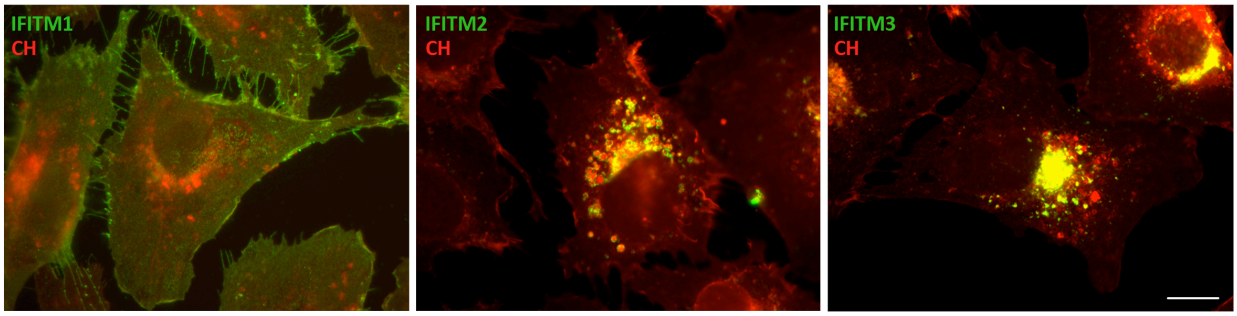

Figure R34. IFITM2 and IFITM3 induce accumulation of cholesterol in endosomal compartments. Analysis of the cholesterol distribution by specific marker filipin (red) in Vero cells stably expressing IFITM1, 2 or 3 (green). Bar=10µm.

These findings collectively indicate that IFITM2 and IFITM3 overexpression in Vero cells results in cholesterol accumulation in endosomal compartments, and subsequently may have a role inhibiting endosomal function and decapsidation upon viral entry.

5.9 IFITM2 induces autophagy and alters LC3 distribution

Also, these innate immunity proteins might act protecting the cells against viral infection by inducing autophagy. Then, we investigated the expression level and the distribution of autophagy marker LC3 upon overexpression of IFITMs. To that end, Vero cells stably expressing IFITM1, 2, 3 or the empty vector were co-stained with specific antibodies against the autophagosome-marker protein LC3 and against MVB/endosomal marker CD63. As shown in **Figure R35**, Vero cells stably expressing IFITMs presented a higher amount of

positive LC3 puncta when compared to Vero cells expressing the empty vector. Intriguingly, IFITM 2 stably expressing cells displayed a massive LC3 puncta accumulation in the cell nucleus periphery. At this cytoplasmic localization, it highly colocalizes with CD63-positive vesicles. In contrast, Vero cells expressing IFITM1 and IFITM3 showed dispersed LC3 distribution over the cell cytoplasm.

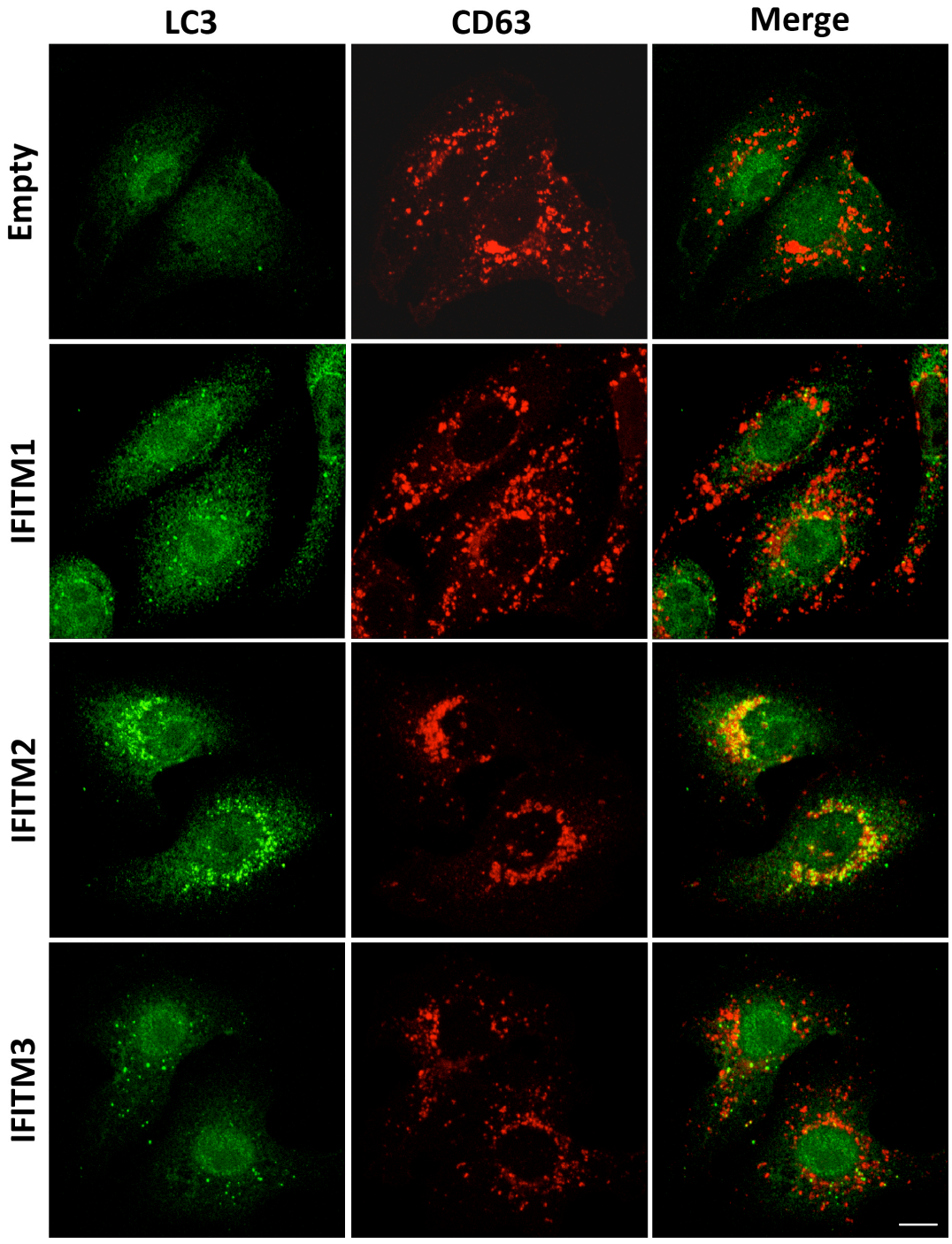

Figure R35. IFITMs induce autophagy and and alter LC3 distribution. Autophagosome distribution analysis in Vero cells stably expressing IFITM1, 2, 3 or the empty vector using autophagosome marker LC3 (green) and

late endosome marker CD63 (red). In IFITM 2 expressing cells, LC3 showed massive LC3 puncta accumulation in the perinuclear area, colocalizing with CD63 endosomal accumulation. Bar=10μm.

These findings suggest that IFITMs overexpression leads to autophagy induction and that IFITM2 overexpression causes a change in normal LC3-positive puncta distribution by recruiting them into specific areas around the cells nucleus that colocalize with late endosomal compartments.

Collectively, these results illustrate a close relationship between innate immunity proteins as IFITMs, the endosomal pathway and autophagy. In summary, IFITM antiviral action could rely on an alteration of the endosomal physiology and this should be object of further studies on antiviral targets at the molecular regulation of late endosome. The finding that IFITM2 expression induces a strong accumulation of LC3 puncta colocalizing with late endosomal marker CD63 will pave the way to future studies on the action of IFITMs in the crossroads of endo-lysosomal regulation and autophagy.

DISCUSSION

Several pathogens, particularly viruses, take advantage of the cellular machinery to fulfill their infectious cycle. Using different strategies to manipulate the host cell, viruses manage to accomplish different steps of the infection, including replication of the viral genome and evasion of the cell immune system response. Autophagy was classically defined as a dynamic process in charge of removing and recycling protein aggregates and damaged organelles. It is now regarded as a mechanism to counteract bacterial and viral infections, recognizing pathogen components to target them for lysosomal degradation. Furthermore, the number of pathways involved in autophagy has expanded over the last years, including the initiation steps of the innate and adaptive immune response upon viral infection (Dreux and Chisari, 2010; Saitoh and Akira, 2010; Sir and Ou, 2010).

Increasing evidence shows that viruses have evolved different strategies not only to evade or subvert autophagy, but also to take advantage of this cellular process. RNA viruses have been reported to benefit from the autophagic machinery by using autophagosome double-membrane vesicles to facilitate their replicative cycle. Such is the case of poliovirus, influenza A, hepatitis C and dengue virus (Richards and Jackson, 2013; Zhang et al., 2014). In contrast, other viruses require inhibition of autophagy to achieve a successful infection (Ku et al., 2008; Pattingre et al., 2005).

Our initial goal in this current work was to study how ASFV regulates autophagy. Since previous reports had not been described this interaction in detail, we designed different strategies to analyze autophagy in the context of ASFV infection. The lipidation of microtubule-associated protein light chain 3 (LC3) is hallmark of autophagy. Upon induction, LC3 cytosolic form (LC3-I) is conjugated to the phospholipid phosphatidylethanolamine (PE) to form the LC3-PE conjugate (LC3-II). This conjugated or lipidated LC3 form is targeted to autophagosomal membranes (Tanida et al., 2008). In fact, conjugation of LC3 occurs at all phases of autophagosome membrane formation and therefore may be useful to monitor the dynamic process of the autophagosome formation.

Initially, we used GFP-tagged LC3 (GFP-LC3) protein to study autophagy in the context of ASFV. Even though we successfully monitored autophagosome formation by transient expression of GFP-LC3 in Vero cells, experiments in the context of ASFV infection could not be performed, due to reductions in cell infectivity after transfection. Moreover, several caveats involving GFP-LC3 transfection have been reported (Hu et al., 2012). Thus, we have

established a method of monitoring autophagosome formation by LC3 expression using a lentiviral transduction system in Vero cells. In order to validate our LC3-expressing Vero (Vero-LC3) cells, we characterized the expression, the subcellular localization and the correct conjugation of this protein. We also confirmed that autophagy was not constitutively active upon LC3 overexpression and that Vero-LC3 cells were equally susceptible to ASFV infection when compared to control cells.

Our findings showed a rapid activation of PI3K/AKT/mTOR signaling cascade through Akt phosphorylation in both Ser-473 and Thr-308 residues early after ASFV infection. This is coincident with previous reports that targeted ASFV infection as an activator of the Akt pathway (Sanchez et al., 2012). This activation leads to an early inhibition of autophagy, a viral mechanism that has been also described for other DNA viruses to promote a more efficient infection (Cooray, 2004). It is interesting to highlight that levels of Akt phosphorylation decreased initially 5 min after infection with ASFV. This reduction correlated with our analysis of LC3-II/LC3-I ratio that showed increased autophagosome formation at 5 mpi. This initial peak of activation can be postulated as an early innate immune response of the cell in the presence of ASFV. Due to the fast entry of the virus into the host cell that occurs within the first hour postinfection (Cuesta-Geijo et al., 2012), our hypothesis is that ASFV might exploit this early transient cell activation to its own benefit, sequestering some components of the autophagosome machinery that will be subsequently used as membrane supplies for viral replication.

ASFV infection does not induce autophagy, neither at early nor at late postinfection times, as revealed by the lack of autophagosomes in the cell. This absence of autophagosome formation was confirmed by using different autophagy inducers as controls. Interestingly, the classical inducer rapamycin yielded a very discrete effect in autophagy levels when compared to the other treatments. This might be due to the allosteric nature of rapamycin in inefficiently inhibiting mTORC1 signaling (Petroulakis et al., 2006). However, treatment with recently discovered autophagy inducer PP242 achieved a stronger induction, as it has been described to be specifically interacting with the catalytic site of mTORC1 (Jacinto et al., 2006).

A massive accumulation of LC3 was detected in ASFV-infected cells that lacked autophagosome formation. This abnormal distribution of LC3 was localized in the

perinuclear region and it colocalized with the viral factory (VF). A similar pattern in LC3 accumulation has been described in vaccinia virus (VV), which its infection also inhibits autophagy in the cell (Moloughney et al., 2011).

In order to further characterize the virus-host interaction in the ASFV-mediated regulation of autophagy, we investigated potential candidates that could be involved in this process. Several genes from other DNA viruses had been already described to inhibit autophagy. This is the case of human herpesvirus 1 (HSV1), which was reported to inhibit autophagy via the interaction of viral protein ICP 34.5 with the host protein Beclin1. Viral Bcl2 homologs encoded by Kaposi's sarcoma herpesvirus (KSHV) and murine gamma-herpesvirus 68 (ϒ-HV68) also inhibit autophagy by a mechanism involving direct interaction with Beclin1 autophagic protein (Ku et al., 2008; Pattingre et al., 2005).

Cellular Bcl2 (cBcl2), the prototype apoptosis inhibitor, has been demonstrated to be an interconnection between autophagy and apoptosis as it negatively regulates autophagy by binding to Beclin1 (Kraft et al., 2010; Sinha et al., 2008). We previously reported that the ASFV cBcl2 homolog, A179L, interacts with pro-apoptotic BH3-only proteins to inhibit apoptosis (Galindo et al., 2008). This interaction was found not only for several BH3-only proteins, such as activated Bid, Bim, Bad, Bmf, Bik, Puma, and DP5 but also for the cellular core pro-apoptotic machinery represented by Bax and Bak.

A similar mechanism of action was described for HS68 vBcl2 (Galindo et al., 2008; Kabeya et al., 2000). HV68 vBcl2 is even more potent than cellular Bcl2, but while HV68 vBcl2 is dispensable for acute HV68 infection, A179L is an essential gene for viral infection (Alonso et al., 2001).

Taking all this into consideration, we tested A179L in the context of autophagy. In this work, we have shown that the ASFV Bcl2 homolog interacts directly with Beclin1 and that the BH3 domain of A179L is required for this binding. Moreover, A179L was found to colocalize with mitochondria and the ER. We propose that the localization of this viral gene to these two organelles is crucial for this protein to exert a dual function in the inhibition of apoptosis and autophagy. Conversely, we did not find an interaction between Beclin1 and the HSV ICP34.5 ASFV homolog *DP71L*. This suggests that these two viral genes differentially exert their function. *DP71L* would control the unfolded protein response while A179L would

harbor the autophagy inhibition function through its interaction with Beclin1. However, these two pathways are thought to be closely related (Criollo et al., 2010; Fimia and Piacentini, 2010).

The capacity of A179L to interact with Beclin1 led us to study the specific role for A179L in the inhibition of autophagosome formation. In the present work, we linked a reduction in the number of autophagosomes with overexpression of A179L, suggesting a role in counteracting the effect of starvation conditions thus preventing autophagosome formation.

We further characterized early steps of ASFV-mediated autophagy regulation in time-of-addition experiments. Induction of autophagy before or immediately after viral infection was detrimental to ASFV replication, demonstrating that the interaction between the virus and autophagy is a dynamic, tightly regulated process during the first hours after infection.

To further confirm whether ASFV targets the autophagic pathway through the inhibition of the autophagosome formation, we analyzed other components of the process, such as the regulation of the autophagic flux by the virus.

The lack of autophagosomes in ASFV-infected cells may be due to either a lack of autophagosome biogenesis or alternatively, due to an extremely high efficiency of autophagy flux. To differentiate these two possibilities we determined the effect of ASFV infection by disrupting the autophagy flux. Bafilomycin A1 (Baf) is a drug that inhibits degradation of autolysosome content by inhibiting the $Na^{+}H^{+}$ pump at the lysosome, thereby blocking LC3 degradation and autophagosome turnover at the lysosome (Rubinsztein et al 2009). In the presence of Baf, accumulation of LC3-II positive puncta would be indicative of efficient autophagic flux, while failure of LC3-II increasing levels in the presence of this inhibitor would be an evidence of a defect in the process prior to degradation at the lysosome (Barth et al 2009). Upon Bafilomycin A1 treatment in ASFV-infected cells, LC3 accumulation was not found in infected cells, supporting that the presence of ASFV disrupts the required cellular machinery for autophagosome formation. A similar effect was also found in vaccinia virus (Moloughney et al., 2011).

To further understand the interaction between ASFV A179L and Beclin1 to inhibit autophagosome formation, we tested whether inducing autophagy in ASFV-infected cells

could revert the virus-mediated inhibition. Our experiments revealed that the effect of ASFV infection upon autophagy could not be reverted by most of the autophagy inducers that we tested. Acquirement of a resistance to autophagy induction has been reported in cells infected by other viruses (Chaumorcel et al., 2008). Interestingly, tamoxifen was the only inducer that reverted the effect of the virus, probably due to its robust induction. Addition of tamoxifen after ASFV infection induced autophagy and also led to VF disaggregation. Taking into consideration that tamoxifen treatment drastically inhibited ASFV infection at early and late postinfection times, it might be interesting to consider tamoxifen in future anti-viral treatments against this virus. Because it takes a great deal of time and money to develop a new drug from a novel chemical compound, it may be easier to use previously approved drugs such as tamoxifen in new applications. Recently reported experiments performed in HCV virus revealed that tamoxifen affects both viral binding and other post-binding events including endocytosis (Murakami et al., 2013).

In our experiments, among all the inhibitors of autophagy tested in the context of ASFV, 3MA inhibitor was used as a negative regulator of ASFV infection. However, since its effect was so broad, affecting several cellular pathways (Caro et al., 1988; Punnonen et al., 1994; Xue et al., 2002), we decided to use a more specific strategy to inhibit autophagy in the context of ASFV. Silencing of ATG5, an E3-ubiquitin ligase essential for autophagosome elongation, was used to target and inhibit the autophagy process. This inhibition negatively affected ASFV infection at both early and late postinfection times. Jointly with results obtained with chemical inhibitors, this suggests that even though the virus inhibits autophagy in infected cells, ASFV may be dependent on the molecular pathway of early autophagosome formation to fulfill its infectious cycle.

Taking into account the fact that LC3 accumulated in the ASFV viral factory (VF), we further analyzed the origin of this viral replication organelle and the similarities with the aggresome. The major steps in viral replication and assembly occur at the viral factory, where all the components to form nascent virions accumulate (Brookes et al., 1996; Nunes et al., 1975; Rouiller et al., 1998). Some authors postulated that similarities between aggresomes and ASFV VF raise the possibility that ASFV uses the aggresome pathway to concentrate cellular and viral proteins, thus facilitating replication and assembly (Netherton and Wileman, 2013) as in other viral diseases (Taylor et al., 2003).

We used several recombinant viruses generated in our lab to study the morphology of the viral replication organelle. It was a single and large structure located near the nucleus lacking a surrounding membrane. It was found typically in the microtubule-organizing center (MTOC), a perinuclear site from where microtubules irradiate to the periphery. Accumulation of fluorescent viral proteins was measured and analyzed in x, y and z planes by confocal microscopy. Moreover, viral DNA, detected by Topro-3 staining did not show a complete superposition with viral proteins in VFs. These observations suggest an organization with segregated functions for DNA replication and viral protein synthesis in VFs. Further studies will be required to confirm this hypothesis. The intermediate filament cytoskeleton (vimentin) characteristically surrounded this structure when it is fully formed. It appeared surrounded by mitochondria but there are not recognizable organelles within this structure when analyzed by electron microscopy (Quetglas et al, 2012). Also, we compared VF morphology in two cell lines that have a different origin. Vero cells are green monkey fibroblasts and WSL are wild swine lung cells. Our findings showed that formation of VFs in WSL cells yielded significantly larger organelles than in Vero cells (Alonso et al., 2013). This can be probably due to the fact that WSL cells better mimic the original host of ASFV.

Then, based in these morphology data of viral factories resembling aggresomes, we further analyzed VF formation as a sequestration of cytoplasmic proteins in these structures. We tested the two canonical aggresome formation pathways that involve HDAC6 and BAG3 proteins. Inhibition of either HDAC6 or BAG3 did not affect the number, formation nor the morphology of VFs. Hence, although the morphology of ASFV VF is similar to that of aggresomes, the mechanism by which these structures are formed was apparently not related. This cannot exclude the possibility of finding new aggresome formation routes that remain unexplored to date.

We have shown here that ASFV infection requires a precise regulation of the autophagy to avoid virus clearance in autophagosomes. In contrast, this process should be strongly inhibited for the virus to establish its replication site and build its replication organelle. Moreover, strong autophagy inductors such as tamoxifen were able to fragment and disperse the ASFV viral factory once it was fully formed. Hence, autophagy regulation appears an important process in the context of ASFV infection.

In our goal to further characterize the interaction between ASFV and the host cell, we focused our attention to the innate immunity pathway. Autophagy has been recently related to the immune response of the cell. The autophagic sequestration of viral components can fuel MHC class II of endogenous antigens (Menendez-Benito and Neefjes, 2007) and the production of type I interferons (IFN) in response to Toll-like receptor 7 (TLR7) (Lee et al., 2007). ASFV has been reported to be modulating the IFN response through different mechanisms. For instance, the A276R viral protein impairs the induction of IFNβ through targeting IRF3 but not IRF7 in a NFκB-independent manner (Correia et al., 2013). Another example is I329L, a viral TLR3 homolog that inhibits the induction of IFN (de Oliveira et al., 2011).

The innate immune response provides the first line of defense against viral infection. That is why many viruses target the IFN pathway in order to counteract the cell response against them. In this thesis, we have studied the possible role of a novel family of IFN-induced proteins (IFITM) in ASFV infection. IFITMs have been reported to inhibit infection of several RNA viruses (Brass et al., 2009), but at the start of this thesis there was nothing published about a possible role of IFITMs in DNA viruses.

After initial confirmation of ASFV susceptibility to IFN treatment, we generated stable IFITM-expressing Vero cells to pursue our experiments. Validation of the stable IFITM expression showed comparable levels to those found in IFN-induced wild type cells. Coincident with previous publications in other cell lines (Feeley et al., 2011a; Huang et al., 2011a), overexpression of IFITM1, 2 or 3 resulted in the exogenous proteins localizing to expanded late endosomal and lysosomal compartments. For endogenous IFITMs, IFITM1 has been reported to be located in the plasma membrane and early endosomes while IFITM2 and 3 are found in late endosomes and lysosomes (Feeley et al., 2011a; Huang et al., 2011a). We could not confirm cellular localization of endogenous IFITM1 and 3, probably due to the lack of specificity of the antibodies to detect simian IFITMs. However, endogenous IFITM2 expression was localized around the nucleus in structures that could resemble mitochondria. This pattern changed when exogenous IFITM2 were expressed, adopting an endosomal distribution. To verify this finding, a double staining against mitochondria and IFITM2 would be required.

Expression of IFITM2 and 3 inhibited ASFV entry. This has been previously reported for other viruses (Diamond and Farzan, 2013). IFITM-mediated viral inhibition has been related to impaired viral-host membrane fusion subsequent to viral binding and endocytosis (Feeley et al., 2011a; Huang et al., 2011a). Also, IFITM3 has been reported to modulate the fluidity and the bending modulus of the cell membrane making it resistant to viral fusion machinery (John et al., 2013).

To test whether ASFV release from the late endosomal compartment was altered in the presence of IFITMs, we analyzed viral uncoating by detecting core viral protein p150. It is important to note that p150 is only detected in uncoated viruses. In the presence of IFITM2 and IFITM3, uncoating of ASFV was decreased, which correlates with the reduction in the number of viral particles entering the cell.

Once we determined the antiviral effect of IFITM2 and IFITM3 in ASFV infection, we hypothesized that this inhibition could be due to an alteration of the endosomal compartments. Analysis of their distribution upon IFITM overexpression revealed that IFITM2 and IFITM3 altered the normal distribution of early and late endosomes and lysosomes. However, this alteration was not found in the presence of IFITM1.

This novel finding supports the above described antiviral role of IFITM2 and IFITM3, since changes in the distribution of the endosomes and the lysosomes could affect viral entry by this pathway. This has special relevance in our model, due to the importance of the endosomal pathway integrity in the context of ASFV infection (Cuesta-Geijo et al, 2012).

IFITM3 has been previously reported to alter the cholesterol homeostasis at the late endosome, leading to cholesterol accumulation and blocking the viral release (Amini-Bavil-Olyaee et al., 2013). In the present study, we proved the presence of cholesterol accumulation upon IFITM2 and IFITM3 overexpression. Taking these findings together with the fact that IFITM2 and IFITM3 are inhibiting ASFV entry, we can hypothesize a mechanism to achieve this inhibition by altering the endosomal pathway, interrupting the cholesterol efflux from the endosome. This is supported by recent findings in our lab that revealed a strong inhibition of ASFV infection upon treatment with drug U18666A that exerts its function by blocking the exit of cholesterol from the endosomal compartments to other

cellular destinations (unpublished data). This causes severe alterations of endosomal maturation and traffic.

We finally studied possible alternative mechanisms underlying IFITM-mediated inhibition of ASFV infection. Therefore, we hypothesized that IFITMs could also exert their antiviral activity by inducing autophagy. Recent data showed that IFITM3 could induce autophagy by analysis of LC3 protein levels (Yount et al., 2012). Taking a similar approach, we found that autophagy levels were increased in the presence of all IFITM1, 2 and 3 proteins, being IFITM2 the highest inducer. Moreover, overexpression of IFITM2 seemed to affect the normal distribution of LC3, adopting a perinuclear pattern colocalizing with late endosomal compartments.

Collectively, these results illustrate a close relationship between innate immunity proteins IFITMs, the endosomal pathway and autophagy. In summary, IFITM antiviral action could rely on an alteration of the endosomal physiology and ongoing studies of our laboratory will focus on antiviral targets at the molecular regulation of late endosome. The finding that IFITM2 expression induces a strong accumulation of LC3 puncta colocalizing with late endosomal marker CD63 will pave the way to future studies on the action of IFITMs in the crossroads of endo-lysosomal regulation and autophagy.

CONCLUSIONS

1. We have established a novel method to monitor autophagosome formation through the stable expression of LC3 protein. This model allows detecting expression and subcellular localization of autophagosomal organelles while preserving normal autophagic competence upon starvation stimuli and upon viral infection.

2. ASFV mediates an inhibition of the autophagy process that persists during the whole infective cycle to ensure optimal viral replication. The infection begins with a brief induction of autophagy immediately after viral entry, followed by a stable and strong inhibition that impairs autophagosome formation that could result in viral clearance.

3. ASFV infection tightly regulates the autophagic pathway. On the one hand it impairs normal autophagic flux and on the other hand it requires this pathway integrity for infectivity and viral factory formation. This has been shown independently with ATG5 silencing and several autophagy inhibitors.

4. ASFV-mediated autophagy inhibition is achieved by the interaction of Bcl2 viral homolog A179L with Beclin1 through its BH3 domain. Point mutation G85A of A179L failed to interact with Beclin1, as described for cBcl2.

5. ASFV viral factory is a single, large cytoplasmic organelle located in the perinuclear area. Intermediate filaments cage around this structure resemble an aggresome. ASFV viral factories are not real aggresomes, as inhibition of both canonical pathways involved in aggresome formation BAG3 and HDAC6, did not alter viral factory formation.

6. IFITMs are a group of transmembrane proteins induced by IFN that have a role in inhibiting several viruses. We have described that IFITM 2 and IFITM3 have an antiviral effect against ASFV.

7. The antiviral mechanism underlying IFITM2 and IFITM3 action against ASFV infection is based in restricting viral entry, due to alterations in endosomal compartments, changes in the cholesterol homeostasis, as well as in the induction of autophagy.

CONCLUSIONES

1. Hemos establecido un nuevo método para monitorizar la formación de autofagosomas mediante la expresión estable de la proteína LC3. Este modelo permite detectar la expresión y la localización subcelular de autofagosomas a la vez que se preserva la competencia autofágica de las células ante estímulos como la deprivación de nutrientes y la infección por el virus.

2. El VPPA produce una inhibición de la autofagia que persiste a lo largo de todo su ciclo infectivo con el fin de asegurar una replicación viral óptima. La infección se inicia con una breve inducción de autofagia inmediatamente después de la entrada del virus que se sigue de una inhibición fuerte y estable que anula la formación de autofagosomas y la posible eliminación del virus.

3. El VPPA regula minuciosamente la ruta autofágica, ya que por un lado inhibe el flujo autofágico normal y por otro requiere la integridad de esta vía para la infectividad y la formación de las factorías virales. Esto se ha demostrado tanto con el silenciamiento de ATG5 como con distintos inhibidores del proceso autofágico.

4. En la búsqueda de proteínas virales implicadas en esta inhibición de la autofagia, se demostró que está mediada por la interacción de A179L, el homólogo viral a Bcl2 con Beclin1 a través del dominio BH3. La mutación puntual G85A anula la capacidad de interacción con Beclin1, del mismo modo que el Bcl2 celular.

5. La factoría viral formada por el VPPA es una estructura única de gran tamaño y localizada en la zona perinuclear similar a un agresoma. Sin embargo, no se trata realmente de un agresoma, ya que la inhibición de las vías involucradas en la formación del agresoma BAG3 y HDAC6, no alteraron la formación de estos orgánulos de replicación viral.

6. Los IFITMs son un grupo de proteínas inducibles por interferón que desempeñan un papel antiviral frente a diversos virus. Hemos descrito por primera vez que IFITM2 e IFITM3 tienen un efecto antiviral frente al VPPA.

7. El mecanismo antiviral de las proteínas IFITM2 e IFITM3 frente al VPPA, se basa en la restricción a nivel de la entrada del virus mediante alteraciones en los compartimentos endosomales, cambios en la homeostasis del colesterol e inducción de la autofagia.

REFERENCES

Abban, C.Y., Meneses, P.I., 2010. Usage of heparan sulfate, integrins, and FAK in HPV16 infection. Virology 403, 1-16.

Afonso, C.L., Piccone, M.E., Zaffuto, K.M., Neilan, J., Kutish, G.F., Lu, Z., Balinsky, C.A., Gibb, T.R., Bean, T.J., Zsak, L., Rock, D.L., 2004. African swine fever virus multigene family 360 and 530 genes affect host interferon response. J Virol 78, 1858-1864.

Ait-Goughoulte, M., Kanda, T., Meyer, K., Ryerse, J.S., Ray, R.B., Ray, R., 2008. Hepatitis C virus genotype 1a growth and induction of autophagy. Journal of virology 82, 2241-2249.

Alcami, A., Carrascosa, A.L., Vinuela, E., 1989. The entry of African swine fever virus into Vero cells. Virology 171, 68-75.

Alessi, D.R., Pearce, L.R., Garcia-Martinez, J.M., 2009. New insights into mTOR signaling: mTORC2 and beyond. Science signaling 2, pe27.

Almazan, F., Rodriguez, J.M., Andres, G., Perez, R., Vinuela, E., Rodriguez, J.F., 1992. Transcriptional analysis of multigene family 110 of African swine fever virus. J Virol 66, 6655-6667.

Almazan, F., Rodriguez, J.M., Angulo, A., Vinuela, E., Rodriguez, J.F., 1993. Transcriptional mapping of a late gene coding for the p12 attachment protein of African swine fever virus. J Virol 67, 553-556.

Alonso, C., Galindo, I., Cuesta-Geijo, M.A., Cabezas, M., Hernaez, B., Munoz-Moreno, R., 2013. African swine fever virus-cell interactions: from virus entry to cell survival. Virus Res 173, 42-57.

Alonso, C., Miskin, J., Hernaez, B., Fernandez-Zapatero, P., Soto, L., Canto, C., Rodriguez-Crespo, I., Dixon, L., Escribano, J.M., 2001. African swine fever virus protein p54 interacts with the microtubular motor complex through direct binding to light-chain dynein. Journal of virology 75, 9819-9827.

Amini-Bavil-Olyaee, S., Choi, Y.J., Lee, J.H., Shi, M., Huang, I.C., Farzan, M., Jung, J.U., 2013. The antiviral effector IFITM3 disrupts intracellular cholesterol homeostasis to block viral entry. Cell Host Microbe 13, 452-464.

Anderson, E.C., Hutchings, G.H., Mukarati, N., Wilkinson, P.J., 1998. African swine fever virus infection of the bushpig (Potamochoerus porcus) and its significance in the epidemiology of the disease. Veterinary microbiology 62, 1-15.

Andjelkovic, M., Alessi, D.R., Meier, R., Fernandez, A., Lamb, N.J., Frech, M., Cron, P., Cohen, P., Lucocq, J.M., Hemmings, B.A., 1997. Role of translocation in the activation and function of protein kinase B. The Journal of biological chemistry 272, 31515-31524.

Andres, G., Garcia-Escudero, R., Salas, M.L., Rodriguez, J.M., 2002. Repression of African swine fever virus polyprotein pp220-encoding gene leads to the assembly of icosahedral core-less particles. J Virol 76, 2654-2666.

Andres, G., Garcia-Escudero, R., Simon-Mateo, C., Vinuela, E., 1998. African swine fever virus is enveloped by a two-membraned collapsed cisterna derived from the endoplasmic reticulum. J Virol 72, 8988-9001.

Andres, G., Garcia-Escudero, R., Vinuela, E., Salas, M.L., Rodriguez, J.M., 2001. African swine fever virus structural protein pE120R is essential for virus transport from assembly sites to plasma membrane but not for infectivity. J Virol 75, 6758-6768.

Andres, G., Simon-Mateo, C., Vinuela, E., 1997. Assembly of African swine fever virus: role of polyprotein pp220. J Virol 71, 2331-2341.

Angulo, A., Vinuela, E., Alcami, A., 1992. Comparison of the sequence of the gene encoding African swine fever virus attachment protein p12 from field virus isolates and viruses passaged in tissue culture. J Virol 66, 3869-3872.

Angulo, A., Vinuela, E., Alcami, A., 1993. Inhibition of African swine fever virus binding and infectivity by purified recombinant virus attachment protein p12. J Virol 67, 5463-5471.

Arias, M., Sanchez-Vizcaino, J.M., Morilla, A., Yoon, K.J., Zimmerman, J.J., 2002. African Swine Fever Eradication: The Spanish Model, Trends in Emerging Viral Infections of Swine. Iowa State Press, pp. 133–139.

Ashford, T.P., Porter, K.R., 1962. Cytoplasmic components in hepatic cell lysosomes. The Journal of cell biology 12, 198-202.

Bakkali, L., Guillou, R., Gonzague, M., Cruciere, C., 1994. A rapid and sensitive chemiluminescence dot-immunobinding assay for screening hybridoma supernatants. Journal of immunological methods 170, 177-184.

Baroudy, B.M., Venkatesan, S., Moss, B., 1982. Incompletely base-paired flip-flop terminal loops link the two DNA strands of the vaccinia virus genome into one uninterrupted polynucleotide chain. Cell 28, 315-324.

Basta, S., Gerber, H., Schaub, A., Summerfield, A., McCullough, K.C., 2010. Cellular processes essential for African swine fever virus to infect and replicate in primary macrophages. Vet Microbiol 140, 9-17.

Bech-Nielsen, S., Fernandez, J., Martinez-Pereda, F., Espinosa, J., Perez Bonilla, Q., Sanchez-Vizcaino, J.M., 1995. A case study of an outbreak of African swine fever in Spain. Br Vet J 151, 203-214.

Behrends, C., Sowa, M.E., Gygi, S.P., Harper, J.W., 2010. Network organization of the human autophagy system. Nature 466, 68-76.

Beltrán-Alcrudo, D., Guberti, V., de Simone, L., DeCastro, J., Rozstalnyy, A., Dietze, K., Wainwright, S., Slingenbergh, J., 2009. African swine fever spread in the Russian Federation and the risk for the region. EMPRES Watch.

Beltrán-Alcrudo, D., Lubroth, J., Depner, K., De La Rocque, S., 2008. African swine fever in the Caucasus. EMPRES Watch.

Bernardes, C., Antonio, A., Pedroso de Lima, M.C., Valdeira, M.L., 1998. Cholesterol affects African swine fever virus infection. Biochim Biophys Acta 1393, 19-25.

Borca, M.V., Carrillo, C., Zsak, L., Laegreid, W.W., Kutish, G.F., Neilan, J.G., Burrage, T.G., Rock, D.L., 1998. Deletion of a CD2-like gene, 8-DR, from African swine fever virus affects viral infection in domestic swine. J Virol 72, 2881-2889.

Borca, M.V., Irusta, P.M., Kutish, G.F., Carillo, C., Afonso, C.L., Burrage, A.T., Neilan, J.G., Rock, D.L., 1996. A structural DNA binding protein of African swine fever virus with similarity to bacterial histone-like proteins. Arch Virol 141, 301-313.

Borca, M.V., Kutish, G.F., Afonso, C.L., Irusta, P., Carrillo, C., Brun, A., Sussman, M., Rock, D.L., 1994. An African swine fever virus gene with similarity to the T-lymphocyte surface antigen CD2 mediates hemadsorption. Virology 199, 463-468.

Bradbury, L.E., Kansas, G.S., Levy, S., Evans, R.L., Tedder, T.F., 1992. The CD19/CD21 signal transducing complex of human B lymphocytes includes the target of antiproliferative antibody-1 and Leu-13 molecules. Journal of immunology 149, 2841-2850.

Brass, A.L., Huang, I.C., Benita, Y., John, S.P., Krishnan, M.N., Feeley, E.M., Ryan, B.J., Weyer, J.L., van der Weyden, L., Fikrig, E., Adams, D.J., Xavier, R.J., Farzan, M., Elledge, S.J., 2009. The IFITM proteins mediate cellular resistance to influenza A H1N1 virus, West Nile virus, and dengue virus. Cell 139, 1243-1254.

Breese, S.S., Jr., DeBoer, C.J., 1966. Electron microscope observations of African swine fever virus in tissue culture cells. Virology 28, 420-428.

Breese, S.S., Jr., Hess, W.R., 1966. Electron microscopy of African swine fever virus hemadsorption. J Bacteriol 92, 272-274.

Brookes, S.M., Dixon, L.K., Parkhouse, R.M., 1996. Assembly of African Swine fever virus: quantitative ultrastructural analysis in vitro and in vivo. Virology 224, 84-92.

Brun, A., Rivas, C., Esteban, M., Escribano, J.M., Alonso, C., 1996. African swine fever virus gene A179L, a viral homologue of bcl-2, protects cells from programmed cell death. Virology 225, 227-230.

Buchkovich, N.J., Yu, Y., Zampieri, C.A., Alwine, J.C., 2008. The TORrid affairs of viruses: effects of mammalian DNA viruses on the PI3K-Akt-mTOR signalling pathway. Nat Rev Microbiol 6, 266-275.

Bulimo, W.D., Miskin, J.E., Dixon, L.K., 2000. An ARID family protein binds to the African swine fever virus encoded ubiquitin conjugating enzyme, UBCv1. FEBS letters 471, 17-22.

Caro, L.H., Plomp, P.J., Wolvetang, E.J., Kerkhof, C., Meijer, A.J., 1988. 3-Methyladenine, an inhibitor of autophagy, has multiple effects on metabolism. Eur J Biochem 175, 325-329.

Carrascosa, A.L., Bustos, M.J., de Leon, P., 2011. Methods for growing and titrating African swine fever virus: field and laboratory samples. Current protocols in cell biology / editorial board, Juan S. Bonifacino ... [et al.] Chapter 26, Unit 26 14.

Carrascosa, J.L., Carazo, J.M., Carrascosa, A.L., Garcia, N., Santisteban, A., Vinuela, E., 1984. General morphology and capsid fine structure of African swine fever virus particles. Virology 132, 160-172.

Carvalho, Z.G., De Matos, A.P., Rodrigues-Pousada, C., 1988. Association of African swine fever virus with the cytoskeleton. Virus research 11, 175-192.

Castello, A., Quintas, A., Sanchez, E.G., Sabina, P., Nogal, M., Carrasco, L., Revilla, Y., 2009. Regulation of host translational machinery by African swine fever virus. PLoS pathogens 5, e1000562.

Chapman, D.A., Tcherepanov, V., Upton, C., Dixon, L.K., 2008. Comparison of the genome sequences of non-pathogenic and pathogenic African swine fever virus isolates. J Gen Virol 89, 397-408.

Chaumorcel, M., Souquere, S., Pierron, G., Codogno, P., Esclatine, A., 2008. Human cytomegalovirus controls a new autophagy-dependent cellular antiviral defense mechanism. Autophagy 4, 46-53.

Chien, C.T., Bartel, P.L., Sternglanz, R., Fields, S., 1991. The two-hybrid system: a method to identify and clone genes for proteins that interact with a protein of interest. Proceedings of the National Academy of Sciences of the United States of America 88, 9578-9582.

Choi, A.M., Ryter, S.W., Levine, B., 2013. Autophagy in human health and disease. N Engl J Med 368, 1845-1846.

Ciechanover, A., 1994. The ubiquitin-proteasome proteolytic pathway. Cell 79, 13-21.

Cobbold, C., Whittle, J.T., Wileman, T., 1996. Involvement of the endoplasmic reticulum in the assembly and envelopment of African swine fever virus. J Virol 70, 8382-8390.

Cobbold, C., Windsor, M., Wileman, T., 2001. A virally encoded chaperone specialized for folding of the major capsid protein of African swine fever virus. Journal of virology 75, 7221-7229.

Colgrove, G.S., Haelterman, E.O., Coggins, L., 1969. Pathogenesis of African swine fever in young pigs. American journal of veterinary research 30, 1343-1359.

Cooray, S., 2004. The pivotal role of phosphatidylinositol 3-kinase-Akt signal transduction in virus survival. The Journal of general virology 85, 1065-1076.

Correia, S., Ventura, S., Parkhouse, R.M., 2013. Identification and utility of innate immune system evasion mechanisms of ASFV. Virus research 173, 87-100.

Costa, J.V., 1990. African Swine Fever, in: Darai, G. (Ed.), Molecular Biology of Iridoviruses, Boston, pp. 247-270.

Costard, S., Porphyre, V., Messad, S., Rakotondrahanta, S., Vidon, H., Roger, F., Pfeiffer, D.U., 2009a. Multivariate analysis of management and biosecurity practices in smallholder pig farms in Madagascar. Prev Vet Med 92, 199-209.

Costard, S., Wieland, B., de Glanville, W., Jori, F., Rowlands, R., Vosloo, W., Roger, F., Pfeiffer, D.U., Dixon, L.K., 2009b. African swine fever: how can global spread be prevented? Philosophical transactions of the Royal Society of London. Series B, Biological sciences 364, 2683-2696.

Criollo, A., Senovilla, L., Authier, H., Maiuri, M.C., Morselli, E., Vitale, I., Kepp, O., Tasdemir, E., Galluzzi, L., Shen, S., Tailler, M., Delahaye, N., Tesniere, A., De Stefano, D., Younes, A.B., Harper, F., Pierron, G., Lavandero, S., Zitvogel, L., Israel, A., Baud, V., Kroemer, G., 2010. IKK connects autophagy to major stress pathways. Autophagy 6, 189-191.

Cuesta-Geijo, M.A., Galindo, I., Hernaez, B., Quetglas, J.I., Dalmau-Mena, I., Alonso, C., 2012. Endosomal maturation, Rab7 GTPase and phosphoinositides in African swine fever virus entry. PLoS ONE 7, e48853.

de Matos, A.P., Carvalho, Z.G., 1993. African swine fever virus interaction with microtubules. Biology of the cell / under the auspices of the European Cell Biology Organization 78, 229-234.

de Oliveira, V.L., Almeida, S.C., Soares, H.R., Crespo, A., Marshall-Clarke, S., Parkhouse, R.M., 2011. A novel TLR3 inhibitor encoded by African swine fever virus (ASFV). Arch Virol 156, 597-609.

de Villiers, E.P., Gallardo, C., Arias, M., da Silva, M., Upton, C., Martin, R., Bishop, R.P., 2010. Phylogenomic analysis of 11 complete African swine fever virus genome sequences. Virology 400, 128-136.

Diamond, M.S., Farzan, M., 2013. The broad-spectrum antiviral functions of IFIT and IFITM proteins. Nature reviews. Immunology 13, 46-57.

Ding, H., Dolan, P.J., Johnson, G.V., 2008. Histone deacetylase 6 interacts with the microtubule-associated protein tau. Journal of neurochemistry 106, 2119-2130.

Dompierre, J.P., Godin, J.D., Charrin, B.C., Cordelieres, F.P., King, S.J., Humbert, S., Saudou, F., 2007. Histone deacetylase 6 inhibition compensates for the transport deficit in Huntington's disease by increasing tubulin acetylation. J Neurosci 27, 3571-3583.

Dreux, M., Chisari, F.V., 2010. Viruses and the autophagy machinery. Cell Cycle 9, 1295-1307.

Elledge, S.J., Mulligan, J.T., Ramer, S.W., Spottswood, M., Davis, R.W., 1991. Lambda YES: a multifunctional cDNA expression vector for the isolation of genes by complementation of yeast and Escherichia coli mutations. Proceedings of the National Academy of Sciences of the United States of America 88, 1731-1735.

Enjuanes, L., Carrascosa, A.L., Moreno, M.A., Vinuela, E., 1976a. Titration of African swine fever (ASF) virus. The Journal of general virology 32, 471-477.

Enjuanes, L., Carrascosa, A.L., Vinuela, E., 1976b. Isolation and properties of the DNA of African swine fever (ASF) virus. J Gen Virol 32, 479-492.

Eskelinen, E.L., Reggiori, F., Baba, M., Kovacs, A.L., Seglen, P.O., 2011. Seeing is believing: the impact of electron microscopy on autophagy research. Autophagy 7, 935-956.

Evans, S.S., Collea, R.P., Leasure, J.A., Lee, D.B., 1993. IFN-alpha induces homotypic adhesion and Leu-13 expression in human B lymphoid cells. Journal of immunology 150, 736-747.

Fan, Q.W., Weiss, W.A., 2011. Autophagy and Akt promote survival in glioma. Autophagy 7, 536-538.

Feeley, E.M., Sims, J.S., John, S.P., Chin, C.R., Pertel, T., Chen, L.M., Gaiha, G.D., Ryan, B.J., Donis, R.O., Elledge, S.J., Brass, A.L., 2011a. IFITM3 inhibits influenza A virus infection by preventing cytosolic entry. PLoS Pathog 7, e1002337.

Feeley, E.M., Sims, J.S., John, S.P., Chin, C.R., Pertel, T., Chen, L.M., Gaiha, G.D., Ryan, B.J., Donis, R.O., Elledge, S.J., Brass, A.L., 2011b. IFITM3 inhibits influenza A virus infection by preventing cytosolic entry. PLoS pathogens 7, e1002337.

Fimia, G.M., Piacentini, M., 2010. Regulation of autophagy in mammals and its interplay with apoptosis. Cell Mol Life Sci 67, 1581-1588.

Fothergill, T., McMillan, N.A., 2006. Papillomavirus virus-like particles activate the PI3-kinase pathway via alpha-6 beta-4 integrin upon binding. Virology 352, 319-328.

Friedman, R.L., Manly, S.P., McMahon, M., Kerr, I.M., Stark, G.R., 1984. Transcriptional and posttranscriptional regulation of interferon-induced gene expression in human cells. Cell 38, 745-755.

Galindo, I., Hernaez, B., Diaz-Gil, G., Escribano, J.M., Alonso, C., 2008. A179L, a viral Bcl-2 homologue, targets the core Bcl-2 apoptotic machinery and its upstream BH3 activators with selective binding restrictions for Bid and Noxa. Virology 375, 561-572.

Galindo, I., Hernaez, B., Munoz-Moreno, R., Cuesta-Geijo, M.A., Dalmau-Mena, I., Alonso, C., 2012. The ATF6 branch of unfolded protein response and apoptosis are activated to promote African swine fever virus infection. Cell Death Dis 3, e341.

Galluzzi, L., Aaronson, S.A., Abrams, J., Alnemri, E.S., Andrews, D.W., Baehrecke, E.H., Bazan, N.G., Blagosklonny, M.V., Blomgren, K., Borner, C., Bredesen, D.E., Brenner, C., Castedo, M., Cidlowski, J.A., Ciechanover, A., Cohen, G.M., De Laurenzi, V., De Maria, R., Deshmukh, M., Dynlacht, B.D., El-Deiry, W.S., Flavell, R.A., Fulda, S., Garrido, C., Golstein, P., Gougeon, M.L., Green, D.R., Gronemeyer, H., Hajnoczky, G., Hardwick, J.M., Hengartner, M.O., Ichijo, H., Jaattela, M., Kepp, O., Kimchi, A., Klionsky, D.J., Knight, R.A., Kornbluth, S., Kumar, S., Levine, B., Lipton, S.A., Lugli, E., Madeo, F., Malomi, W., Marine, J.C., Martin, S.J., Medema, J.P., Mehlen, P., Melino, G., Moll, U.M., Morselli, E., Nagata, S., Nicholson, D.W., Nicotera, P., Nunez, G., Oren, M., Penninger, J., Pervaiz, S., Peter, M.E., Piacentini, M., Prehn, J.H., Puthalakath, H., Rabinovich, G.A., Rizzuto, R., Rodrigues, C.M., Rubinsztein, D.C., Rudel, T., Scorrano, L., Simon, H.U., Steller, H., Tschopp, J., Tsujimoto, Y., Vandenabeele, P., Vitale, I., Vousden, K.H., Youle, R.J., Yuan, J., Zhivotovsky, B., Kroemer, G., 2009. Guidelines for the use and interpretation of assays for monitoring cell death in higher eukaryotes. Cell death and differentiation 16, 1093-1107.

Gamerdinger, M., Kaya, A.M., Wolfrum, U., Clement, A.M., Behl, C., 2011. BAG3 mediates chaperone-based aggresome-targeting and selective autophagy of misfolded proteins. EMBO reports 12, 149-156.

Gannage, M., Dormann, D., Albrecht, R., Dengjel, J., Torossi, T., Ramer, P.C., Lee, M., Strowig, T., Arrey, F., Conenello, G., Pypaert, M., Andersen, J., Garcia-Sastre, A., Munz, C., 2009. Matrix protein 2 of influenza A virus blocks autophagosome fusion with lysosomes. Cell host & microbe 6, 367-380.

Garcia-Beato, R., Salas, M.L., Vinuela, E., Salas, J., 1992. Role of the host cell nucleus in the replication of African swine fever virus DNA. Virology 188, 637-649.

Garcia-Escudero, R., Andres, G., Almazan, F., Vinuela, E., 1998. Inducible gene expression from African swine fever virus recombinants: analysis of the major capsid protein p72. J Virol 72, 3185-3195.

Garcia-Mata, R., Bebok, Z., Sorscher, E.J., Sztul, E.S., 1999. Characterization and dynamics of aggresome formation by a cytosolic GFP-chimera. The Journal of cell biology 146, 1239-1254.

Garcia-Mata, R., Gao, Y.S., Sztul, E., 2002. Hassles with taking out the garbage: aggravating aggresomes. Traffic 3, 388-396.

Gietz, D., St Jean, A., Woods, R.A., Schiestl, R.H., 1992. Improved method for high efficiency transformation of intact yeast cells. Nucleic acids research 20, 1425.

Gomez-Puertas, P., Rodriguez, F., Oviedo, J.M., Brun, A., Alonso, C., Escribano, J.M., 1998. The African swine fever virus proteins p54 and p30 are involved in two distinct steps of virus attachment and both contribute to the antibody-mediated protective immune response. Virology 243, 461-471.

Gonzalez, A., Talavera, A., Almendral, J.M., Vinuela, E., 1986. Hairpin loop structure of African swine fever virus DNA. Nucleic Acids Res 14, 6835-6844.

Granja, A.G., Nogal, M.L., Hurtado, C., Salas, J., Salas, M.L., Carrascosa, A.L., Revilla, Y., 2004. Modulation of p53 cellular function and cell death by African swine fever virus. Journal of virology 78, 7165-7174.

Granja, A.G., Perkins, N.D., Revilla, Y., 2008. A238L inhibits NF-ATc2, NF-kappa B, and c-Jun activation through a novel mechanism involving protein kinase C-theta-mediated up-regulation of the amino-terminal transactivation domain of p300. J Immunol 180, 2429-2442.

Guarente, L., 1993. Strategies for the identification of interacting proteins. Proceedings of the National Academy of Sciences of the United States of America 90, 1639-1641.

Gutierrez, M.G., Master, S.S., Singh, S.B., Taylor, G.A., Colombo, M.I., Deretic, V., 2004. Autophagy is a defense mechanism inhibiting BCG and Mycobacterium tuberculosis survival in infected macrophages. Cell 119, 753-766.

Hanahan, D., 1983. Studies on transformation of Escherichia coli with plasmids. Journal of molecular biology 166, 557-580.

Hay, N., Sonenberg, N., 2004. Upstream and downstream of mTOR. Genes & development 18, 1926-1945.

Heath, C.M., Windsor, M., Wileman, T., 2001. Aggresomes resemble sites specialized for virus assembly. The Journal of cell biology 153, 449-455.

Hernaez, B., Alonso, C., 2010. Dynamin- and clathrin-dependent endocytosis in African swine fever virus entry. J Virol 84, 2100-2109.

Hernaez, B., Cabezas, M., Munoz-Moreno, R., Galindo, I., Cuesta-Geijo, M.A., Alonso, C., 2013. A179L, a new viral Bcl2 homolog targeting Beclin 1 autophagy related protein. Curr Mol Med 13, 305-316.

Hernaez, B., Diaz-Gil, G., Garcia-Gallo, M., Ignacio Quetglas, J., Rodriguez-Crespo, I., Dixon, L., Escribano, J.M., Alonso, C., 2004a. The African swine fever virus dynein-binding protein p54 induces infected cell apoptosis. FEBS Lett 569, 224-228.

Hernaez, B., Escribano, J.M., Alonso, C., 2004b. Switching on and off the cell death cascade: African swine fever virus apoptosis regulation, in: Alonso, C. (Ed.), Viruses and apoptosis. Springer, Berlin, pp. 57-70.

Hernaez, B., Escribano, J.M., Alonso, C., 2006. Visualization of the African swine fever virus infection in living cells by incorporation into the virus particle of green fluorescent protein-p54 membrane protein chimera. Virology 350, 1-14.

Hernaez, B., Escribano, J.M., Alonso, C., 2008. African swine fever virus protein p30 interaction with heterogeneous nuclear ribonucleoprotein K (hnRNP-K) during infection. FEBS Lett 582, 3275-3280.

Hideshima, T., Bradner, J.E., Wong, J., Chauhan, D., Richardson, P., Schreiber, S.L., Anderson, K.C., 2005. Small-molecule inhibition of proteasome and aggresome function induces synergistic antitumor activity in multiple myeloma. Proceedings of the National Academy of Sciences of the United States of America 102, 8567-8572.

Hingamp, P.M., Arnold, J.E., Mayer, R.J., Dixon, L.K., 1992. A ubiquitin conjugating enzyme encoded by African swine fever virus. The EMBO journal 11, 361-366.

Hingamp, P.M., Leyland, M.L., Webb, J., Twigger, S., Mayer, R.J., Dixon, L.K., 1995. Characterization of a ubiquitinated protein which is externally located in African swine fever virions. Journal of virology 69, 1785-1793.

Hu, D., Wu, J., Xu, L., Zhang, R., Chen, L., 2012. A method for the establishment of a cell line with stable expression of the GFP-LC3 reporter protein. Molecular medicine reports 6, 783-786.

Huang, I.C., Bailey, C.C., Weyer, J.L., Radoshitzky, S.R., Becker, M.M., Chiang, J.J., Brass, A.L., Ahmed, A.A., Chi, X., Dong, L., Longobardi, L.E., Boltz, D., Kuhn, J.H., Elledge, S.J., Bavari, S., Denison, M.R., Choe, H., Farzan, M., 2011a. Distinct patterns of IFITM-mediated restriction of filoviruses, SARS coronavirus, and influenza A virus. PLoS Pathog 7, e1001258.

Huang, I.C., Bailey, C.C., Weyer, J.L., Radoshitzky, S.R., Becker, M.M., Chiang, J.J., Brass, A.L., Ahmed, A.A., Chi, X., Dong, L., Longobardi, L.E., Boltz, D., Kuhn, J.H., Elledge, S.J., Bavari, S., Denison, M.R., Choe, H., Farzan, M., 2011b. Distinct patterns of IFITM-mediated restriction of filoviruses, SARS coronavirus, and influenza A virus. PLoS pathogens 7, e1001258.

Hubbert, C., Guardiola, A., Shao, R., Kawaguchi, Y., Ito, A., Nixon, A., Yoshida, M., Wang, X.F., Yao, T.P., 2002. HDAC6 is a microtubule-associated deacetylase. Nature 417, 455-458.

Inoue, Y., Klionsky, D.J., 2010. Regulation of macroautophagy in Saccharomyces cerevisiae. Seminars in cell & developmental biology 21, 664-670.

Iyer, L.M., Aravind, L., Koonin, E.V., 2001. Common origin of four diverse families of large eukaryotic DNA viruses. J Virol 75, 11720-11734.

Jacinto, E., Facchinetti, V., Liu, D., Soto, N., Wei, S., Jung, S.Y., Huang, Q., Qin, J., Su, B., 2006. SIN1/MIP1 maintains rictor-mTOR complex integrity and regulates Akt phosphorylation and substrate specificity. Cell 127, 125-137.

Jacinto, E., Loewith, R., Schmidt, A., Lin, S., Ruegg, M.A., Hall, A., Hall, M.N., 2004. Mammalian TOR complex 2 controls the actin cytoskeleton and is rapamycin insensitive. Nature cell biology 6, 1122-1128.

Jackson, W.T., Giddings, T.H., Jr., Taylor, M.P., Mulinyawe, S., Rabinovitch, M., Kopito, R.R., Kirkegaard, K., 2005. Subversion of cellular autophagosomal machinery by RNA viruses. PLoS biology 3, e156.

Jiang, D., Weidner, J.M., Qing, M., Pan, X.B., Guo, H., Xu, C., Zhang, X., Birk, A., Chang, J., Shi, P.Y., Block, T.M., Guo, J.T., 2010. Identification of five interferon-induced cellular proteins that inhibit west nile virus and dengue virus infections. Journal of virology 84, 8332-8341.

John, S.P., Chin, C.R., Perreira, J.M., Feeley, E.M., Aker, A.M., Savidis, G., Smith, S.E., Elia, A.E., Everitt, A.R., Vora, M., Pertel, T., Elledge, S.J., Kellam, P., Brass, A.L., 2013. The CD225 domain of IFITM3 is required for both IFITM protein association and inhibition of influenza A virus and dengue virus replication. J Virol 87, 7837-7852.

Johnston, J.A., Ward, C.L., Kopito, R.R., 1998. Aggresomes: a cellular response to misfolded proteins. The Journal of cell biology 143, 1883-1898.

Jordan, T.X., Randall, G., 2012. Manipulation or capitulation: virus interactions with autophagy. Microbes and infection / Institut Pasteur 14, 126-139.

Kabeya, Y., Mizushima, N., Ueno, T., Yamamoto, A., Kirisako, T., Noda, T., Kominami, E., Ohsumi, Y., Yoshimori, T., 2000. LC3, a mammalian homologue of yeast Apg8p, is localized in autophagosome membranes after processing. The EMBO journal 19, 5720-5728.

Kabeya, Y., Mizushima, N., Yamamoto, A., Oshitani-Okamoto, S., Ohsumi, Y., Yoshimori, T., 2004. LC3, GABARAP and GATE16 localize to autophagosomal membrane depending on form-II formation. Journal of cell science 117, 2805-2812.

Karim, M.R., Kanazawa, T., Daigaku, Y., Fujimura, S., Miotto, G., Kadowaki, M., 2007. Cytosolic LC3 ratio as a sensitive index of macroautophagy in isolated rat hepatocytes and H4-II-E cells. Autophagy 3, 553-560.

Kawaguchi, Y., Kovacs, J.J., McLaurin, A., Vance, J.M., Ito, A., Yao, T.P., 2003. The deacetylase HDAC6 regulates aggresome formation and cell viability in response to misfolded protein stress. Cell 115, 727-738.

Ke, P.Y., Chen, S.S., 2011. Activation of the unfolded protein response and autophagy after hepatitis C virus infection suppresses innate antiviral immunity in vitro. The Journal of clinical investigation 121, 37-56.

Khakpoor, A., Panyasrivanit, M., Wikan, N., Smith, D.R., 2009. A role for autophagolysosomes in dengue virus 3 production in HepG2 cells. The Journal of general virology 90, 1093-1103.

Kirkegaard, K., Taylor, M.P., Jackson, W.T., 2004. Cellular autophagy: surrender, avoidance and subversion by microorganisms. Nat Rev Microbiol 2, 301-314.

Kleiboeker, S.B., 2002. Swine fever: classical swine fever and African swine fever. Vet Clin North Am Food Anim Pract 18, 431-451.

Kleiboeker, S.B., Scoles, G.A., 2001. Pathogenesis of African swine fever virus in Ornithodoros ticks. Anim Health Res Rev 2, 121-128.

Kleiboeker, S.B., Scoles, G.A., Burrage, T.G., Sur, J., 1999. African swine fever virus replication in the midgut epithelium is required for infection of Ornithodoros ticks. Journal of virology 73, 8587-8598.

Kopito, R.R., 2000. Aggresomes, inclusion bodies and protein aggregation. Trends in cell biology 10, 524-530.

Kraft, C., Peter, M., Hofmann, K., 2010. Selective autophagy: ubiquitin-mediated recognition and beyond. Nat Cell Biol 12, 836-841.

Ku, B., Woo, J.S., Liang, C., Lee, K.H., Hong, H.S., E, X., Kim, K.S., Jung, J.U., Oh, B.H., 2008. Structural and biochemical bases for the inhibition of autophagy and apoptosis by viral BCL-2 of murine gamma-herpesvirus 68. PLoS pathogens 4, e25.

Kuma, A., Hatano, M., Matsui, M., Yamamoto, A., Nakaya, H., Yoshimori, T., Ohsumi, Y., Tokuhisa, T., Mizushima, N., 2004. The role of autophagy during the early neonatal starvation period. Nature 432, 1032-1036.

Kuznar, J., Salas, M.L., Vinuela, E., 1980. DNA-dependent RNA polymerase in African swine fever virus. Virology 101, 169-175.

Lange, U.C., Adams, D.J., Lee, C., Barton, S., Schneider, R., Bradley, A., Surani, M.A., 2008. Normal germ line establishment in mice carrying a deletion of the Ifitm/Fragilis gene family cluster. Molecular and cellular biology 28, 4688-4696.

Lange, U.C., Saitou, M., Western, P.S., Barton, S.C., Surani, M.A., 2003. The fragilis interferon-inducible gene family of transmembrane proteins is associated with germ cell specification in mice. BMC Dev Biol 3, 1.

Lee, H.K., Lund, J.M., Ramanathan, B., Mizushima, N., Iwasaki, A., 2007. Autophagy-dependent viral recognition by plasmacytoid dendritic cells. Science 315, 1398-1401.

Levine, B., Deretic, V., 2007. Unveiling the roles of autophagy in innate and adaptive immunity. Nat Rev Immunol 7, 767-777.

Lewin, A.R., Reid, L.E., McMahon, M., Stark, G.R., Kerr, I.M., 1991. Molecular analysis of a human interferon-inducible gene family. Eur J Biochem 199, 417-423.

Li, G., Jiang, H., Chang, M., Xie, H., Hu, L., 2011. HDAC6 alpha-tubulin deacetylase: a potential therapeutic target in neurodegenerative diseases. J Neurol Sci 304, 1-8.

Liang, C., E, X., Jung, J.U., 2008. Downregulation of autophagy by herpesvirus Bcl-2 homologs. Autophagy 4, 268-272.

Liang, X.H., Jackson, S., Seaman, M., Brown, K., Kempkes, B., Hibshoosh, H., Levine, B., 1999. Induction of autophagy and inhibition of tumorigenesis by beclin 1. Nature 402, 672-676.

Liang, X.H., Kleeman, L.K., Jiang, H.H., Gordon, G., Goldman, J.E., Berry, G., Herman, B., Levine, B., 1998. Protection against fatal Sindbis virus encephalitis by beclin, a novel Bcl-2-interacting protein. Journal of virology 72, 8586-8596.

Lu, J., Pan, Q., Rong, L., He, W., Liu, S.L., Liang, C., 2011. The IFITM proteins inhibit HIV-1 infection. Journal of virology 85, 2126-2137.

Ma, X.M., Blenis, J., 2009. Molecular mechanisms of mTOR-mediated translational control. Nature reviews. Molecular cell biology 10, 307-318.

Mammucari, C., Milan, G., Romanello, V., Masiero, E., Rudolf, R., Del Piccolo, P., Burden, S.J., Di Lisi, R., Sandri, C., Zhao, J., Goldberg, A.L., Schiaffino, S., Sandri, M., 2007. FoxO3 controls autophagy in skeletal muscle in vivo. Cell metabolism 6, 458-471.

Marsh, M., Helenius, A., 2006. Virus entry: open sesame. Cell 124, 729-740.

Martins, A., Ribeiro, G., Marques, M.I., Costa, J.V., 1994. Genetic identification and nucleotide sequence of the DNA polymerase gene of African swine fever virus. Nucleic Acids Res 22, 208-213.

Matsuyama, A., Shimazu, T., Sumida, Y., Saito, A., Yoshimatsu, Y., Seigneurin-Berny, D., Osada, H., Komatsu, Y., Nishino, N., Khochbin, S., Horinouchi, S., Yoshida, M., 2002. In vivo destabilization of dynamic microtubules by HDAC6-mediated deacetylation. The EMBO journal 21, 6820-6831.

Mebus, C.A., Dardiri, A.H., 1980. Western hemisphere isolates of African swine fever virus: asymptomatic carriers and resistance to challenge inoculation. American journal of veterinary research 41, 1867-1869.

Menendez-Benito, V., Neefjes, J., 2007. Autophagy in MHC class II presentation: sampling from within. Immunity 26, 1-3.

Menges, C.W., Baglia, L.A., Lapoint, R., McCance, D.J., 2006. Human papillomavirus type 16 E7 up-regulates AKT activity through the retinoblastoma protein. Cancer research 66, 5555-5559.

Mijaljica, D., Prescott, M., Devenish, R.J., 2011. Microautophagy in mammalian cells: revisiting a 40-year-old conundrum. Autophagy 7, 673-682.

Miskin, J.E., Abrams, C.C., Goatley, L.C., Dixon, L.K., 1998. A viral mechanism for inhibition of the cellular phosphatase calcineurin. Science 281, 562-565.

Mizushima, N., Yoshimori, T., 2007. How to interpret LC3 immunoblotting. Autophagy 3, 542-545.

Mizushima, N., Yoshimori, T., Levine, B., 2010. Methods in mammalian autophagy research. Cell 140, 313-326.

Moffatt, P., Gaumond, M.H., Salois, P., Sellin, K., Bessette, M.C., Godin, E., de Oliveira, P.T., Atkins, G.J., Nanci, A., Thomas, G., 2008. Bril: a novel bone-specific modulator of mineralization. Journal of bone and mineral research : the official journal of the American Society for Bone and Mineral Research 23, 1497-1508.

Moloughney, J.G., Monken, C.E., Tao, H., Zhang, H., Thomas, J.D., Lattime, E.C., Jin, S., 2011. Vaccinia virus leads to ATG12-ATG3 conjugation and deficiency in autophagosome formation. Autophagy 7, 1434-1447.

Monaghan, P., Cook, H., Hawes, P., Simpson, J., Tomley, F., 2003. High-pressure freezing in the study of animal pathogens. J Microsc 212, 62-70.

Montgomery, R.E., 1921. On a form of a swine fever occurring in British East African (Kenya Colony). J. Comp. Path. Therap 34, 159-191 y 243-262.

Moreno, M.A., Carrascosa, A.L., Ortin, J., Vinuela, E., 1978. Inhibition of African swine fever (ASF virus replication by phosphonoacetic acid. J Gen Virol 39, 253-258.

Moss, B., 2001. Poxviridae: the viruses and their replication., in: Fields BN, K.D., Howley PM, Chanock RM, Hirsch MS, Melnick JL, Monath TP, Roizman B. (Ed.), Fields Virology., 4th ed. Lippincott-Raven Press, Philadelphia, pp. 2849–2883.

Munoz, M., Freije, J.M., Salas, M.L., Vinuela, E., Lopez-Otin, C., 1993. Structure and expression in E. coli of the gene coding for protein p10 of African swine fever virus. Arch Virol 130, 93-107.

Murakami, Y., Fukasawa, M., Kaneko, Y., Suzuki, T., Wakita, T., Fukazawa, H., 2013. Selective estrogen receptor modulators inhibit hepatitis C virus infection at multiple steps of the virus life cycle. Microbes Infect 15, 45-55.

Nakagawa, I., Amano, A., Mizushima, N., Yamamoto, A., Yamaguchi, H., Kamimoto, T., Nara, A., Funao, J., Nakata, M., Tsuda, K., Hamada, S., Yoshimori, T., 2004. Autophagy defends cells against invading group A Streptococcus. Science 306, 1037-1040.

Nakashima, A., Tanaka, N., Tamai, K., Kyuuma, M., Ishikawa, Y., Sato, H., Yoshimori, T., Saito, S., Sugamura, K., 2006. Survival of parvovirus B19-infected cells by cellular autophagy. Virology 349, 254-263.

Netherton, C.L., McCrossan, M.C., Denyer, M., Ponnambalam, S., Armstrong, J., Takamatsu, H.H., Wileman, T.E., 2006. African swine fever virus causes microtubule-dependent dispersal of the trans-golgi network and slows delivery of membrane protein to the plasma membrane. J Virol 80, 11385-11392.

Netherton, C.L., Wileman, T.E., 2013. African swine fever virus organelle rearrangements. Virus Res 173, 76-86.

Nimmerjahn, F., Milosevic, S., Behrends, U., Jaffee, E.M., Pardoll, D.M., Bornkamm, G.W., Mautner, J., 2003. Major histocompatibility complex class II-restricted presentation of a cytosolic antigen by autophagy. Eur J Immunol 33, 1250-1259.

Nunes, J.F., Vigario, J.D., Terrinha, A.M., 1975. Ultrastructural study of African swine fever virus replication in cultures of swine bone marrow cells. Arch Virol 49, 59-66.

Ogawa, M., Yoshimori, T., Suzuki, T., Sagara, H., Mizushima, N., Sasakawa, C., 2005. Escape of intracellular Shigella from autophagy. Science 307, 727-731.

Orvedahl, A., Alexander, D., Talloczy, Z., Sun, Q., Wei, Y., Zhang, W., Burns, D., Leib, D.A., Levine, B., 2007. HSV-1 ICP34.5 confers neurovirulence by targeting the Beclin 1 autophagy protein. Cell host & microbe 1, 23-35.

Orvedahl, A., MacPherson, S., Sumpter, R., Jr., Talloczy, Z., Zou, Z., Levine, B., 2010. Autophagy protects against Sindbis virus infection of the central nervous system. Cell host & microbe 7, 115-127.

Pahl, H.L., Baeuerle, P.A., 1996. Control of gene expression by proteolysis. Current opinion in cell biology 8, 340-347.

Pai, M.T., Tzeng, S.R., Kovacs, J.J., Keaton, M.A., Li, S.S., Yao, T.P., Zhou, P., 2007. Solution structure of the Ubp-M BUZ domain, a highly specific protein module that recognizes the C-terminal tail of free ubiquitin. Journal of molecular biology 370, 290-302.

Paludan, C., Schmid, D., Landthaler, M., Vockerodt, M., Kube, D., Tuschl, T., Munz, C., 2005. Endogenous MHC class II processing of a viral nuclear antigen after autophagy. Science 307, 593-596.

Pan, I.C., Hess, W.R., 1984. Virulence in African swine fever: its measurement and implications. American journal of veterinary research 45, 361-366.

Park, J.R., Hockenbery, D.M., 1996. BCL-2, a novel regulator of apoptosis. Journal of cellular biochemistry 60, 12-17.

Pattingre, S., Tassa, A., Qu, X., Garuti, R., Liang, X.H., Mizushima, N., Packer, M., Schneider, M.D., Levine, B., 2005. Bcl-2 antiapoptotic proteins inhibit Beclin 1-dependent autophagy. Cell 122, 927-939.

Payne, E., Bowles, M.R., Don, A., Hancock, J.F., McMillan, N.A., 2001. Human papillomavirus type 6b virus-like particles are able to activate the Ras-MAP kinase pathway and induce cell proliferation. Journal of virology 75, 4150-4157.

Pena, L., Yanez, R.J., Revilla, Y., Vinuela, E., Salas, M.L., 1993. African swine fever virus guanylyltransferase. Virology 193, 319-328.

Penrith, M.L., Thomson, G.R., Bastos, A.D., Phiri, O.C., Lubisi, B.A., Du Plessis, E.C., Macome, F., Pinto, F., Botha, B., Esterhuysen, J., 2004. An investigation into natural resistance to African swine fever in domestic pigs from an endemic area in southern Africa. Rev Sci Tech 23, 965-977.

Perez, J., Fernandez, A.I., Sierra, M.A., Herraez, P., Fernandez, A., Martin de las Mulas, J., 1998. Serological and immunohistochemical study of African swine fever in wild boar in Spain. The Veterinary record 143, 136-139.

Perreira, J.M., Chin, C.R., Feeley, E.M., Brass, A.L., 2013. IFITMs restrict the replication of multiple pathogenic viruses. Journal of molecular biology 425, 4937-4955.

Petersen, J., Drake, M.J., Bruce, E.A., Riblett, A.M., Didigu, C.A., Wilen, C.B., Malani, N., Male, F., Lee, F.H., Bushman, F.D., Cherry, S., Doms, R.W., Bates, P., Briley, K., Jr., 2014. The major cellular sterol regulatory pathway is required for Andes virus infection. PLoS pathogens 10, e1003911.

Petroulakis, E., Mamane, Y., Le Bacquer, O., Shahbazian, D., Sonenberg, N., 2006. mTOR signaling: implications for cancer and anticancer therapy. Br J Cancer 94, 195-199.

Pim, D., Massimi, P., Dilworth, S.M., Banks, L., 2005. Activation of the protein kinase B pathway by the HPV-16 E7 oncoprotein occurs through a mechanism involving interaction with PP2A. Oncogene 24, 7830-7838.

Plowright, W., Parker, J., Peirce, M.A., 1969. African swine fever virus in ticks (Ornithodoros moubata, murray) collected from animal burrows in Tanzania. Nature 221, 1071-1073.

Plowright, W., Parker, J., Staple, R.F., 1968. The growth of a virulent strain of African swine fever virus in domestic pigs. J Hyg (Lond) 66, 117-134.

Polo-Jover, F., Sánchez-Botija, C., 1961. La Peste porcina africana en España. Bull Off Int Epizoot 55, 107-147.

Populo, H., Lopes, J.M., Soares, P., 2012. The mTOR Signalling Pathway in Human Cancer. Int J Mol Sci 13, 1886-1918.

Porstmann, T., Santos, C.R., Griffiths, B., Cully, M., Wu, M., Leevers, S., Griffiths, J.R., Chung, Y.L., Schulze, A., 2008. SREBP activity is regulated by mTORC1 and contributes to Akt-dependent cell growth. Cell metabolism 8, 224-236.

Portugal, R., Martins, C., Keil, G.M., 2012. Novel approach for the generation of recombinant African swine fever virus from a field isolate using GFP expression and 5-bromo-2'-deoxyuridine selection. J Virol Methods 183, 86-89.

PROMed-Mail, 2012. PRO/AH> African swine fever - Russia (10): control, food chain International Society for Infectious Diseases.

Punnonen, E.L., Marjomaki, V.S., Reunanen, H., 1994. 3-Methyladenine inhibits transport from late endosomes to lysosomes in cultured rat and mouse fibroblasts. European journal of cell biology 65, 14-25.

Quetglas, J.I., Hernaez, B., Galindo, I., Munoz-Moreno, R., Cuesta-Geijo, M.A., Alonso, C., 2012. Small rho GTPases and cholesterol biosynthetic pathway intermediates in african Swine Fever virus infection. J Virol 86, 1758-1767.

Ramiro-Ibanez, F., Ortega, A., Brun, A., Escribano, J.M., Alonso, C., 1996. Apoptosis: a mechanism of cell killing and lymphoid organ impairment during acute African swine fever virus infection. J Gen Virol 77 (Pt 9), 2209-2219.

Ramiro-Ibanez, F., Ortega, A., Ruiz-Gonzalvo, F., Escribano, J.M., Alonso, C., 1997. Modulation of immune cell populations and activation markers in the pathogenesis of African swine fever virus infection. Virus Res 47, 31-40.

Reunanen, H., Punnonen, E.L., Hirsimaki, P., 1985. Studies on vinblastine-induced autophagocytosis in mouse liver. V. A cytochemical study on the origin of membranes. Histochemistry 83, 513-517.

Reyes-Turcu, F.E., Horton, J.R., Mullally, J.E., Heroux, A., Cheng, X., Wilkinson, K.D., 2006. The ubiquitin binding domain ZnF UBP recognizes the C-terminal diglycine motif of unanchored ubiquitin. Cell 124, 1197-1208.

Rez, G., Meldolesi, J., 1980. Freeze-fracture of drug-induced autophagocytosis in the mouse exocrine pancreas. Lab Invest 43, 269-277.

Richards, A.L., Jackson, W.T., 2013. How positive-strand RNA viruses benefit from autophagosome maturation. J Virol 87, 9966-9972.

Rivera, J., Abrams, C., Hernaez, B., Alcazar, A., Escribano, J.M., Dixon, L., Alonso, C., 2007a. The MyD116 African swine fever virus homologue interacts with the catalytic subunit of protein phosphatase 1 and activates its phosphatase activity. J Virol 81, 2923-2929.

Rivera, J., Abrams, C., Hernaez, B., Alcazar, A., Escribano, J.M., Dixon, L., Alonso, C., 2007b. The MyD116 African swine fever virus homologue interacts with the catalytic subunit of protein phosphatase 1 and activates its phosphatase activity. Journal of virology 81, 2923-2929.

Roberts, H., Smith, J., Drew, T., 2014. African Swine Fever in wild boar in Ukraine, Preliminary Outbreak Assessment. Department of Environment, Food and Rural Affairs, Veterinary Science Team.

Rodriguez, I., Nogal, M.L., Redrejo-Rodriguez, M., Bustos, M.J., Salas, M.L., 2009. The African swine fever virus virion membrane protein pE248R is required for virus infectivity and an early postentry event. J Virol 83, 12290-12300.

Rodriguez, J.M., Garcia-Escudero, R., Salas, M.L., Andres, G., 2004. African Swine Fever Virus Structural Protein p54 Is Essential for the Recruitment of Envelope Precursors to Assembly Sites. J Virol 78, 4299-1313.

Rodriguez, J.M., Salas, M.L., Vinuela, E., 1992. Genes homologous to ubiquitin-conjugating proteins and eukaryotic transcription factor SII in African swine fever virus. Virology 186, 40-52.

Rodriguez, J.M., Salas, M.L., Vinuela, E., 1996. Intermediate class of mRNAs in African swine fever virus. J Virol 70, 8584-8589.

Rojo, G., Chamorro, M., Salas, M.L., Vinuela, E., Cuezva, J.M., Salas, J., 1998a. Migration of mitochondria to viral assembly sites in African swine fever virus-infected cells. Journal of virology 72, 7583-7588.

Rojo, G., Chamorro, M., Salas, M.L., Vinuela, E., Cuezva, J.M., Salas, J., 1998b. Migration of mitochondria to viral assembly sites in African swine fever virus-infected cells. J Virol 72, 7583-7588.

Rojo, G., Garcia-Beato, R., Vinuela, E., Salas, M.L., Salas, J., 1999. Replication of African swine fever virus DNA in infected cells. Virology 257, 524-536.

Ropolo, A., Tomasini, R., Grasso, D., Dusetti, N.J., Cerquetti, M.C., Iovanna, J.L., Vaccaro, M.I., 2004. Cloning of IP15, a pancreatitis-induced gene whose expression inhibits cell growth. Biochemical and biophysical research communications 319, 1001-1009.

Rouiller, I., Brookes, S.M., Hyatt, A.D., Windsor, M., Wileman, T., 1998. African swine fever virus is wrapped by the endoplasmic reticulum. J Virol 72, 2373-2387.

Rubinsztein, D.C., Cuervo, A.M., Ravikumar, B., Sarkar, S., Korolchuk, V., Kaushik, S., Klionsky, D.J., 2009. In search of an "autophagomometer". Autophagy 5, 585-589.

Saitoh, T., Akira, S., 2010. Regulation of innate immune responses by autophagy-related proteins. J Cell Biol 189, 925-935.

Salas, J., Salas, M.L., Vinuela, E., 1988. Effect of inhibitors of the host cell RNA polymerase II on African swine fever virus multiplication. Virology 164, 280-283.

Salas, M.L., Kuznar, J., Vinuela, E., 1981. Polyadenylation, methylation, and capping of the RNA synthesized in vitro by African swine fever virus. Virology 113, 484-491.

Salas, M.L., Kuznar, J., Vinuela, E., 1983. Effect of rifamycin derivatives and coumermycin A1 on in vitro RNA synthesis by African swine fever virus. Brief report. Arch Virol 77, 77-80.

Salas, M.L., Rey-Campos, J., Almendral, J.M., Talavera, A., Vinuela, E., 1986. Transcription and translation maps of African swine fever virus. Virology 152, 228-240.

Sanchez, E.G., Quintas, A., Perez-Nunez, D., Nogal, M., Barroso, S., Carrascosa, A.L., Revilla, Y., 2012. African swine fever virus uses macropinocytosis to enter host cells. PLoS Pathog 8, e1002754.

Sarbassov, D.D., Guertin, D.A., Ali, S.M., Sabatini, D.M., 2005. Phosphorylation and regulation of Akt/PKB by the rictor-mTOR complex. Science 307, 1098-1101.

Scheffner, M., Nuber, U., Huibregtse, J.M., 1995. Protein ubiquitination involving an E1-E2-E3 enzyme ubiquitin thioester cascade. Nature 373, 81-83.

Schelhaas, M., Shah, B., Holzer, M., Blattmann, P., Kuhling, L., Day, P.M., Schiller, J.T., Helenius, A., 2012. Entry of human papillomavirus type 16 by actin-dependent, clathrin- and lipid raft-independent endocytosis. PLoS pathogens 8, e1002657.

Schieke, S.M., Phillips, D., McCoy, J.P., Jr., Aponte, A.M., Shen, R.F., Balaban, R.S., Finkel, T., 2006. The mammalian target of rapamycin (mTOR) pathway regulates mitochondrial oxygen consumption and oxidative capacity. The Journal of biological chemistry 281, 27643-27652.

Schmid, D., Pypaert, M., Munz, C., 2007. Antigen-loading compartments for major histocompatibility complex class II molecules continuously receive input from autophagosomes. Immunity 26, 79-92.

Schoggins, J.W., Wilson, S.J., Panis, M., Murphy, M.Y., Jones, C.T., Bieniasz, P., Rice, C.M., 2011. A diverse range of gene products are effectors of the type I interferon antiviral response. Nature 472, 481-485.

Shapira, S.D., Gat-Viks, I., Shum, B.O., Dricot, A., de Grace, M.M., Wu, L., Gupta, P.B., Hao, T., Silver, S.J., Root, D.E., Hill, D.E., Regev, A., Hacohen, N., 2009. A physical and regulatory map of host-influenza interactions reveals pathways in H1N1 infection. Cell 139, 1255-1267.

Simon-Mateo, C., Andres, G., Almazan, F., Vinuela, E., 1997. Proteolytic processing in African swine fever virus: evidence for a new structural polyprotein, pp62. J Virol 71, 5799-5804.

Sinha, S., Colbert, C.L., Becker, N., Wei, Y., Levine, B., 2008. Molecular basis of the regulation of Beclin 1-dependent autophagy by the gamma-herpesvirus 68 Bcl-2 homolog M11. Autophagy 4, 989-997.

Sir, D., Chen, W.L., Choi, J., Wakita, T., Yen, T.S., Ou, J.H., 2008. Induction of incomplete autophagic response by hepatitis C virus via the unfolded protein response. Hepatology 48, 1054-1061.

Sir, D., Ou, J.H., 2010. Autophagy in viral replication and pathogenesis. Mol Cells 29, 1-7.

Smith, G.A., Enquist, L.W., 2002. Break ins and break outs: viral interactions with the cytoskeleton of Mammalian cells. Annu Rev Cell Dev Biol 18, 135-161.

Smith, S.E., Koegl, M., Jentsch, S., 1996. Role of the ubiquitin/proteasome system in regulated protein degradation in Saccharomyces cerevisiae. Biological chemistry 377, 437-446.

Spangle, J.M., Munger, K., 2010. The human papillomavirus type 16 E6 oncoprotein activates mTORC1 signaling and increases protein synthesis. Journal of virology 84, 9398-9407.

Stefanovic, S., Windsor, M., Nagata, K.I., Inagaki, M., Wileman, T., 2005a. Vimentin rearrangement during African swine fever virus infection involves retrograde transport along microtubules and phosphorylation of vimentin by calcium calmodulin kinase II. Journal of virology 79, 11766-11775.

Stefanovic, S., Windsor, M., Nagata, K.I., Inagaki, M., Wileman, T., 2005b. Vimentin rearrangement during African swine fever virus infection involves retrograde transport along microtubules and phosphorylation of vimentin by calcium calmodulin kinase II. J Virol 79, 11766-11775.

Studier, F.W., 1991. Use of bacteriophage T7 lysozyme to improve an inducible T7 expression system. Journal of molecular biology 219, 37-44.

Suarez, C., Gutierrez-Berzal, J., Andres, G., Salas, M.L., Rodriguez, J.M., 2010. African swine fever virus protein p17 is essential for the progression of viral membrane precursors toward icosahedral intermediates. J Virol 84, 7484-7499.

Surviladze, Z., Sterk, R.T., DeHaro, S.A., Ozbun, M.A., 2013. Cellular entry of human papillomavirus type 16 involves activation of the phosphatidylinositol 3-kinase/Akt/mTOR pathway and inhibition of autophagy. Journal of virology 87, 2508-2517.

Tabares, E., Sanchez Botija, C., 1979. Synthesis of DNA in cells infected with African swine fever virus. Arch Virol 61, 49-59.

Takahashi, M.N., Jackson, W., Laird, D.T., Culp, T.D., Grose, C., Haynes, J.I., 2nd, Benetti, L., 2009. Varicella-zoster virus infection induces autophagy in both cultured cells and human skin vesicles. Journal of virology 83, 5466-5476.

Takeshige, K., Baba, M., Tsuboi, S., Noda, T., Ohsumi, Y., 1992. Autophagy in yeast demonstrated with proteinase-deficient mutants and conditions for its induction. The Journal of cell biology 119, 301-311.

Tanida, I., Ueno, T., Kominami, E., 2008. LC3 and Autophagy, in: Deretic, V. (Ed.), Autophagosome and Phagosome, Methods in Molecular Biology ed. Humana Press, Totowa, NJ (USA).

Taylor, M.P., Kirkegaard, K., 2007. Modification of cellular autophagy protein LC3 by poliovirus. Journal of virology 81, 12543-12553.

Taylor, M.P., Kirkegaard, K., 2008. Potential subversion of autophagosomal pathway by picornaviruses. Autophagy 4, 286-289.

Teodoro, J.G., Branton, P.E., 1997. Regulation of apoptosis by viral gene products. J Virol 71, 1739-1746.

Thumm, M., Egner, R., Koch, B., Schlumpberger, M., Straub, M., Veenhuis, M., Wolf, D.H., 1994. Isolation of autophagocytosis mutants of Saccharomyces cerevisiae. FEBS letters 349, 275-280.

Tsukada, M., Ohsumi, Y., 1993. Isolation and characterization of autophagy-defective mutants of Saccharomyces cerevisiae. FEBS letters 333, 169-174.

Valdeira, M.L., Geraldes, A., 1985. Morphological study on the entry of African swine fever virus into cells. Biol Cell 55, 35-40.

Webb, J.L., Ravikumar, B., Rubinsztein, D.C., 2004. Microtubule disruption inhibits autophagosome-lysosome fusion: implications for studying the roles of aggresomes in polyglutamine diseases. The international journal of biochemistry & cell biology 36, 2541-2550.

Wieland, B., Dhollander, S., Salman, M., Koenen, F., 2011. Qualitative risk assessment in a data-scarce environment: a model to assess the impact of control measures on spread of African Swine Fever. Prev Vet Med 99, 4-14.

Wileman, T., 2006. Aggresomes and autophagy generate sites for virus replication. Science 312, 875-878.

Wileman, T., 2007. Aggresomes and pericentriolar sites of virus assembly: cellular defense or viral design? Annu Rev Microbiol 61, 149-167.

Wilkins, C., Woodward, J., Lau, D.T., Barnes, A., Joyce, M., McFarlane, N., McKeating, J.A., Tyrrell, D.L., Gale, M., Jr., 2013. IFITM1 is a tight junction protein that inhibits hepatitis C virus entry. Hepatology 57, 461-469.

Xu, Y., Jagannath, C., Liu, X.D., Sharafkhaneh, A., Kolodziejska, K.E., Eissa, N.T., 2007. Toll-like receptor 4 is a sensor for autophagy associated with innate immunity. Immunity 27, 135-144.

Xue, L., Borutaite, V., Tolkovsky, A.M., 2002. Inhibition of mitochondrial permeability transition and release of cytochrome c by anti-apoptotic nucleoside analogues. Biochemical pharmacology 64, 441-449.

Yanez, R.J., Rodriguez, J.M., Nogal, M.L., Yuste, L., Enriquez, C., Rodriguez, J.F., Vinuela, E., 1995. Analysis of the complete nucleotide sequence of African swine fever virus. Virology 208, 249-278.

Yang, Z., Klionsky, D.J., 2010. Mammalian autophagy: core molecular machinery and signaling regulation. Current opinion in cell biology 22, 124-131.

Yount, J.S., Karssemeijer, R.A., Hang, H.C., 2012. S-palmitoylation and ubiquitination differentially regulate interferon-induced transmembrane protein 3 (IFITM3)-mediated resistance to influenza virus. The Journal of biological chemistry 287, 19631-19641.

Zhang, F., Moon, A., Childs, K., Goodbourn, S., Dixon, L.K., 2010. The African swine fever virus DP71L protein recruits the protein phosphatase 1 catalytic subunit to dephosphorylate eIF2alpha and inhibits CHOP induction but is dispensable for these activities during virus infection. J Virol 84, 10681-10689.

Zhang, R., Chi, X., Wang, S., Qi, B., Yu, X., Chen, J.L., 2014. The regulation of autophagy by influenza A virus. BioMed research international 2014, 498083.

Zhang, Y., Li, N., Caron, C., Matthias, G., Hess, D., Khochbin, S., Matthias, P., 2003. HDAC-6 interacts with and deacetylates tubulin and microtubules in vivo. The EMBO journal 22, 1168-1179.

Zsak, L., Lu, Z., Burrage, T.G., Neilan, J.G., Kutish, G.F., Moore, D.M., Rock, D.L., 2001a. African swine fever virus multigene family 360 and 530 genes are novel macrophage host range determinants. J Virol 75, 3066-3076.

Zsak, L., Lu, Z., Kutish, G.F., Neilan, J.G., Rock, D.L., 1996. An African swine fever virus virulence-associated gene NL-S with similarity to the herpes simplex virus ICP34.5 gene. J Virol 70, 8865-8871.

Zsak, L., Sur, J.H., Burrage, T.G., Neilan, J.G., Rock, D.L., 2001b. African Swine Fever virus (asfv) multigene families 360 and 530 genes promote infected macrophage survival. ScientificWorldJournal 1, 97.

PUBLICATIONS